Determination of thorium by Organic bases

By G. S. DESHMUKH and J. XAVIER

(Received December 13, 1954)

Jefferson[1] and Hartwell[2] reported the use of various amines and organic bases for the quantitative estimation of thorium in presence of rare earths. Further work by Atanasiu[3] and Schiotz[4] and Ismail and Hartwood[5] showed that pyridine, quinoline and hexamine are effective for the separation of thorium from cerium earths. An investigation along these lines seemed to promise well because it was considered that among the numerous hitherto uninvestigated organic bases, suitable precipitants might be found for the quantitative determination of thorium and its separation from rare earths and other familar congeners. Series of trial experiments were therefore carried out using *o*-tolidine, dianisidine, *p*-phenylenediamine, *o*-anisidine and *o*-phenetidine as precipitants for thorium. The present communication reports results obtained with the above bases and shows that *o*-anisidine and *o*-phenetidine afford a quantitative separation of thorium from trivalent rare earths.

Experimental

The organic bases used as precipitants were of Merck's reagent grade quality and were purified by repeated recrystallisation or/and distillation. An aqueous thorium chloride (or nitrate) solution was prepared and its thorium content was determined by *m*-nitrobenzoic[6] and sebacic acids.[7] In the case of *o*-tolidine, dianisidine and *p*-phenylenediamine the following procedure was adopted for precipitating the corresponding thorium complex.

To an aliquot quantity (10 ml.) of the thorium solution about 20–30 ml. of alcohol was added and the solution was heated to 90° C. A saturated alcoholic solution of the base was now run in a thin stream with constant stirring till the precipitation was complete, followed by about 5–10 ml. of alcohol. The contents were boiled for a couple of minutes. The precipitate was allowed to settle for an hour, filtered through Whatman 40, washed with cold alcohol, dried and ignited to ThO_2. For obtaining reproducible and accurate results, it is necessary to add the precipitant to an almost boiling hot solution of thorium salt containing an equivalent volume of alcohol and also to continue boiling at least for a few minutes after the complete precipitation of the thorium complex.

A representative group of results is given in Table I.

Since cerium and other trivalent rare earths are also precipitated by the above organic bases under the above experimental conditions, whose adaptability in quantitative analysis is restricted only to the determination of thorium in its aqueous solution.

Series of experiments carried out with *o*-phenetidine and *o*-anisidine, however, showed that these ammines could be used for the precipitation of thorium and its separation from trivalent rare earths e. g. Ce, La, Y and Er.

To a known volume of the thorium solution mixed with varying quantities of the above trivalent salt solutions and an equal portion of alcohol, an alcoholic solution of *o*-phenetidine or *o*-anisidine was added. The

TABLE I

Expt. No.	Wt. of ThO_2 (g.)	Wt. of ThO_2 (g.)			Difference		
	m-nitrobenzoic acid (a)	*o*-tolidine (b)	dianisidine (c)	*p*-phenylenediamine (d)	a~b	a~c	a~d
1	0.0640	0.0640	0.0638	0.0641	. .	0.0002	0.0001
2	0.0922	0.0919	0.0923	0.0923	0.0003	0.0001	0.0001
3	0.1152	0.1148	0.1149	0.1153	0.0004	0.0003	0.0001
4	0.1164	0.1164	0.1165	0.1165	. .	0.0001	0.0001
5	0.1378	0.1379	0.1376	0.1378	0.0001	0.0002	. .
6	0.1390	0.1392	0.1388	0.1390	0.0002	0.0002	. .

1) A.M. Jefferson, *J. Amer. Chem. Soc.*, **24**, 540 (1902).
2) B.L. Hartwell, ibid. **25**, 1128 (1903).
3) I.A. Atanasiu, *Ber.*, **60B**, 2507 (1927).
4) A.B. Schiotz, *Tids. Kemi. Farm. Terapi.*, **14**, 270 (1917).
5) A.M. Ismail, and H.F. Harwood, *Analyst*, **62**, 185 (1937).
6) A.C. Neish, *Chem. News*, **90**, 196, 201 (1904).
7) T.C. Smith and C. James, *J. Amer. Chem. Soc.*, **34**, 281 (1912).

CHEMISTRY HALL LIBRARY

precipitate appeared gradually and was complete in about 20–30 minutes. It was kept aside for six hours, filtered through Whatman 40, washed initially with cold alcohol and then repeatedly with hot 50% alcohol. The precipitate was dissolved in a minimum quantity of dilute 2N-HCl, the solution diluted further to about 50 ml. and thorium reprecipitated. This was washed finally with alcohol, dried and ignited to constant weight as ThO_2.

TABLE II

Expt No.	Wt. of ThO_2 (g.) *m*-nitrobenzoic acid (a)	Wt. of X_2O_3 (g.) added	Wt. of ThO_2 (g.) *o*-phenetidine (b)	Wt. of ThO_2 (g.) *o*-anisidine (c)	Difference a~b	Difference a~c
1	0.0640	0.0580	0.0642	0.0644	0.0002	0.0004
2	0.0922	0.0886	0.0926	0.0924	0.0004	0.0002
3	0.1152	0.1022	0.1150	0.1154	0.0002	0.0004
4	0.1164	0.1162	0.1166	0.1166	0.0002	0.0002
5	0.1378	0.1162	0.1376	0.1380	0.0002	0.0002
6	0.1390	0.1228	0.1394	0.1390	0.0004	. .

X=Ce, La, Y or Er

Results in Table II show that the double precipitation effects a quantitative separation of thorium from the trivalent rare earths used in the present investigation. The interference of other familiar congeners of thorium in its determination by the above precipitants is under investigation.

Grateful thanks of the authors are due to Professor S. S. Joshi for facilities and to the National Institute of Sciences of India for award of a research fellowship to one of us (G. S. D.) during the course of the above work

Summary

Quantitative estimation of thorium by precipitating it from aqueous thorium chloride (or nitrate) solution by *o*-tolidine, dianisidine, *p*-phenylenediamine, *o*-anisidine and *o*-phenetidine has been studied. The precipitated complex is ignited to constant weight and determined gravimetrically as ThO_2.

The use of *o*-anisidine and *o*-phenetidine for the separation of thorium from trivalent cerium has been suggested.

Chemical Laboratories Benaras Hindu University
&
The Indian Association for the Cultivation of Science Calcutta

---

Micelle Formation and Solubilization in Benzene by Fatty Acid Salts of Higher Amines

By Ayao KITAHARA

(Received September 20, 1954)

Introduction

Whilst numerous investigations have been made on the micelle formation as well as the solubilization both of which take place in *aqueous solutions* of detergents, little is known about the similar phenomena in *non-aqueous solutions*.

Some investigators[1,2] have assumed the micelle formation of detergents in non-polar solvents. However,it is not necessarily certain that detergent molecules can aggregate to micelles spontaneously when they are dissolved in non-polar solvents, because the present theories regarding the micelle formation in aqueous solutions of detergents can not be applied to a case when a solvent is a non-polar one. Hence, the more experimental

1) M. van der Waarden, *J. Colloid Sci.*, 5, 448 (1950). S. Kaufmann and C. R. Singleterry, *J. Colloid Sci.*, 7, 453 (1952). M.B. Mathews and E. Hirschhorn, *J. Colloid Sci.*, 8, 86 (1953).

2) Recently, Palit et al. have observed the enhancement in dissolving power for water into non-polar solvent with the presence of detergent such as fatty acid salts of higher amines, and this apparent solubilization was assumed to be parallel phenomena with micelle formation. See: S. R. Ralit and V. Venkateswarlu, *Proc. Roy. Soc.*, A208, 542 (1951); *J. Chem. Soc.*, 1954, 2129.

evidences are desired concerning the micelle formation as well as the solubilization which may take place in non-aqueous solutions of detergents, especially when the solvents are non-polar ones.

Experimental

Preparation of Detergents.—It was presumed that fatty acid salts of higher aliphatic amines are the most favourable materials as detergents for the present purpose. A series of compounds were prepared in possibly purified states in the following way.

Commercial dodecylamine and octadecylamine were purified by distillation under reduced pressure. The fraction having b.p. 131–133°C under 15 mmHg and those having b.p. 188–190°C under 4 mmHg were collected. Commercial propionic and butylic acid were dried by means of anhydrous copper sulfate and purified by distillation. For the other fatty acids, the products of Nihon Yushi Co. were used. The neutralization of amines with acids was carried out at room temperature. The solvents used in the preparation and the melting points of the products are summarized in Table I.

All the purified compounds were white and crystalline. The fluctuation of their melting points was ±1°C. Butylate and caproate of dodecylamine were strongly hygroscopic.

When the reaction of amines and acids was carried out at about 150°C instead of room temperature, substances having different melting points were obtained. The infra-red absorption spectra of reaction products from dodecylamine and propionic acid or capric acid were taken in nujol on a Perkin-Elmer 112 instrument. The products (1) obtained at high temperature showed absorptions at 1630 and 3300 cm^{-1}. The former absorption is attributed to the carbonyl group of

Table I

Preparation and Melting Points of Detergents

Detergent	Solvent used in neutralization	Solvent used in recrystallization	m.p. °C
Dodecylamine propionate	Benzene and *n*-Hexane	—	54–56
„ butylate	*n*-Hexane	*n*-Hexane	39–41
„ caproate	„	„	31–33
„ caprylate	„	—	43–45
„ capriate	Benzine	*n*-Hexane	60–61
„ laurate	„	„	62–64
„ myristate	„	„	64
„ palmitate	„	„	70–71
Octadecylamine propionate	Acetone	Benzine+Acetone	69–72
„ butylate	„	Benzine	56–58
„ caproate	„	„	46–47
„ caprylate	„	Acetone	52–54
„ capriate	„	„	59–61
„ laurate	„	„	62–64
„ myristate	„	—	71–72
„ palmitate	„	—	78–79

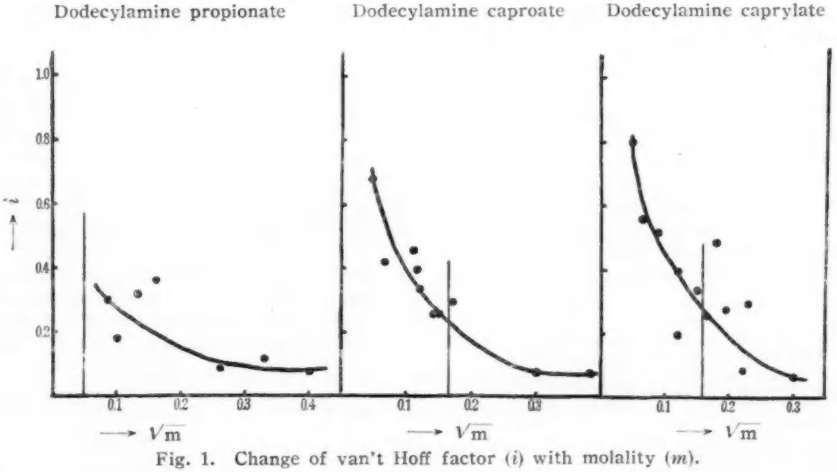

Fig. 1. Change of van't Hoff factor (i) with molality (m).

acid amide and the latter to its amide group. On the other hand, the corresponding products (2) obtained at room temperature had absorptions at 1400 and 1600 cm^{-1}. These two absorption peaks are attributed to carboxylic ions. Therefore, compounds (1) are acid amides, and (2) are fatty acid salts of higher amines having the structure of $[RCOO^-]$ $[H^+_3NR']$[3].

Determination of van't Hoff Factors.—For the purpose of ascertaining micelle formation, the van't Hoff factors (i) for dodecylamine propionate, caproate and caprylate in benzene were determined at various concentrations by means of cryoscopy (Fig. 1). The measurement was carried out with the usual Beckmann's apparatus.

Measurements of Solubilization.—The limiting amount of solubilized water into a benzene solution of a detergent was determined by the following simple method. Five cc. of solution was put into a test tube. By means of a micro-burette, water was added in portions of 0.002–0.003 cc. After addition of each portion the solution was vigorously shaken 50–250 times, and then put to stand for half an hour. The occurrence of turbidity was detected by means of Tyndall light. Near the limit of solubilization, Tyndall light was observed one or two days after water had been added in order to ascertain the attainment of equilibrium. The limit of solubilization was confirmed by the occurrence of faint turbidity. The measurements were carried out at 26°C.

Results and Discussion

Formation of Micelle.—The relation between the van't Hoff factor (i) and the root of molality was given in Fig. 1. At these concentrations the depression of temperature was insufficient to be observed accurately by a Beckmann's thermometer. Accordingly the data are not so accurate and show fluctuation. But these are adequate for qualitative discussion.

In aqueous solutions the critical concentration of micelle formation of ionic detergents has been discussed from the relation between an osmotic coefficient and a concentration.[4] In non-polar solvents micelle formation may be discussed with van't Hoff factor in place of an osmotic coefficient, because an ionic dissociation in non-polar solvent is doubtful. Therefore, Fig. 1 will be useful for the discussion of micelle formation in benzene.

In the cases of dodecylamine caproate and caprylate, the van't Hoff factors show a remarkable decrease at a range of the concentration in the manner similar to the well-known cases of osmotic coefficients in aqueous solutions. It is thought that this remarkable decrease shows the initiation of micelle formation at this range. In the case of dodecylamine propionate, the remarkable decrease was not observed within the concentration range of this experiment. Its range of the initiation of micelle formation seems to be in the left side of the obtained curve, but in this range no measurement was accurately carried out because of the slight depression of temperature. In any case the values of i at higher concentration are sufficient to show that micelles have been formed. It will be, therefore, concluded that micelle formation begins to take place at a certain concentration for these detergents. The phenomenon of solubilization should take place as the result of micelle formation.

On the other hand, the van't Hoff factors of acid amides in benzene have shown only slight decreases at comparable concentrations. For example, van't Hoff factors of dodecyl amide of caproic acid was 1.0 and 0.55 at 0.20 and 0.32 of $\sqrt{m}$, respectively. It is, therefore, assumed that micelles have not been formed at these concentrations in the case of acid amides.

Solubilization of Water.—The amount of solubilized water was plotted against the concentration of detergents, correction being made with respect to the solubility of water in benzene (Figs. 2 and 3). The salts of

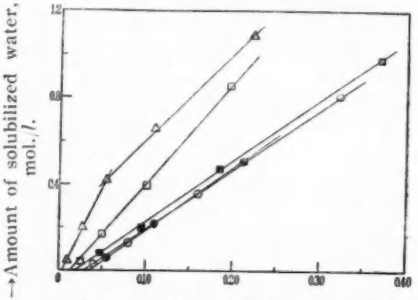

Fig. 2. The relation between solubilized water and concentration of salts of dodecylamine.

△ dodecylamine propionate
□ " butylate
■ " caproate
○ " caprylate
● " capriate

3) Fatty acid salts of amines and acid amides were prepared, ( ) keeping R'=12 and changing R from 3, 4, 6, 8, ..., 16, and (b) keeping R'=18 and R in the same way. It was found that the caproates (R=6) both of (a) and ( ) have the lowest melting points in the case of fatty acid salts of amines.

4) J. W. McBain, "Colloid Science", D. C. Heath & Co., Boston, (1950), p. 242.

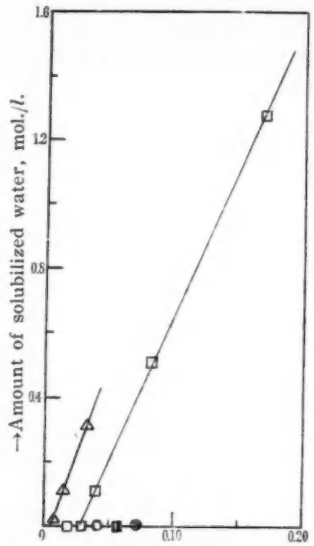

Fig. 3. The relation between solubilized water and concentration of salts of octadecylamine.

△ octadecylamine propionate
□ " butylate
■ " caproate
○ " caprylate
● " capriate

octadecylamine had less solubility as compared with those of dodecylamine. It was, therefore, hardly possible to carry out the measurement at higher concentrations similar to the later case. In octadecylamine caproate, caprylate and capriate, no solubilization was observed even at the concentrations 0.055, 0.040 and 0.077 mol./*l*., respectively. The measurements on laurate, myristate and palmitate of dodecylamine as well as on those of octadecylamine were impossible because of their limited solubility in benzene. The acid amides, i.e. the reaction products at higher temperature, showed no solubilization at comparable concentrations, corresponding to the slight variance of the van't Hoff factor.

The amount of solubilized water was found to be proportional to the concentration of detergents except for the higher concentration range of dodecylamine propionate. In the concentration range 0.005 – 0.4 mol./*l*. the relation can be expressed by the formula

$$S=\alpha(C-\beta)$$

where, S=amount of solubilized water, mol./*l*.,
C=concentration of detergents, mol./*l*.,
α, β=constants.

The values of α and β are given in Table II.

TABLE II
VALUES OF α AND β

Detergent	α	β(mol./*l*.)
Dodecylamine propionate	7.2	0.002
" butylate	4.6	0.012
" caproate	2.9	0.020
" caprylate	2.8	0.030
" capriate	2.9	0.035
Octadecylamine propionate	12	0.005
" butylate	9.0	0.028
" caproate	—	>0.055
" caprylate	—	>0.040
" capriate	—	>0.070

The value of α is taken as a measure of solubilizing power, i.e. the number of moles of water which is solubilized per one mole of a detergent. The value of β gives the critical micelle concentration which is obtained from the measurement of the solubilization of water.

From the curve of Fig. 1 a critical concentration of micelle formation cannot be sharply recognized. But it is seen from the comparison between the values of β and Fig. 1 that the value of the critical micelle concentration from the data of solubilization (the value of β) is within the steep range of decreasing in the curve. The vertical lines of Fig. 1 show the values of β, the unit of concentration being corrected. It will be, therefore, concluded that the idea of micelle formation which is suggested from the cryoscopical experiment is not in conflict with that of micelle formation from solubilization.

It is seen from Table II that the critical micelle concentration increases with the chain length of the acid part as well as of the amine part and that the small critical micelle concentration corresponds to the great solubilizing power. The relation between the critical micelle concentration and the chain length is entirely different from the cases of aqueous solutions. Accordingly, the mechanism of the micelle formation in the benzene solution seems to be quite different from that in the aqueous solution.

The author wishes to express his thanks to Prof. H. Akamatsu for his suggestions.

Summary

Fatty acid salts of higher aliphatic amines were prepared and used as detergents. The micelle formation in the benzene solution was verified from the relation between the van't Hoff factor and the concentration. It was shown that the amount of solubilized

water is proportional to the concentration of the detergent. The value of the critical micelle concentration was determined from the extraporation of the proportionality. This value is within the region of the remarkable decrease in the curve between the van't Hoff factor and the concentration. With the increases of the carbon number of the amine or the acid part, the critical micelle concentration increases and the solubilizing power decreases. This result is quite different from that of aqueous solutions.

Department of Chemistry, Faculty of Science, Tōhō University, Chiba

---

Lower Electronic States of the Free NH_2 *Radical*[1]

By Jiro HIGUCHI

(Received October 20, 1954)

Introduction

Free radicals like CH_2, CH_3, NH_2 and others have been assumed to be intermediates in many chemical reactions, but their existence has not definitely been identified. Recently, the flash technique was applied to the spectroscopy by Porter[2], and the existence of some free radicals has been identified. For such polyatomic free radicals, however, only limited information should be expected about the electronic states and the structures, because at present many levels have not yet been identified experimentally even for stable molecules. Thus, it is very difficult to determine the course of such reactions as photolysis or electric discharge, in which the role of electronic excited states is of great significance. The theoretical interpretation is, therefore, very important not only as a supplement to observation but as the discussion of chemical reaction, in which such a radical is assumed to exist as an intermediate.

The so-called α band of ammonia has long been known from emission spectra of oxy-ammonia flames and electric discharges through ammonia,[3] and has long been suspected of being due to the free NH_2 radical. Recently, Herzberg and Ramsay[4] observed the α bands in absorption in photodecomposed ammonia by using a flash technique and confirmed the fact that the free NH_2 radical is responsible for the α band. Little, has, however, been done on the theoretical interpretation.

Thus, the lower electronic states and the structure of the free NH_2 radical are theoretically investigated in the present work. The method used is the LCAO-SCF one developed by Roothaan[5] and the SCF calculation is performed for the ground state only. The energy levels of the lower excited states are computed by use of the ground state MO's without configuration interaction, because some reasonable results have been obtained on the CH radical in a similar way[6] and such reliable results may also be expected here if reasonable values of energy integrals can be used.

Outline of Calculation

The calculation was performed by assuming the spatial configuration of the NH_2 radical as an isosceles triangle, and taking the x and y axes in the molecular plane and the z axis being perpendicular to the plane as shown in Fig. 1. The internuclear distance between the nitrogen and the hydrogen was

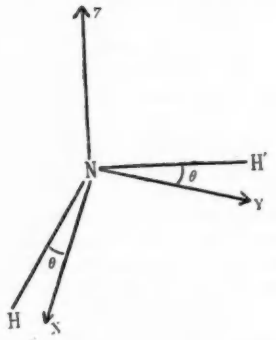

Fig. 1. Axes for the NH_2 radical.

1) A preliminary account of the present paper was given in *J. Chem. Phys.*, **22**, 1467 (1954).
2) G. Porter, *Proc. Roy. Soc.* (*London*), **A200**, 284 (1950).
3) W. B. Rimmer, *Proc. Roy. Soc.* (*London*), **A103**, 696 (1923); F. Fowler and J.S. Badami, *Proc. Roy. Soc.* (*London*), **A133**, 325 (1931); A. G. Gaydon, *Proc. Roy. Soc.* (*London*), **A181**, 197 (1942).
4) G. Herzberg and D.A. Ramsay, *J. Chem. Phys.*, **20**, 347 (1952); *Discussion Faraday Soc.*, No. 14, 11 (1952).
5) C.C.J. Roothaan, *Rev. Mod. Phys.*, **23**, 69 (1951).
6) J. Higuchi, *J. Chem. Phys.*, **22**, 1339 (1954).

taken as 1.01 Å as in the equilibrium distance of the ammonia molecule[7].

NH_2 is a nine-electron radical, and the LCAO-SCF calculation was carried out by taking the seven atomic orbitals n, s, x, y, z, h and h' into consideration, which mean $1s$, $2s$, $2px$, $2py$, $2pz$ orbitals of nitrogen atom, $1s$ of one hydrogen (the side of the x axis) and $1s$ of the other hydrogen, respectively. The interactions between all electrons were explicitly included but the orthogonality between n and h or h' was assumed, because its overlap integral is fairly small in comparison with the others[8].

The atomic orbitals used were the Hartree-Fock SCF AO's in the ^4S state of nitrogen[9] and in the ^2S state of hydrogen. The majority of the two-center integrals is, however, very difficult to calculate, and it was, therefore, assumed that the use of Slater AO's[10] instead of the SCF AO's gives satisfactory approximations of the two-center integrals, and they were taken from the table by Kotani and Amemiya.[11] The core-field energies were, however, obtained from the Fock equations of the ^4S state of nitrogen atom as in the case of the CH radical[5]. The one-electron three-center integrals for the nitrogen-hydrogen type were calculated by following Oohata's method[12], but for the hydrogen-hydrogen type were taken from the table by Hirschfelder and Weygandt[13], while the two-electron integrals were approximately obtained by modifying Mulliken's approximation[14].

7) H. Sponer, "Molekülspektren I. Tabellen", Verlag Julius Springer Berlin, (1935) p. 80.

8) $S_{nh}=0.0678$, while $S_{sh}=0.5601$ and $S_{\sigma h}=0.4187$.

9) D. R. Hartree and W. Hartree, *Proc. Roy. Soc.* (*London*), **A193**, 299 (1948).

10) $n=(\delta^6/\pi)^{1/2}r\exp(-\delta r)$, $s=(\xi^5/3\pi)^{1/2}r\exp(-\delta r)$, $\sigma=(\delta^5/\pi)^{1/2}r\exp(-\delta r)\cos\theta$, $\pi=(\delta^5/\pi)^{1/2}r\exp(-\delta r)\sin\theta\begin{Bmatrix}\cos\phi\\ \sin\phi\end{Bmatrix}$ and $h=(1/\pi)^{1/2}\exp(-r)$. In the present paper, δ and δ' are chosen as 1.90 and 6.757, respectively.

11) M. Kotani and A. Amemiya, *Proc. Phys. Math. Soc. Japan*, **22**, Extra No. 1 (1940).

12) K. Oohata, *Busseiron Kenkyu*, **50**, 38 (1952).

13) J.O. Hirschfelder and C.N. Weygandt, *J. Chem. Phys.*, **6**, 806 (1938).

14) R. S. Mulliken, *J. chim. phys.*, **46**, 500 and 521 (1949).

Some values calculated by Mulliken's approximation are rather small as compared with the exact values, for example in the case of the one-electron integrals for the hydrogen-hydrogen type. In the present work, therefore, the two-electron three-center integrals were obtained from the exact value of one-electron three-center integrals as follows:

$(\alpha\beta:\gamma\delta)=(1/4)T_{\alpha\beta}T_{\gamma\delta}[(\alpha\alpha:\gamma\gamma)+(\beta\beta:\gamma\gamma)+(\alpha\alpha:\delta\delta)+(\beta\beta:\delta\delta)]$ where

$T_{\alpha\beta}=2(P_{\gamma\delta}:\alpha\beta)/[(P_{\gamma\delta}:\alpha\alpha)+(P_{\gamma\delta}:\beta\beta)]$.

Here the $P_{\gamma\delta}$ is the point which was found by maximizing the overlapping charge $\chi_\gamma\chi_\delta d\tau$ along the internuclear axis. This approximation gives fairly good results in two-center integrals but somewhat doubtful results from the point of view of physical meaning. It is, therefore, more desirable to use the higher order expansion of atomic orbitals.

LACO MO's ϕ's which are formed by these seven atomic orbitals χ_p's were chosen so that they belong in sets to irreducible representations of the symmetry C_{2v} of NH_2, and they are reduced to[15]

$$\begin{aligned}
K(a_1)&=n\\
1a_1&=a_{11}(s)+a_{12}(x+y)+a_{13}(h+h')\\
2a_1&=a_{21}(s)+a_{22}(x+y)+a_{23}(h+h')\\
3a_1&=a_{31}(s)+a_{32}(x+y)+a_{33}(h+h')\\
1b_1&=z\\
1b_2&=a_{44}(x-y)+a_{45}(h-h')\\
2b_2&=a_{54}(x-y)+a_{55}(h-h')
\end{aligned}\qquad(1)$$

Here the order of increasing number for the MO's within each symmetry species is the order of increasing energy. The coefficients a_{tp}'s of atomic orbitals χ_p's were chosen to satisfy the orthonormality conditions:

$$\int\bar{\phi}_t{}^\nu\phi_j{}^\nu d\tau^\nu=\sum_{p,q}\bar{a}_{tp}S_{pq}a_{jq}=\delta_{tj},\qquad(2)$$

where the overlap integrals S_{pq}'s are defined by

$$S_{pq}=\overline{S}_{qp}=\int\bar{\chi}_p\chi_q d\tau.\qquad(3)$$

The electronic structure of the $^2B_1$ state, which has been considered to be the ground state of the NH_2 radical, is given as resulting from configuration $(1a_1)^2(1b_2)^2(2a_1)^2(1b_1)^1$, and the total nine electron normalized wave function Φ for this state is then built up as an antisymmetrized product of these LCAO MO's and the energy of this state is given by

$$E=\int\bar{\Phi}\mathfrak{H}\Phi d\tau.\qquad(4)$$

where

$$\mathfrak{H}=\sum_{\mu=1}^{9}\left(-\frac{1}{2}\Delta_\nu-\frac{7}{r_{N\nu}}-\frac{1}{r_{H\nu}}-\frac{1}{r_{H'\nu}}\right)+\frac{1}{2}\sum_{\substack{(\mu,\nu=1)\\ \mu\neq\nu}}^{9}\frac{1}{r^{\mu\nu}}\qquad(5)$$

Introducing the notations

$$H_t=\int\bar{\phi}_t{}^\nu\left(-\frac{1}{2}\Delta_\nu-\frac{7}{r_{N\nu}}-\frac{1}{r_{H\nu}}-\frac{1}{r_{H'\nu}}\right)\psi_t{}^\nu d\tau^\nu\qquad(6)$$

$$J_{tj}=\int\bar{\phi}_t{}^\mu\bar{\phi}_j{}^\nu\frac{1}{r^{\mu\nu}}\phi_t{}^\mu\phi_j{}^\nu d\tau^{\mu\nu}\qquad(7)$$

$$K_{tj}=\int\bar{\phi}_t{}^\mu\bar{\phi}_j{}^\nu\frac{1}{r^{\mu\nu}}\varphi_j{}^\mu\phi_t{}^\nu d\tau^{\mu\nu}\qquad(8)$$

and

$$H'_t=H_t+2J_{ns}-K_{ns},\qquad(6')$$

one obtains

$$\begin{aligned}
E=&2H_n+J_{nn}+2H'_{1a_1}+2H'_{1b_2}+2H'_{2a_1}\\
&+H'_{1b_1}+J_{1a_11a_1}+4J_{1a_11b_2}-2K_{1a_11b_2}\\
&+4J_{1a_12a_1}-2K_{1a_12a_1}+2J_{1a_11b_1}-K_{1a_11b_1}\\
&+J_{1b_21b_2}+4J_{1b_22a_1}-2K_{1b_22a_1}+2J_{1b_21b_1}\\
&-K_{1b_21b_1}+J_{2a_12a_1}+2J_{2a_11b_1}-K_{2a_11b_1}.
\end{aligned}\qquad(9)$$

15) In the present work, the choice of the symmetry axis is made according to Mulliken.

To obtain the $1a_1$, $1b_2$ and $2a_1$ orbitals, a variational procedure was carried out for the energy of state (4), subject to the orthonormality conditions of the MO's (1). It can be shown that this variational process leads to the following equation

$$(\boldsymbol{H}'+\boldsymbol{G})\boldsymbol{a}_i=\epsilon_{ii}\boldsymbol{S}\boldsymbol{a}_i. \tag{10}$$

Here the column vectors $\boldsymbol{a}_i$'s give the coefficients of the AO's in the ia_1 and ib_2 orbitals. $\boldsymbol{S}$ is a hermitian matrix with elements given by (3); $\boldsymbol{H}'$ is the core-field energy matrix with elements

$$H'_{pq}=\bar{H}'_{qp}=\int\chi_p^{\nu}\left(-\frac{1}{2}\Delta_{\nu}-\frac{7}{r_{N\nu}}-\frac{1}{r_{H\nu}}-\frac{1}{r_{H'\nu}}\right)\chi_q^{\nu}d\tau^{\nu}+2(pq:nn)-(pn:nq), \tag{11}$$

where

$$(pq:rt)=\int\bar{\varphi}_p^{\mu}\bar{\varphi}_r^{\nu}\frac{1}{r^{\mu\nu}}\varphi_q^{\mu}\varphi_t^{\nu}d\tau^{\mu\nu}.^{16)} \tag{12}$$

$\boldsymbol{G}$ is the electronic interaction matrix with elements

$$\begin{aligned}G_{pq}=\bar{G}_{qp}=&2(pq:1a_11a_1)-(p1a_1:1a_1q)\\&+2(pq:1b_21b_2)-(p1b_2:1b_2q)\\&+2(pq:2a_12a_1)-(p2a_1:2a_1q)\\&+(pq:1b_11\bar{b}_1)-(1/2)(p1b_1:1b_1q).\end{aligned} \tag{13}$$

The procedure followed in the calculation is to assume values of $\boldsymbol{a}_i$'s in (1) consistent with the orthonormality conditions (2), compute the G_{pq}'s by (13), solve Eq. (10) for ϵ_{ii} and a new set $\boldsymbol{a}_i$'s and repeat until self-consistency is attained.

LCAO MO's

The LCAO MO's of the lowest energy of the $^2B_1$ state by the SCF procedure are given in Table I, and the orbital energies are

TABLE I

LCAO-SCF MO'S FOR THE $^2B_1$ STATE

$K(a_1)=n$

$$1a_1=\begin{pmatrix}0.762\\0.759\\0.753\\0.742\\0.737\end{pmatrix}(s)+\begin{pmatrix}0.151\\0.132\\0.112\\0.067\\0.000\end{pmatrix}(x+y)+\begin{pmatrix}0.156\\0.166\\0.179\\0.200\\0.211\end{pmatrix}(h+h')$$

$$2a_1=-\begin{pmatrix}0.618\\0.578\\0.531\\0.355\\0.000\end{pmatrix}(s)+\begin{pmatrix}0.533\\0.561\\0.590\\0.661\\0.707\end{pmatrix}(x+y)+\begin{pmatrix}0.245\\0.237\\0.227\\0.159\\0.000\end{pmatrix}(h+h')$$

$$3a_1=\begin{pmatrix}1.031\\1.075\\1.111\\1.183\\1.235\end{pmatrix}(s)+\begin{pmatrix}0.580\\0.527\\0.464\\0.281\\0.000\end{pmatrix}(x+y)-\begin{pmatrix}0.856\\0.875\\0.883\\0.891\\0.898\end{pmatrix}(h+h')$$

$1b_1=z$

$$1b_2=\begin{pmatrix}0.397\\0.389\\0.386\\0.385\\0.392\end{pmatrix}(x-y)+\begin{pmatrix}0.532\\0.503\\0.479\\0.449\\0.431\end{pmatrix}(h-h')$$

$$2b_2=\begin{pmatrix}0.746\\0.777\\0.805\\0.851\\0.866\end{pmatrix}(x-y)+\begin{pmatrix}0.968\\0.949\\0.948\\0.967\\0.983\end{pmatrix}(h-h')$$

at the bond angle of $\begin{pmatrix}90^\circ\\115^\circ\\120^\circ\\150^\circ\\180^\circ\end{pmatrix}$, respectively.

plotted in Fig. 2. These LCAO MO's are

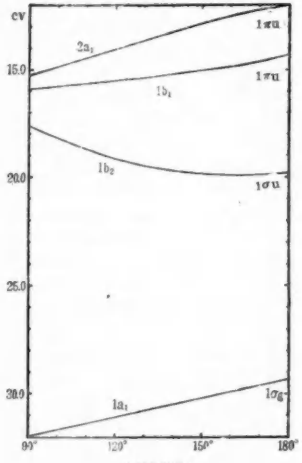

Fig. 2. Ionization energies for the $^2B_1$ state of the NH_2 radical. The value for the linear form are given as the extrapolated one from the non-linear form.

considered to be reasonable for that state, and their electronic properties can be regarded as corresponding to those of H_2O by Ellison and Shull[17] and by Maeda[18], which are also calculated by the LCAO-SCF method, because the NH_2 and H_2O are molecules belonging to the same symmetry group C_{2v}. That is, the $1a_1$ orbital indicates strong bonding property, for the coefficient of s is much larger than the others, but $2a_1$ orbital is weakly bonding due to strong s-p mixing in the nitrogen orbitals of the MO at the bond angle near the equilibrium point. Such natures of the σ orbitals discussed in the case of the CH radical[6] are considered to be quite similar to those of the a_1 orbitals in

16) Orbitals φ_p's mean either AO's χ_p's or MO's ϕ_p's.

17) F. O. Ellison and H. Shull, *J. Chem. Phys.*, 21, 1420 (1953).

18) S. Maeda, *Busseiron Kenkyu*, 70, 101 (1954).

this case. That is, the a_1 (or σ) orbital of the lowest energy except the inner shell is strongly bonding but the a_1 (or σ) orbitals of higher energies are weakly bonding.

It is seen that the coefficients of $x-y$ in the $1b_2$ orbitals are almost independent of the bond angle, while others are not. On the other hand, the hybridized orbitals used in the electron pair bond theory[19] are written as follows:

$$\begin{aligned}\psi_1 &= (1/2)^{1/2}(s)\cos\alpha - (1/2)(x+y)\sin\alpha \\ &\quad + (1/2)(x-y) \\ \psi_2 &= (1/2)^{1/2}(s)\cos\alpha - (1/2)(x+y)\sin\alpha \\ &\quad - (1/2)(x-y) \\ \psi_3 &= (s)\sin\alpha + (1/2)^{1/2}(x+y)\cos\alpha\end{aligned} \tag{14}$$

where

$$\sin\alpha = (1-\tan\theta')/(1+\tan\theta') \tag{15}$$

and ψ_1 and ψ_2 are equivalent orbitals with their charge clouds extending along two straight lines which make an angle θ' with the x- and y-axis, respectively. In these orbitals (14), the coefficients of $x-y$ are also independent of the bond angle or the angle between the directions of their charge clouds. It is of interest to see that the LCAO-SCF calculation comes to the same conclusion for the coefficient of $x-y$ as the electron pair bond theory.

The localized symmetry orbitals of the NH_2 radical can be obtained by a unitary transformation of the two of the a_1 orbitals as shown by Pople[20] in the case of H_2O, and they are given in Table II. In these orbitals, $1a_1'$ and $2a_1'$ may be said to represent the a_1 lone pair and the a_1 bonding orbital, respectively. It is evident that the lone pair orbital $1a_1'$ has mainly s character, especially at the bond angle of 90°, but has not a perfect s character as it has in the electron pair bond theory, and the relationship between the coefficients of s and $x+y$ is also complicated. This may be due to the influence of ionic character.

TABLE II

LOCALIZED SYMMETRY ORBITALS FOR THE $^2B_1$ STATE

$K(a_1)=n$

$$1a_1' = \begin{pmatrix}0.975\\0.953\\0.920\\0.740\\0.000\end{pmatrix}(s) - \begin{pmatrix}0.159\\0.214\\0.277\\0.476\\0.707\end{pmatrix}(x+y)$$

$$2a_1' = \begin{pmatrix}-0.113\\-0.038\\+0.049\\+0.360\\+0.737\end{pmatrix}(s) + \begin{pmatrix}0.531\\0.535\\0.533\\0.464\\0.000\end{pmatrix}(x+y) + \begin{pmatrix}0.290\\0.290\\0.289\\0.256\\0.211\end{pmatrix}(h+h')$$

$1b_1=z$

$$1b_2 = \begin{pmatrix}0.397\\0.389\\0.386\\0.385\\0.392\end{pmatrix}(x-y) + \begin{pmatrix}0.532\\0.503\\0.479\\0.449\\0.431\end{pmatrix}(h-h')$$

at the bond angle of $\begin{pmatrix}90°\\115°\\120°\\150°\\180°\end{pmatrix}$, respectively.

The "LCAO orbital energies" represent good approximation to the ionization energies of corresponding electron shells. In the present work, the calculated value of $2a_1$ orbital is 14.4 ev which is the minimum ionization energy at the equilibrium bond angle for the $^2B_1$ state. This value approximately corresponds to the removal of an electron from $2a_1$ orbital, but it is somewhat higher than the observed one of 11.05 ev.[21]

In spite of the fact that both the $2a_1$ and $1b_1$ orbitals turn into the $1\pi_u$ orbital in the linear form, the ionization energy of $2a_1$ is lower than that of $1b_1$, and neither value shows the same value at the bond angle of 180° in Fig. 2. This is due to the fact that the NH_2 radical has an unpaired electron: the $2a_1$ orbital is filled by two electrons with paired spins while the $1b_1$ has only one electron, and further the electronic repulsion in the former is stronger than in the latter. In view of these facts, the ground state of the CH_2 radical is probably the $^3B_1$ state, for the energy of the $^1A_1$ state $(1a_1)^2(1b_2)^2(2a_1)^2$ is considered to be higher than that of the B_1 states $(1a_1)^2(1b_2)^2(2a_1)^1(1b_1)^1$ and also the $^3B_1$ state may be the most stable.

Using the LCAO MO's in Table I without configuration interaction, the dipole moment for the corresponding bond angle can be calculated and is shown in Table III. These

TABLE III

DIPOLE MOMENT

Bond angle	90°	105°	120°	150°	180°
Dipole moment D. ($N^-H_2^+$)	1.75	1.32	0.83	−0.14	0.00

values may be rather small but not considered to be unreasonable as compared with the value of the ammonia molecule of 1.40 D.[22] This correspondence may be due to the similarity of electronic structures between the NH_2 radical and the ammonia molecule. But such correspondence does not exist in the relationship between the CH radical and the methane molecule, for there is a consi-

19) For example, see T. Inui and S. Yanagawa, "Group Representation and Atoms and Molecules", Shokabo, Tokyo, (1950) p. 253.

20) J.A. Pople, *J. Chem. Phys.*, **21**, 2234 (1953).

21) J.C. Devins and M. Burton *J. Am. Chem. Soc.*, **76**, 2618 (1954).

22) L.G. Wesson, "Table of Electric Dipole Moments", The Technology Press. Massachusetts Institute of Technology, (1948) p. 2.

derable difference in the electronic structure, that is, the former has lone pair electrons but the electrons in the latter are all bonding[1], and the lone pair electrons make a substantial contribution to the dipole moments[23].

Electronic States and Structures

By using the LCAO MO's given in Table I, the energies of the lower electronic states were calculated without configuration interaction, and are shown in Fig. 3. They may

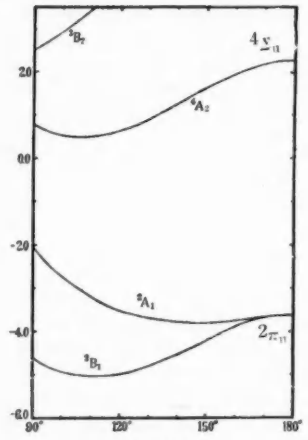

Fig. 3. Lower electronic states of the free NH_2 radical (without configuration interaction). The origin of energy is chosen to be $N(^4S)+2H(^2S)$.

be considered to be fairly reasonable, if the good result of the CH radical[1] obtained by the similar procedure is referred to. The electronic configurations of these states are as follows:

$^2B_1$: $K(1a_1)^2(1b_2)^2(2a_1)^2(1b_1)^1$
$^2A_1$: $K(1a_1)^2(1b_2)^2(2a_1)^1(1b_1)^2$
$^4A_2$: $K(1a_1)^2(1b_2)^2(2a_1)^1(1b_1)^1(2b_2)^1$
$^2B_2$: $K(1a_1)^2(1b_2)^1(2a_1)^2(1b_1)^2$.

Herzberg[24] showed that, in the upper state of the α bands, the bond angle is fairly large and possibly 180° while, in the lower state, it has an intermediate value. According to Luft's estimation,[25] the equilibrium bond angles of the lower and the upper state are 110° and 135–160°, respectively. These results are very close to the values of the present calculation for the $^2B_1$ and the $^2A_1$ state. The calculated value of a $^2B_1 \rightarrow {}^2A_1$ transition (1.8 ev) is also in fairly good agreement with the experimental result, which was observed in absorption spectrum in the region of 4500–7400 Å. In view of these facts, the present calculation may be said to give the theoretical interpretation of the α bands as follows: this spectrum is due to the free NH_2 radical, and the upper and the lower states are the $^2A_1$ and the $^2B_1$ state, respectively.

The calculated $^2B_2$ state was, however, higher than that predicted by Mulliken[4]. This is mainly due to the facts that the present calculation ignores configuration interaction and that the variational procedure is carried out for the $^2B_1$ state only. Especially, the second $^2B_2$ state $K(1a_1)^2(1b_2)^2(2a_1)^2(2b_2)^1$ is very close to the lowest $^2B_2$ state, and then the effect of configuration interaction may not be disregarded.

In the previous section, the similarity of electronic structures for the nitrogen atoms in the NH_2 radical and in the ammonia molecule has been discussed from the point of view of dipole moment. Besides this, such similarity can be deduced from their structures, that is, the tetrahedral structure of bond angle is almost perfectly preserved in the ground state of the NH_2 radical as in the ammonia molecule. On the other hand, the HCO angle of the HCO radical is also scarcely changed from that of the formaldehyde molecule in the photochemical reaction,[27] and this may be also due to the preservation of the electronic structure for the carbon atom. In view of these facts, the bond angle of the ground state may scarcely be changed in such reactions due to the preservation of electronic structure for the atom whose bond is ruptured. In the excited states, however, such property is not preserved in the case of the NH_2 radical and of the HCO radical. The analogous relationship between the ground and the excited state can be seen in molecules such as HCN[27], C_2H_2[28] and others, in which the linear form is not preserved in the excitation of an electron from the bonding orbital to the non- or anti-bonding orbital.

The results in the present work are, however, qualitatively satisfying, but can not be conclusive because of the method used, the approximate values in the many-center integrals and the ignorance of configuration interaction. It may be desiable to investigate these points more accurately, though they, in part, have been discussed by the present author in his calculation of CH[1].

23) A. B. F. Duncan and J. A. Pople, *Trans. Faraday Soc.*, **49**, 217 (1953).
24) G. Herzberg, private communication.
25) N.W. Luft, *Discussion Faraday Soc.*, No. 14, 114 (1952).
26) D.A. Ramsay, *J. Chem. Phys.*, **21**, 960 (1953).
27) G. Herzberg and K.K. Innes, to be published.
28) C. W. King and C. K. Ingold, *Nature*, **169**, 1101 (1952); K. K. Innes, *J. Chem. Phys.*, **22**, 863 (1954).

Summary

LCAO MO's and ionization potentials have been calculated for the $^2B_1$ state of the free NH_2 radical by using the LCAO-SCF method. The interactions of all electrons have been explicitly considered, but the orthogonal relationship between the 1*s* orbitals of nitrogen and hydrogen was assumed. Using these MO's the lower electronic states have also been investigated without configuration interaction. The calculated value of a $^2B_1 \rightarrow {}^2A_1$ transition is 1.8 ev in fairly good agreement with the observed one of the α bands of ammonia in the region of 4500 to 7400 Å. The calculated bond angles of the $^2B_1$ and the $^2A_1$ state are about 110° and 150°, respectively. These results are in good agreement with the observation and the opinion by Herzberg and Ramsay and the estimation by Luft.

The author wishes to thank Dr. S. Shida for his helpful advice and encouragement, Dr. K. Niira for his useful suggestions and Mr. S. Maeda and Mr. K. Oohata for their kind discussion and permission to use the unpublished data on the auxiliary function of the three-center integrals. He also expresses his thanks to Dr. G. Herzberg for his kind communication.

Laboratory of Physical Chemistry,
Tokyo Institute of Technology,
Tokyo

Grain Growth of Silver Chloride Suspensions in Polyvinyl Alcohol

By Yasushi Ohyama and Kiyoshi Futaki

(Received December 6, 1954)

Introduction

Aqueous suspensions of silver chloride in the presence of protective colloid such as gelatin are usually called emulsion in photography. It is well known that grains of silver halide formed by mixing silver nitrate solution with alkali halide solution quickly coagulate and precipitate when the protective colloid is absent. In the aqueous solution of gelatin, not only is this coagulation or precipitation inhibited, but the grain growth is also retarded. The grain-growth, however, is not so completely inhibited as in polyvinyl alcohol described later, but is smooth enough to fulfil the requirements of emulsion-making in the photographic industry.

On the contrary silver halide emulsions prepared with polyvinyl alcohol as protective colloid consist of very fine grains not exceeding 0.1 μ and 0.05 μ in diameter for bromide and chloride respectively. They scarcely grow by the prolonged ripening at rather high temperature, because the grain-growth is inhibited by its extraordinarily strong adsorption to the silver halide grain and the lack of active substances ordinarily found in gelatin. The function of these active substances is to accelerate the grain-growth. In the following, the role of these substances is disscussed.

The author reported previously[1] that it becomes very turbid as soon as traces of some sulfur-containing substances are added to the suspension, and this increase in turbidity is the evidence of grain growth in the suspension. This was confirmed by the electron micrograph. The amount of addition necessary to produce the increase of turbidity (i.e. the growth of grains) differs very widely from one to another. This grain-growth can easily be traced by the nephelometric method, and can be described as functions of time and temperature of ripening and amounts of active substances added. Substances tested and reported in the previous paper are limited only in some sorts of sulfur-containing compounds known as chemical sensitizers in photography, e.g. thiosinamine, thiosulphates, rhodanine, the N-alkyl-thiones of Kendall[2] and their derivatives. These substances, however, with few exceptions, produce heavy fog during ripening from lack of stability of the complex compounds with silver halide.

In this paper the author will present some other types of active substances, much more important for the investigation of physical

1) Y. Ohyama, Royal Photographic Society Centenary Conference, London, Sept. (1953) (Proceeding is now in press).

2) J. D. Kendall, 9th Internat. Congress of Phot., Paris, 235 (1935).

ripening of photographic emulsion and for the understanding of the role of gelatine. They do not produce fog but increase stability of the emulsion in many cases. Compounds now investigated include a large number of substances not containing active sulfur, e.g. N-alkyl homologues of guanidine, pyrrolidone, pyridone, quinolone, 2-iminobenzothiazoline, etc. High molecular compounds such as polyvinyl pyrrolidone or albumin have also been tested and their activities are confirmed.

Experimental

The grain-growth can be traced by the nephelometric method as was previously reported[1], because in the region of the sizes in question (between 0.05 μ and 0.25 μ in diameter) it was confirmed by Evva[3] and Ammann-Brass[4] that the increase of turbidity of the suspension is in linear proportion to the mean graindiameter. To 12 ml. of aqueous solutions of active substances with varying concentration (10 ml. of this solution may be replaced by alcohol if needed for substances sparingly soluble in water), 10 ml. of 6% solution of polyvinyl alcohol and 4 ml. of 0.6 M NaCl solution are added. The mixture is heated to 70°C, and 4 ml. of 0.2 M silver nitrate solution (70°C) is added in 15 seconds. After drawing out 2 ml. of this suspension of AgCl at 2, 4, 8 and 16 min. after the addition of silver ions, it is diluted with 20 ml. of cold water and the turbidity is measured. This is done by measuring the intensity of a parallel light beam which passes through a glass cuvette (1 cm. depth) containing the diluted suspension with the aid of a photocell at two points: just behind the cuvette and 20 cm away from it. Afterwards this rather complicated method was replaced by a simple measurement of optical absporption and this is designated as the transmission method.

In the previous report[1], dealing with sulfur-containing chemical sensitizers, the addition of active substances was effected after the emulsification (formation of fine suspension of silver chloride) was accomplished. In this report, however, the addition was effected before the emulsification except for the case specially cited. Usually this has no influence upon the turbidity obtained at the same period of ripening and also the activity of the substance used is identical. The new method is very convenient for the experiments at high concentration and particularly suitable for a thermally coagulating substance such as albumin.

3) F. Evva, *Z. wiss. Phot.* **47**, 39, (1952).

4) H. Ammann-Brass, *Sci. et Ind. Phot.*, [2], **23**, 249, (1952).

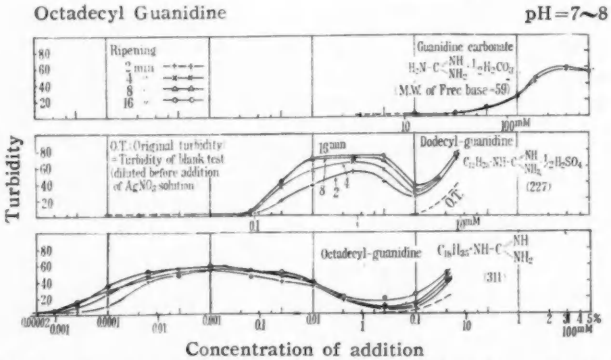

Fig. 1. Ripening characteristics of guanidine derivatives (Part. 1).

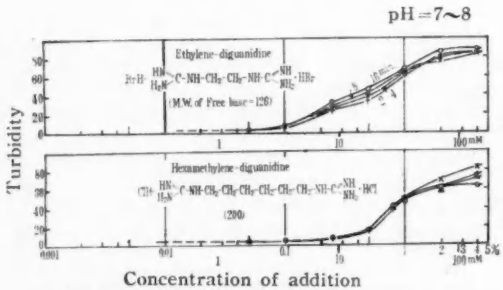

Fig. 2. Ripening characteristics of guanidine derivatives (Part. 2).

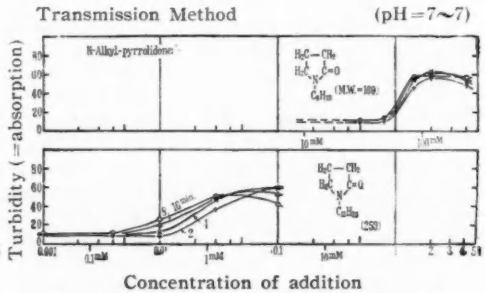

Fig. 3. Ripening characteristics of pyrrolidones.

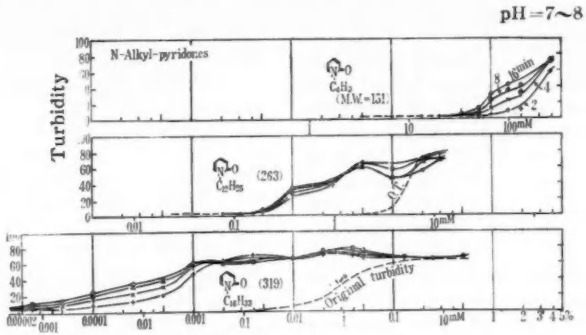

Fig. 4. Ripening characteristics of pyridones.

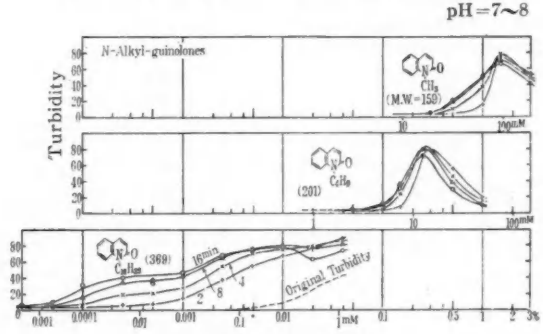

Fig. 5. Ripening characteristics of quinolones.

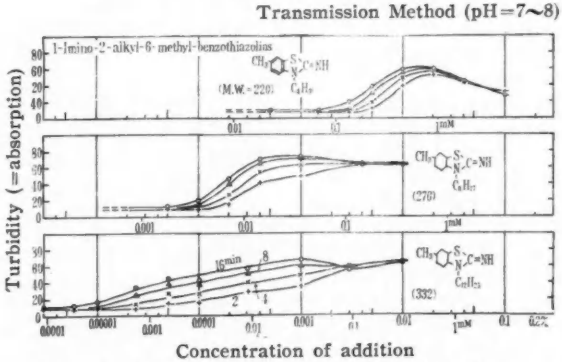

Fig. 6. Ripening characteristics of 2-imino-thiazolines.

Results and Discussion

(a) **Ripening Characteristics.**—If turbidity is plotted against the concentration (on logarithmic scale) of added substance in the emulsion, taking ripening (or heating) time as parameter, characteristic curves of many substances are obtained. Using these diagrams, comparisons of their activities and also ripening characteristics at various concentrations are easily recognizable at a glance. Fig. 1, and Fig. 2 show some examples of these characteristic curves of the guanidine series. Fig. 3, 4, 5 and 6 are those of pyrrolidone, pyridone, quinolone and 2-imino-thiazoline series respectively.

(b) **Activity and its Dependance on Molecular Weight.**—Activity defined as the reciprocal of the minimum addition concentration (in milli mol.) which causes definite

turbidity-increase is valuable for the comparison of the activities of many substances and can also be used for the determination of the relation between activity and the molecular weight or the chemical constitution of active substances. The choice of the comparison point may be optional, turbidity increase of 2, 10, 20 or 40 units (or absorption of 15, 20, 30 or 40% for transmission method) are convenient and usually 10 unit increase (or absorption of 20%) was preferred.

Fig. 7, 8 and 9 show the relation between activities and molecular weights of N-alkyl homologues of the above mentioned substances. Symbols of G, PQ and IT represent guanidine, pyridone (and also pyrrolidone) quinolone and 2-imino-thiazoline series respectively. It is very astonishing to know that activities in these several series of

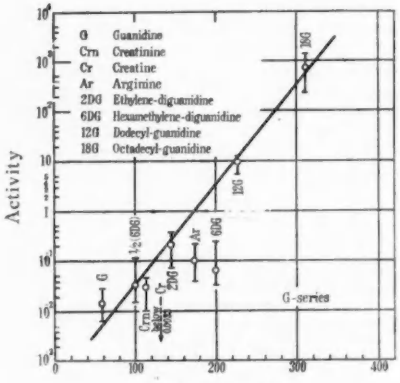

Fig. 7. Relation between activities and molecular weight of guanidine series.

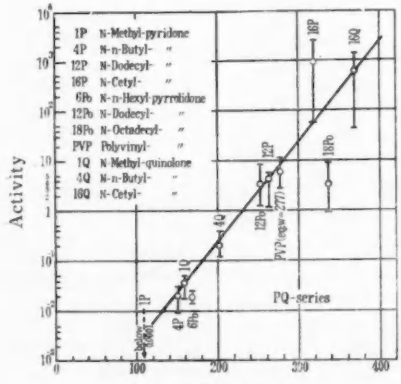

Fig. 8. Relation between activities and molecular weight of pyrrolidone, pyridone and quinolone series.

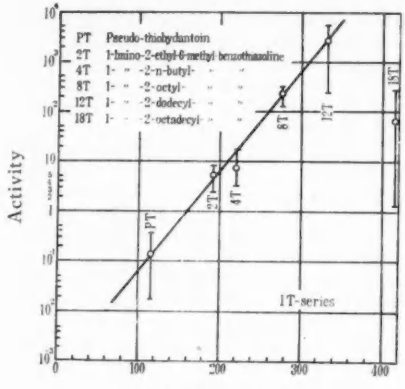

Fig. 9. Relation between activities and molecular weight of imino-thiazoline series.

substances increase markedly with increasing molecular weight by introducing alkyl radicals of increasing numbers of carbon atoms. The relation between activity (A) and molecular weight (M) can be expressed approximately in the following equation,

$$\log_{10} A = \frac{M}{50} - \alpha$$

where α is constant in each series. The equation states that the increase in molecular weight by 50 enhances the activity 10 times in each series of substances. It is varied as far as the molecular weight reaches 300–400.

(c) **General Constitution of Active Substances.**—The above mentioned active substances have the following general chemical constitution,

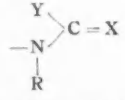

where X is O or NH and Y is $-NH_2$, $-NH-$, $-N=$, $-CH=CH-$, $-CH_2-CH_2-$, $-O-$, $-S-$, or radicals constituting heterocyclic ring with N atom adjacent to central carbon atom. R is alkyl, aryl or aralkyl radical usually up to 20 carbon atoms. It is interesting to recall here that sulfur containing active substances previously reported by the author[1], with few exceptions have chemical constitution in accord with this general structure if X is taken as S, for example thioacetanilide, isothiocyanates, thiourea derivatives, rhodanines or the N-alkyl thiones of Kendall[2].

Of course, there are many active substances which do not coincide with the above mentioned general constitution such as thiosulphates, xanthates, alkylamines, heterocyclic amines or many thiol compounds. Some of them were reported already[1] and others will be reported in another paper.

(d) **Polyfunctional Derivatives and Effective Molecular Weight.**—As is shown in Fig. 7, the activity and molecular weight relation for hexamethylene-diguanidine is irregular whereas ethylene-diguanidine is regular, and if the molecular weight of hexamethylene-diguanidine is divided by 2, the position of the substance falls just on the line and we are able to conclude that the effective equivalent weight of hexamethylene-diguanidine is one half of its real molecular weight.

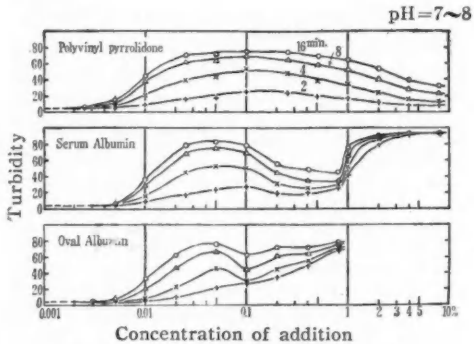

Fig. 10. Ripening characteristics of albumins and polyvinyl-pyrrolidone.

It supports the assumption that hexamethylene-diguanidine adsorbs, on the surface of silver chloride particles, by both active functional ends, whereas ethylene-diguanidine cannot bend enough, because of the shorter chain length. Polyvinyl-pyrrolidone is also active and is almost 10 times as powerful as ordinary active gelatine, and the grain-growth of silver chloride suspension in the mixture with polyvinyl-alcohol is very smooth and rapid as in a gelatinous solution (usual photographic emulsion). The ripening characteristic curve is shown in Fig. 10 and it is possible to estimate the effective equivalent weight of polyvinyl-pyrrolidone from the relation between activity and molecular weight of pyrrolidone derivatives (Fig. 8). The figure obtained is about 277* and it means that every one, two or three pyrrolidone radicals in this long chain molecule** adsorb to the surface of silver chloride. It is interesting to notice that ripening characteristic curves of oval and serumalbumin (also shown in Fig. 10) closely resemble that of polyvinyl-pyrrolidone, considering that their chemical constitutions differ so far and the latter may also be used as an artificial substitute for the former in medical application.

(e) **Influence of Carboxyl Group and Amide Linkage.**—Also in Fig. 7 data on some amino acids having guanyl group, such as arginine, creatine and creatinine are shown. Arginine is not so active as is expected from its molecular weight, and creatine is practically inactive (if active, its activity is below 0.003), whereas creatinine is fairly active (a little below the line). This means that the carboxyl group hinder the activity to a great extent and the amide linkage has scarcely any influence on the activity.

Conclusions

(1) Many substances which accelerate the grain growth of silver chloride suspension in polyvinyl-alcohol were found. Most of them are organic compounds having in their molecule at least one sulfur atom or one nitrogen atom. The most simple compounds are mercaptans or amines of the aliphatic or aromatic series.

(2) Many of them are, however, more complicated compounds having general chemical constitutions as follows,

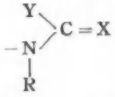

where X is O, NH, or S, and Y is NH_2, $-NH-$, $-N=$, $-CH=CH-$, $-CH_2-CH_2-$, $-O-$, $-S-$ or radicals constituting the heterocyclic ring with N atom adjacent to central C atom. R is alkyl, aryl or aralkyl radical usually up to 20 C atoms (or vinyl radical for polyvinyl compounds).

(3) Their activities, difined as the reciprocal of the minimum added concentration (in milli mol.) which causes definite turbidity increase, differ very widely from one to another, and increase with increasing numbers of C atoms in R of above general constitutions up to about 16–20 atoms.

(4) The relation between activity (A) and molecular-weight (M) can be expressed in the equation.

$$\log_{10} A = \frac{M}{50} - \alpha$$

(5) Activities of polyfunctional compounds fit more reasonably to the above equation

* The sum of atomic weight of one unit vinyl-pyrrolidone is 111 and $277 = {}^1/_2(2\times111+3\times111)$

** The sample used in this experiment is Albigen, which have a molecular weight of about 25,000.

in which molecular weight is replaced by the effective equivalent weight, which is defined as the molecular weight divided by the number of effective functional groups. And from this effective equivalent weight the mode of adsorption of the active substance can be estimated.

(6) Usually at about a molecular weight of 300–400, the activity for acceleration of the grain-growth reaches its maximum, where the grain-growth of AgCl suspension in polyvinyl-alcohol will take place at very low concentration (about 0.0003 mM≒0.00001%) of an active substance.

(7) From these and other evidences, it may be concluded that in most cases acceleration of the grain-growth is optimum when only the surface of grain is partially covered (at least a few %) with active substances, and the remainder of the surface is occupied by the adsorbed layer of polyvinyl-alcohol.

Research Section, Kyoto Factory.
Mitsubishi Paper Mills Co.,
Kyoto

Acetylation of Holocellulose in Fibrous State

By Toshikazu FUJIMURA*

(Received December 27, 1954)

When wood pulp is used as raw-material for cellulose acetate, the effect of pentosan comes into question. In a previous paper, it was reported that pentosan hindered acetylation of holocellulose with acetic anhydride—acetic acid—sulfuric acid system[1]. Because the product is gradually dispersed in that case, acetylation process in acetic anhydride—benzene—sulfuric acid system, which keeps its fibrous state and proceeds layer by layer, seems suitable to be used to disclose the hindering effect of pentosan and the structure of holocellulose. In this paper, the change of acetic acid content with the time of acetylation was compared with the equation, the rate-determining step of which is internal diffusion or surface resistance. The process of acetylation of single fiber was also observed by birefringence, based on the small little birefringence of the acetate. Then, the effect of alkaline refining on acetylation was studied and compared with beech sulfite rayon pulp and Bemberg rayon, which have circular section.

Derivation of Theoretical Rate Equation

The equation which was suggested for the combustion of spherical pyrite particle, was modified for a cylinder of infinite length[2]. It was assumed as follows:

(1) The reaction is so fast that the progress of acetylated layer is controlled by the migration rate of the reagent.

(2) The migration velocity at the surface is proportional to the difference of concentration.

(3) Diffusion in the acetylated layer follows Fick's law.

(4) Steady state is attained in a short time.

(5) The concentration of reagent in the surrounding medium is constant.

From the assumption (4), (2) and (3) respectively, the following relations are established per unit length,

$$2\pi R dm'/dt = 2\pi r dm/dt = 2\pi r'' dm''/dt = -2\pi r'' a(dr''/dt) \quad (1)$$

$$dm'/dt = k(C^* - C') \quad (2)$$

$$dm/dt = D dc/dr \quad (3)$$

where:

a: mass of reagent to react with unit volume of fiber.

R, r'': outer radius, unreacted radius of fiber.

C^*, C', C'': Concentration of reagent in the surrounding medium, at the surface and at the interface of unreacted layer.

m', m'', m: Migrated mass of reagent at the surface, at the interface of unreacted layer and in acetylated layer of radius r.

Rearranging (3) and combining (1) gives

$$Ddc = (dm/dt)dr = -ar''(dr''/dt)dr/r$$

Integrating from r'' to R

$$D(C' - C'') = -\ln(R/r'')ar''(dr''/dt) \quad (4)$$

Combining (2) and (1) yields

$$C' = C^* + ar''(dr''/dt)/kR \quad (5)$$

Combining (5) and (4)

$$(C^* - C'')dt = a\{1/kr + \ln(R/r'')/D\}(r''dr'')$$

Integrating between zero and t

$$(C^* - C'')t = a[(1/2k + R/4D)R - r''^2/2kR + \{r''\ln(R/r'')/2D + r''/4D\}r'']$$

r'' becomes zero when t is T

$$(C^* - C'')T = a(1/2k + R/4D)R$$

i) When surface resistance is rate-determining, $k \ll D$, $t/T = 1 - (r''/R)^2$

---

* Present addres: Kokoku Rayon and Pulp Co. Ltd., Yatsushiro Mill, Kumamoto.

1) T. Fujimura, *J. Chem. Soc. Japan (Ind. Chem. Sec.)*, **56**, 99 (1953).

2) S. Yagi and D. Kunii, *J. Chem. Soc. Japan (Ind. Chem. Sec.)*, **56**, 131 (1953).

ii) When internal diffusion is rate-determining,

$k \gg D$, $t/T = 1-(r''/R)^2\{1-2\ln(r''/R)\}$

When it is converted into acetic acid content,

i) $t/T = 9A/(10-7A)$

ii) $t/T = 1-(10-16A)\{1-\ln(10-16A)+\ln(10-7A)\}/(10-7A)$

Because acetic acid content A is calculated, assuming no volume change by acetylation,

$A = 180\{1-(r''/R)^2\}/[162(r''/R)^2+288\{1-(r''/R)^2\}]$

Then,

$(r''/R)^2 = (10-16A)/(10-7A)$

Materials and Methods

As material, beech wood fiber was selected because of its nearly cylindrical form. Holocellulose was prepared by treating five times with sodium chlorite[3]. Its yield was 81.6% and it contained 33.3% pentosan and 3.45% lignin. The rayon pulp was commercial beech sulfite pulp. Bemberg rayon of 40 denier/30 was used.

Acetylating reagent was prepared by heating acetic anhydride—benzene—sulfuric acid mixture on water bath for two hours to convert into sulfoacetic acid[4]. After the separate samples of material were treated with acetylating reagent in separate flasks dipped in thermostat for various times respectively, they were filtered, washed successively with ethanol, water and again ethanol, and finally air dried.

The alkaline-refining time was five hours and the liquid ratio was 1:40. The refined product was filtered and washed first by aq. alkali of the same concentration and temperature as the treating alkali, then water, 10% acetic acid and again water, and finally air dried.

Acetic acid content was determined by alkaline saponification method. Retardation was measured by quartz-wedge.

Results

1. Holocellulose.—Acetylating conditions and the results are given in Tables I, II, III, IV and V. In the initial stage readily reacting portion is observed. Pretreatment, boiling with acetic acid as well as replacing successively with water and acetic acid, accelerates the reaction. Lowering liquid ratio to 1:50 has no remarkable effect, but in the final stage the acetic acid content is a little decreased. By reducing acetic anhydride or sulfuric acid content, as well as by lowering the temperature, the reaction is retarded. The yield first decreases abruptly

TABLE I

CONDITIONS OF ACETYLATION

Expt. No.	Pre-treating	Temp. °C	Ac_2O	C_5H_5	H_2SO_4	Liquid ratio
F-11	Air drying	30	100	300	1.8	100
F-12	Replacing	30	100	300	1.8	100
F-13	Boiling	30	100	300	1.8	100
F-21	Air drying	30	100	300	1.8	50
F-22	Air drying	30	50	300	0.9	100
F-23	Air drying	30	100	300	0.9	100
F-31	Air drying	45	100	300	1.8	100
F-32	Air drying	15	100	300	1.8	100

TABLE II

CHANGE OF ACETIC ACID CONTENT WITH TIME

Expt. No.	Acetic acid content (%) at time (hr.)								
	½	1	2	4	6	8	15	20	25
F-11	14.4	16.6	20.1	25.4	30.6	34.7	47.7	57.4	62.6
F-12	42.9	44.9	46.8	50 7	55.1	56.5	61.5	—	65.6
F-13	44.5	45.5	47.6	50.6	53.5	57.4	61.6	—	65.2
F-21	13.5	18.3	21.1	—	31.9	36.7	49.0	—	59.1
F-22	14.4	15.5	16.1	20.2	23.1	26.1	33.2	—	43.8
F-23	15 7	17.4	19.7	22.6	27.0	30.2	42.7	47.3	48.9
F-31	21.7	26.2	38.7	43.2	54.2	58.6	64.0	67.2	68.2
F-32	13.4	14.9	15.9	16.6	18.7	19.1	22.5	26.0	29.1

TABLE III

CHANGE OF BIREFRINGENCE WITH TIME

Expt. No.	Birefringence (×1000) at time (hr.)								
	½	1	2	4	6	8	15	20	25
F-11	13.4	14.9	17.9	17.9	—	12.8	8.5	5.4	4.1
F-12	9.5	8.3	5.5	5.4	6.0	5.0	7.3	—	4.7
F-13	4.3	9.0	6.1	6.3	5.5	4.7	3.8	—	3.2
F-21	12.6	14.2	8.2	10.2	7.9	6.3	4.4	—	3.4
F-22	9.6	7.2	7.7	10.2	12.1	8.4	8.8	—	6.0
F-23	13.4	9.1	9.5	9.7	13.7	10.1	7.0	5.7	11.3
F-31	9.7	5.3	7.7	9.4	5.6	4.7	—	—	4.2
F-32	14.1	13.4	10.8	8.2	15.2	13.2	11.3	9.5	9.6

TABLE IV

CHANGE OF YIELD WITH TIME

Expt. No.	Yield (%) at time (hr.)								
	½	1	2	4	6	8	15	20	25
F-11	91.7	90.1	90.4	85.7	90.0	87.7	85.2	80.2	79.9
F-12	97.9	92.8	92.3	87.2	78.1	77.2	89.9	—	69.4
F-13	90.9	96.6	94.9	81.4	78.2	76.3	90.8	—	90.7
F-21	91.2	94.4	89.2	—	87.7	90.6	84.8	—	79.4
F-22	89.4	90.8	87.8	88.6	88.0	82.4	86.3	—	83.5
F-23	88.4	88.7	89.3	91.3	88.7	87.4	88.6	82.6	85.1
F-31	90.7	89.8	87.6	84.3	84.5	86.9	71.9	67.6	59.7
F-32	90.4	89.3	90.9	87.8	85.9	—	90.1	87.1	82.1

TABLE V

CHANGE OF PENTOSAN CONTENT WITH TIME

Expt. No.	Content (%) at time (hr.)				
	½	2	6	15	25
F-11	37.7	39.4	41.1	40.0	43.5
F-12	40.6	41.2	44.2	39.3	—
F-13	40.3	40.0	41.3	34.4	34.5
F-21	34.1	39.7	37.7	26.3	24.0
F-22	36.7	37.7	37.9	26.1	41.1
F-23	37.1	37.8	39.7	41.2	55.4
F-31	47.9	37.0	—	35.2	42.3
F-32	45.6	37.2	47.3	47.8	35.8

3) L. E. Wise, M. Murphy and A. A. D'Addieco, *Paper Trade J.*, **122**, No. 2, 35 (1946).

4) I. Sakurada et al., *J. Chem. Soc. Japan* (*Ind. Chem. Sec.*), **37**, 127, 1339 (1934).

and then stays constant. Pentosan is not entirely lost. Birefringence decreases at first abruptly, then increases and finally gradually again decreases, but its value is scattered.

2. Alkali Refined Holocellulose.—The refined products shown in Table VI were

TABLE VI

REFINING CONDITIONS AND RESULTS

Expt. No.	Refining		Total Yield %	α-Cellulose		Pentosan	
	Temp. °C	NaOH %		Cont. %	Yield %	Cont. %	Yield %
C-41	15	1	63.0	80.9	90.7	27.6	52.1
C-43	15	4	55.9	92.0	91.5	14.8	24.8
C-44	15	8	52.2	94.8	88.0	12.3	19.3
C-42	15	17.5	49.9	96.6	85.9	10.6	16.0
W-62	60	1	66.5	76.8	90.9	29.7	59.4
W-61	60	4	55.9	88.5	88.0	17.3	29.0
H-52	95	1	64.7	77.3	89.0	31.2	60.5
H-51	95	0.2	67.7	75.2	93.4	31.3	65.2
Raw material			100	56.2	100	33.3	100
RP			100	90.9	100	5.1	100

acetylated at 30°C. The acetylating mixture was composed of 100 parts acetic anhydride, 300 parts benzene and 1.8 parts sulfuric acid, and the liquid ratio used was 1 : 100. The results are shown in Tables VII, VIII, IX and X.

TABTE VII

CHANGE OF ACETIC ACID CONTENT WITH TIME

Expt. No.	Acetic acid content (%) at time (hr)								
	½	1	2	4	6	8	15	20	25
C-41	5.6	6.1	7.3	9.4	11.5	13.5	21.2	25.5	29.2
C-43	4.3	6.4	8.1	8.5	11.9	13.5	18.4	22.3	—
C-44	3.7	4.9	5.1	7.9	8.6	10.4	10.3	13.0	—
C-42	2.0	2.1	2.2	2.3	3.0	3.8	3.7	4.4	6.2
W-62	6.8	8.2	9.4	13.5	15.5	17.6	22.7	26.7	31.6
W-61	3.2	4.9	6.3	8.7	9.9	12.8	19.9	24.1	29.8
H-52	5.5	6.8	7.6	8.9	11.2	13.9	22.6	26.0	30.6
H-51	5.4	5.8	6.8	8.9	12.5	14.4	20.3	25.5	30.2
P-72	1.5	2.8	2.8	3.9	5.3	5.8	10.6	11.9	13.7

TABLE IX

CHANGE OF BIREFRINGENCE WITH TIME

Expt. No.	Birefringence (×1000) at time (hr)								
	½	1	2	4	6	8	15	20	25
C-41	21.8	17.7	18.3	17.0	13.4	17.8	14.6	16.1	13.2
C-43	18.1	21.6	14.9	18.4	12.9	17.2	15.6	15.3	4.5
C-44	19.2	21.1	24.1	15.0	20.7	18.5	13.6	24.3	16.3
C-42	25.1	29.6	28.5	28.9	28.2	30.1	29.6	27.1	20.7
W-62	16.7	24.3	20 5	25.1	17.7	18.2	17.6	17.6	16.9
W-61	17.9	18.4	15.1	19.9	16.7	15.9	17.3	11.9	14.9
H-52	15.4	16.2	16.1	20.4	18.1	18.3	16.6	15.6	14.3
H-51	15.4	12.3	15.5	15.7	18.4	14.5	17.6	17.1	14.1
P-72	11.8	11.5	12.0	9.7	13.0	12.5	11.8	11.7	11.3

TABLE X

CHANGE OF PENTOSAN WITH TIME

Expt. No.	Content (%)		
	½	6	25
C-41	33.2	37.8	33.2
C-43	13.5	14.2	14.8
C-44	14.7	15.2	15.1
C-42	16.1	11.4	11.4
W-62	33.6	32.4	28.8
W-61	16.8	16.5	19.4
H-52	31.5	32.9	26.0
H-51	34.0	32.0	32.9
P-72	7.1	7.7	6.4

The product refined with concentrated cold alkaline education reacted with difficulty. Refining temperature affects little on the reaction rate, but product refined at 60°C seems to be a little superior. The further refined products exhibit less initial decrease of yield, less abrupt change of acetic acid content and more diffused loss of birefringence. Pentosan is apparently little changed.

3. Bemberg Rayon and Pulp.—As shown in Table XI, the reaction is slow. Soaping has no effect. Birefringence decreases naturally.

TABLE VIII

CHANGE OF YIELD WITH TIME

Expt. No.	Yield (%) at time (hr.)								
	½	1	2	4	6	8	15	20	25
C-41	92.8	94.4	95.9	—	95.7	95.9	94.4	93.6	92.0
C-43	96.4	95.2	88.2	93.7	95.8	94.6	96.4	96.0	—
C-44	97.4	97.6	98.4	95.7	95.8	93.5	94.7	92.3	—
C-42	94.8	95.0	95.8	98.2	98.6	95.5	96.4	96.2	97.7
W-62	93.6	90.4	91.4	91.8	89.9	92.4	91.8	92.4	103.2
W-61	96.3	95.0	95.9	95.6	95.2	95.8	93.6	93.5	92.1
H-52	102.0	101.4	100.7	101.8	101.4	100.7	99.0	99.3	94.6
H-51	92.8	95.1	94.1	93.3	93.5	92.2	93.2	93.2	86.2
P-72	105.0	106.1	100.3	106.9	100.1	101.3	95.2	100.0	100.4

TABLE XI
ACETYLATION OF BEMBERG RAYON

Expt. No.	Change with time (hr.)											
	½	1	2	4	6	8	15	20	25	50	100	200
	Acetic acid content (%)											
B-81	2.2	3.1	3.2	3.1	3.4	4.2	4.6	4.6	4.5			
B-82	1.4	1.7	3.1	2.8	3.5	3.7	4.8	5.0	5.3	7.6	11.7	13.1
B-83	14.2	22.7	24.1	24.7	27.6	27.6	32.9	34.5		48.7	51.1	54.5
	Yield (%)											
B-81	94.6	97.0	97.6	98.1	97.3	97.0	95.3	96.4	96.0			
B-82	98.8	99.8	98.1	98.5	98.4	97.7	97.7	96.4	97.6	94.8	94.2	96.7
B-83	97.1	96.9	92.9	93.6	94.2	93.5	93.4	98.5	86.4	82.2	85.9	89.4
	Birefringence (×1000)											
B-81	22.9	21.7	24.8	21.7	20.5	21.3	22.3	21.5	21.1			
B-82	26.8	26.4	25.0	22.2	24.1	22.1	21.6	22.9	20.3	21.3	20.2	19.5
B-83	25.6	21.3	22.1	20.8	20.0	20.1	18.0	18.7	19.1	19.0	16.1	9.1

Discussion

1. Unreacted Radius.—Assuming that pentosan is concentrated at outer layer and preferentially acetylated,

$$A=-\frac{180(1-x^2/y)/162+120(x^2-1)/132}{x^2/y+288(1-x^2/y)/162+216(x^2-1)/132}$$

where x: unreacted radius/radius excluding pentosan.
$X=1/(1-P)$: total radius/radius excluding pentosan
P: content of pentosan in product
y: yield of product, fraction of theoretical value.

Then, $x^2=(10-16A)y/(10-7A)(1-P)-2yP/(1-P)$

x is plotted against time fraction, which is arranged so as to lay the last experimental point on the calculated line of reaction controlled by surface-resistance, which is given as a full line in the figure. The broken line shows the case controlled by internal diffusion. As shown in Figs. 1, 2, 3 and 4, air-dried holocellulose tends to follow the reaction controlled by surface resistance regardless of the composition of acetylating mixture, acetylating temperature and degree of refin-

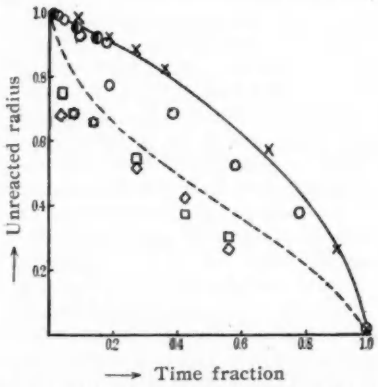

Fig. 1. Effect of pretreatment and temperature on acetylation rate of holocellulose.
(○, at 45°C; ×, at 30°C; ◐, at 15°C (air-dried); □, ◇: replacing or boiling with acetic acid)

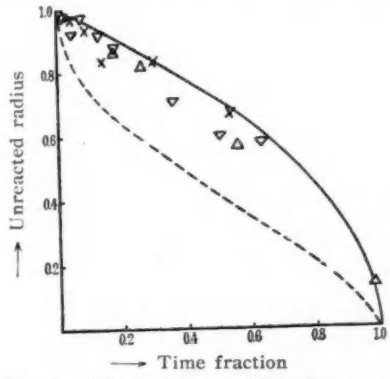

Fig. 2. Effect of composition of reagent on acetylation rate of holocellulose.
(△, +, ▽: low liquid ratio, low acetic anhydride or low sulfuric acid)

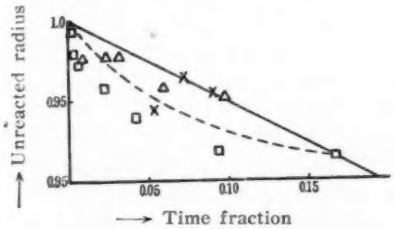

Fig. 3. Effect of cold alkali concentration on acetylation rate of refined holocellulose.
(×, △, □: 1%, 4%, 8% NaOH)

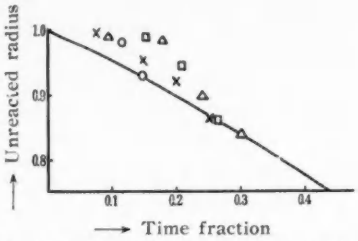

Fig. 4. Effect of warm and hot alkali concentration on acetylation rate of refined holocellulose.
(×, △, ○, □: 1%, 4% at 60°C; 1%, 0.2% at 95°C)

ing. Pretreated sample follows close by the curve controlled by internal diffusion. Hence pentosan layer may hinder the acetylation in air-dried state, but pretreatment would remove the hindrance. Figs. 5 and 6 shows

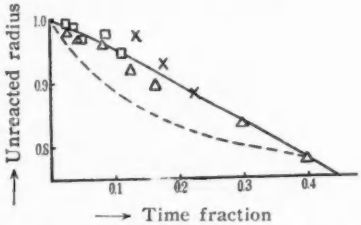

Fig. 5. Acetylation rate of air-dried rayon pulp and bemberg rayon.
(△, □, ×: rayon, soaped, rayon, pulp)

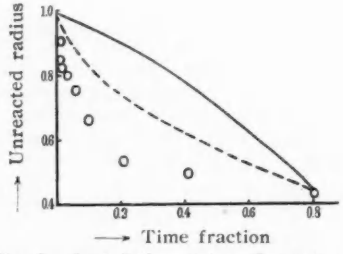

Fig. 6. Acetylation rate of pretreated bemberg rayon.

that not only pretreated Bemberg rayon but also air-dried rayon is likely counted as the type controlled by internal diffusion.

2. Relation to Structure.—Steep increase of acetic acid content and loss of yield in initial stage may be derived from the readily reacting and dispersing amorphous portion, for its magnitude is almost independent of acetylating conditions. The behavior of birefringence is elucidated by considering that initially it is reduced by acetylation of the accessible part, secondly it is raised by loss of amorphous portion, both bringing about the increase of residual crystallinity, and thirdly it is reduced again gradually by acetylation of crystalline region. Since the final acetic acid content is higher than the value corresponding to the birefringence and the yield is low, so acetolysis might have occurred.

3. Effect of Refining.—Slower reaction resulting from cold concentrated alkali refining is likely due to hornification, the loss of accessible portion or transformation into cellulose hydrate. The low reactivity of the sample refined with more dilute alkali than 4% is explained probably by the incomplete removal of the acetylation hindering layer and its gelatinization. The slow reaction of pulp and Bemberg rayon may be ascribed to more compact structure.

4. Behavior of Pentosan.—The content of pentosan in the product is apparently rather higher. Slight solubility of acetate and the easy production of oxymethylfurfural may be responsible for this. If all pentosan in holocellulose is preferentially acetylated, its acetic acid content should amount to 24.8%, but the value of only 12% observed in its initial stage suggests that pentosan is not exclusively accessible.

Summary

Acetylation in fibrous state of holocellulose, its alkali-refined product, rayon pulp and Bemberg rayon was undertaken to disclose the effect of pentosan and the structure of holocellulose.

1) Acetylation of air-dried holocellulose is roughly controlled by surface resistance, regardless of various ratios depending on conditions of acetylation and degree of refining. The rate of pretreated sample seems to be determined by internal diffusion.

2) The birefringence decreases at first abruptly and then increases and finally decreases again. The final higher birefringence compared to acetic acid content may be ascribed to acetolysis. Definite amorphous portion is acetylated easily at the initial stage and lost, so that residual crystallinity, and also birefringence, increase.

3) By alkali-refining, acetylation is retarded and initial abrupt change, which is caused by the amorphous portion is diffused. There is optimum point in the concentration of refining alkali, probably relating to hornification, loss of amorphous portion, transformation of crystal form and hindrance by residual pentosan layer. The refining temperature affects the acetylation slightly.

4) Pentosan in product is not reduced apparently, probably due to oxymethylfurfural yielding and poor solubility of acetate. Also pentosan may not be entirely accessible at initial stage.

The author wishes to thank Prof. H. Sobue for his guidance and inspiration.

Department of Applied Chemistry,
Faculty of Engineering,
Yamanashi University, Kofu

On the Thermal Dissociation of Organic Compounds. VII. The Urea Linkage (1,3-Dibenzylurea and 1-isopropyl 3 3 diethylurea in Alcohols)

By Teruaki MUKAIYAMA

(Received, July 26, 1954)

Introduction

As described in the previous reports[1-4], ureas thermally dissociate into isocyanates and amines:

$$RHNCONHR \rightleftarrows R-N=C=O+H_2NR.$$

The kinetics of the thermal dissociation of ureas in various fatty acids have been studied and the results show that the rate of dissociation increases as the acidity of the solvent acid increases. A general acid catalysis for the thermal dissociation of urea in fatty acids can be shown as,

$$RHNCONHR+R'COOH \rightleftarrows R'COO^-+RNH_2+RNH_2CO^+$$
$$\downarrow -H^+$$
$$R-N=C=O$$

In this experiment, the kinetic data on the thermal dissociation of ureas in alcohols have been determined in order to gain an understanding of the dissociation of ureas in a very weak acid, as in alcohols.

By the present experiment, benzyl N-phenylcarbamate, m.p. 78°, was obtained on heating 1,3-diphenylurea in a large excess of benzyl alcohol at 170° for 3 hrs. In this case, the mechanism shown by equation (1) and (2) can be considered.

$$C_6H_5HNCONHC_6H_5 \rightleftarrows C_6H_5N=C=O+H_2NC_6H_5 \quad (1)$$

$$C_6H_5N=C=O+HOCH_2C_6H_5 \rightleftarrows C_6H_5HNCOOCH_2C_6H_5 \quad (2)$$

The dissociation reaction of urea is a reversal of the formation reaction and the addition of isocyanate and amine to form urea proceeds very rapidly, when accompanied by a liberation of heat. In eq. (1), the equilibrium between urea and isocyanate—amine is in favor of the left side of the reaction. When urea is heated in alcohol, isocyanate dissociated forms urethane according to eq. (2) which removes a considerable part of isocyanate, the equilibrium will be disturbed and a readjustment must take place. Thereupon an additional amount of urea will dissociate, forming isocyanate and amine until the equilibrium is again established.

Thus, when urea is reacted in a large excess of alcohol, if the reaction (1) is the rate-determining step, the rate of dissociation of urea becomes measurable if one determines the amount of amine formed according to eq. (1).

As has been previously mentioned, 1,3-diphenylurea dissociates more readily than 1,3-dibenzylurea used in the present experiment and the use of the former urea seemed to be convenient for the kinetic study because it dissociates at a lower temperature than the latter. In the titration of aniline formed from the former urea, however, the change in pH at the equivalence point is small, which makes the experiment difficult. Therefore 1,3-dibenzylurea and 1-isopropyl-3,3-diethylurea which form strong bases were used.

Experimental

Materials.—1,3-Dibenzylurea was prepared from benzyl isocyanate[5] and water, m.p. 167°C, recrystallized from ethanol.

1-Isopropyl-3,3-diethylurea was prepared from isopropyl isocyanate[6] and diethylamine, m.p. 66°C,

1) T. Hoshino, T. Mukaiyama and H. Hoshino, *J. Am. Chem. Soc.*, **74**, 3097 (1952).
2) T. Hoshino, T. Mukaiyama and H. Hoshino, This Bulletin, **25**, 392 (1952).
3) T. Mukaiyama and T. Matsunaga, *J. Am. Chem. Soc.*, **75**, 6209 (1953).
4) T. Mukaiyama, S. Ozaki and T. Hoshino, This Bulletin, **27**, 578 (1954).
5) T. Curtius and E. Boetzlen, *J. prakt. Chem.*, **64**, 316 (1901).
6) O. Hambsch, *J. prakt. Chem.*, **125**, 182 (1930).

recrystallized from petroleum ether.

The following alcohols were used: benzyl alcohol, b.p. 112°C at 20 mm.; anisyl alcohol, b.p. 147°C at 20 mm.; 1,2-propanediol b.p. 91°C at 16 mm.; ethylene glycol, b.p. 120°C at 20 mm.; diethylene glycol, b.p. 137°C at 15 mm.; triethylene glycol, b.p. 166°C at 15 mm.; 1,4-butanediol, b.p. 136°C at 24mm.; glycerol, b.p. 185°C at 23 mm.:

Procedure and Analysis.—In carrying out the dissociation reaction, a definite quantity of alcohol was measured into a 20 ml. reaction tube having a ground stopper. The reaction tubes were then placed in a thermostat for 20 min. in order to allow them to attain the constant temperature. Thereupon a small glass tube containing a weighed amount of urea was put into the alcohol and shaken hard to dissolve out the urea. At appropriate intervals of time the tubes were removed from the thermostat and the reaction was stopped by rapid cooling with cold water. The temperature control of the reaction thermostat was accurate to ±0.05°C within the temperature range 165—190°C using a tetraline-mercury regulator. The amounts of amine produced were determined by titration with 0.1 normal hydrochloric acid, back-titration being carried out with 0.1 normal sodium hydroxide, using methyl red as indicator.

Results and Discussion

The steps in the thermal dissociation of urea in alcohol are believed to proceed *via* equations (3) and (4)

$$\mathrm{RHNCONHR} \underset{k_2}{\overset{k_1}{\rightleftharpoons}} \mathrm{RNCO}+\mathrm{H_2NR} \qquad (3)$$

$$\mathrm{RNCO}+\mathrm{HOR'} \underset{k_4}{\overset{k_3}{\rightleftharpoons}} \mathrm{RHNCOOR'} \qquad (4)$$

The first step is a reversible reaction for which the differential equation is

$$-\frac{d(\mathrm{A})}{dt}=\frac{d(\mathrm{C})}{dt}=k_1(\mathrm{A})-k_2(\mathrm{B})\,(\mathrm{C}) \qquad (5)$$

The symbols *A*, *B* and *C* are used for urea, isocyanate and amine, respectively. The rate of change of the concentration of the isocyanate is the difference between the rates of its formation from urea (3) and urethane (4) and the rates of its reaction to form both urethane (4) and urea (3).

$$\frac{d(\mathrm{B})}{dt}=k_1(\mathrm{A})-k_2(\mathrm{B})\,(\mathrm{C})-k_3(\mathrm{B})\,(\mathrm{D})+k_4(\mathrm{E}) \qquad (6)$$

The symbols *D* and *E* are used for alcohol and urethane.

The rate of reaction of alcohol and isocyanate and that of amine and isocyanate are very fast in comparison with that of dissociation of urea and of urethane. Thus, the concentration of isocyanate remains small and the rate of change of its concentration $\frac{d(\mathrm{B})}{dt}$ is small, compared with the rate $k_1(\mathrm{A})$ at which it is formed from urea. This means in view of eq. (6) that $\frac{d(\mathrm{B})}{dt}$ is a small difference between relatively large quantities so that it may be neglected in comparison with them. Consequently, eq. (6) approximates closely to

$$0=k_1(\mathrm{A})-k_2(\mathrm{B})\,(\mathrm{C})-k_3(\mathrm{B})\,(\mathrm{D})+k_4(\mathrm{E})$$

and $$(\mathrm{B})=\frac{k_1(\mathrm{A})+k_4(\mathrm{E})}{k_2(\mathrm{C})+k_3(\mathrm{D})}$$

Introduction of the values of (B) into eq. (5) leads to

$$-\frac{d(\mathrm{A})}{dt}=\frac{d(\mathrm{C})}{dt}=k_1(\mathrm{A})-k_2\left\{\frac{k_1(\mathrm{A})+k_4(\mathrm{E})}{k_2(\mathrm{C})+k_3(\mathrm{D})}\right\}\cdot(\mathrm{C}) \qquad (7)$$

If *D* is in great excess compared with *A*, the second term in eq. (7) becomes negligible and the amount of amine formed in the reaction directly gives the amount of urea dissociated.

The amount of amine formed according to eq. (3) was determined by the titration. On plotting the logarithm of the amount of amine formed at regular intervals of time a linear relationship was obtained. This indicates that the reaction was of a first order. The rate constant is given by the gradient of such a plot[7], as show in Fig. 1.

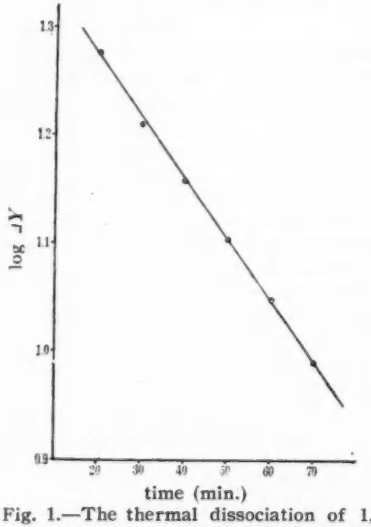

Fig. 1.—The thermal dissociation of 1,3-dibenzylurea in benzyl alcohol at 179.8°C: the plot of log ΔY against time.

7) E. A. Guggenheim, *Phil. Mag.*, 2, 538 (1926).

(a) 1,3-Dibenzylurea (1 mole) in Alcohol (100 moles*).—The alcohols were benzyl alcohol, anisyl alcohol, 1,2-propanediol, ethylene glycol, diethylene glycol, triethylene glycol, 1,4-butanediol and glycerol. The results are shown in Table I. The rates were of the first order with respect to 1,3-dibenzylurea. As an example of a typical run, the thermal dissociation of 1,3-dibenzylurea in benzyl alcohol at 179.8°C is shown in Fig. 1.

TABLE I

THE RATE CONSTANTS OF THE THERMAL DISSOCIATION OF 1,3-DIBENZYLUREA IN ALCOHOLS

Alcohols	t°(C)	$k_1 \times 10^2$ (min.$^{-1}$)
Benzyl Alcohol	190.5	2.86
	185.7	2.00
	179.8	1.25
	175.3	0.80
	166.7	0.46
Ethylene Glycol	185.2	2.63
	179.1	1.73
	176.0	1.32
	173.5	1.12
	166.4	0.56
Glycerol	186.3	2.61
	184.5	2.28
	180.2	1.70
	177.5	1.34
	173.3	0.95
Anisyl Alcohol	184.5	2.38
Triethylene Glycol	184.5	1.66
Diethylene Glycol	184.5	1.37
1,2-Propanediol	180.4	1.14
1,4-Butanediol	184.7	0.967

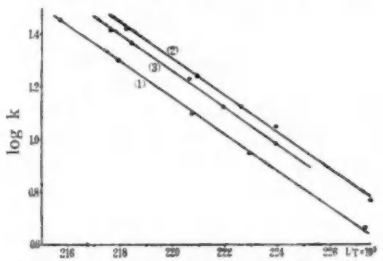

Fig. 2. The thermal dissociation of 1,3-dibenzylurea in benzyl alcohol (1), ethylene glycol (2) and glycerol (3): the plot of 1/T against log K.

The kinetic data were further analyzed by means of the Arrhenius equation

$$\ln k = \ln A - (E/RT)$$

and by the absolute rate equation

$$\ln (k/T) = \ln R\kappa/Nh + \Delta S^{\neq}/R - \Delta H^{\neq}/RT$$

The transmission coefficient, κ, was set equal to unity. The calculated kinetic and thermodynamic functions are collected in Table II.

In Table III, the percentage of dissociated urea in the thermal dissociation of 1,3-dibenzylurea (1 mole) in benzyl alcohol, ethylene glycol and glycerol (each alcohols 100 moles) are shown against time.

TABLE II

KINETIC AND THERMODYNAMIC FUNCTIONS FOR THE THERMAL DISSOCIATION OF 1,3-DIBENZYLUREA IN ALCOHOLS

Alcohol	T°	$A \times 10^{11}$ (sec.$^{-1}$)	E(kcal.)	$\Delta H^{\neq}$(kcal.)	$\Delta S^{\neq}$(cal. mol.$^{-1}$ deg.$^{-1}$)	$\Delta E^{\neq}$(kcal.)
Benzyl alcohol	458.9	4.62	31.8	32.2	−6.02	34.4
Ethylene glycol	458.4	1.69	30.6	30.6	−8.01	34.3
Glycerol	457.7	2.42	31.0	30.7	−7.30	34.3

TABLE III

THE PERCENTAGE OF DISSOCIATED 1,3-DIBENZYLUREA (1 MOLE) IN ALCOHOLS (100 moles) *vs.* TIME

Solvent	Temperature (°C)	Time (min.) 20	40	60	80	100	Rate constant ($k_1 \times 10^2$) (min.$^{-1}$)
Benzyl alcohol	185.7	10.4	19.2	25.5	30.1	33.0	2.00
Ethylene glycol	185.2	17.1	38.2	49.9	56.7	61.2	2.63
Glycerol	181.5	26.9	48.3	63.0	72.9	80.8	2.28

As is seen from Table III, the amount of dissociated urea in ethylene glycol is nearly twice that in benzyl alcohol and that in glycerol is nearly 2.5 times that in benzyl alcohol, while the rate constants, as measured by the amount of benzylamine produced, of dissociation in these three alcohols are nearly equal. This suggests that the velocities of dissociation of urea in alcohols are dependent on the concentration of the hydroxylic group in the solvent alcohols.

The result can be explained by postulating

the formation of an intermediate complex in equilibrium with urea and alcohol as shown in eq. (8), which dissociates into an isocyanate, an amine and alcohols *via* the rate-determing step according to eq. (9)

$$\text{urea}+\text{alcohols} \rightleftarrows (\text{urea-alcohols}) \quad (8)$$

$$(\text{urea-alcohols}) \xrightarrow{k_1} \text{isocyanate}+\text{amine}+\text{alcohols} \quad (9)$$

$$\text{isocyanate}+\text{alcohol} \rightleftarrows \text{urethane} \quad (10)$$

$$\text{urethane}+\text{alcohols} \rightleftarrows (\text{urethane-alcohols}) \quad (11)$$

The concentration of the complex is given by the following equation,

$$(C_{\text{complex}}) = K \cdot (C_{\text{urea}}) \cdot (C_{\text{alcohol}})$$

and the velocity of dissociation is therefore expressed as,

$$v = k_1 \cdot K \cdot (C_{\text{urea}}) \cdot (C_{\text{alcohol}})$$

(b) 1-Isopropyl-3,3-diethylurea (1 mole) in Alcohols (100 moles).—The alcohols were benzyl alcohol, anisyl alcohol, diethylene glycol, triethylene glycol and glycerol. The results are shown in Table IV. The rates

TABLE IV

THE RATE CONSTANTS OF THE THERMAL DISSOCIATION OF 1-ISOPROPYL-3,3-DIETHYLUREA IN ALCOHOLS

Alcohols	t(°C)	$k \times 10^2$ (min.$^{-1}$)
Benzyl alcohol	169.7	0.99
Anisyl alcohol	169.7	1.20
Ethylene glycol	184.5	fast
Glycerol	169.7	1.53
Triethylene glycol	184.5	1.04
Diethylene glycol	184.5	2.00

were of the first order with respect to 1-isopropyl-3,3-diethylurea.

In the process of dissociation of ureas, the one nitrogen atom of urea accepts a proton to form an amine and the other nitrogen atom donates a proton to form an isocyanate.[4] The consideration leads to the conclusion that there are two roles of the solvents which control the dissociation.

(a) Ability of solvents to accept a proton from a urea molecule, namely basicity.

(b) Ability of solvents to donate a proton to a urea molecule, namely acidity.

As to the effect of the solvents, it is shown by the present experiment that the rate of dissociation increases in the series,

ethylene glycol>glycerol>anisyl alcohol>benzyl alcohol>1,2-propanediol>diethylene glycol, triethylene glycol>1,4-butanediol.

The rates of dissociation in these eight alcohols differ slightly; however, the rates of dissociation in ethylene glycol and in glycerol are faster than in anisyl alcohol and that in anisyl alcohol is faster than in benzyl alcohol. The basicities of these four alcohols are expected to increase in the following order, which coincides with that of the rates of dissociation.

ethylene glycol>glycerol>anisyl alcohol>benzyl alcohol.

This will lead to the consideration that the stronger the basicities of alcohols the faster the rates of dissociation.

Also, the fact that the rate of dissociation in ethylene glycol is faster than in all other dihydric alcohols (i.e., 1,2-propanediol, diethylene glycol, triethylene glycol and 1,4-butanediol) will show that the larger the molecular size the slower the rates of dissociation.

In order to compare the solvent effects of fatty acids and of alcohols on the thermal dissociation of ureas, the rate constants of the dissociation of 1,3-dibenzylurea and 1-isopropyl-3,3-diethylurea in fatty acids described in the previous report[4] are listed in Table. V.

TABLE V

THE RATE CONSTANTS OF THE THERMAL DISSOCIATION OF 1,3-DIBENZYLUREA AND 1-ISOPROPYL-3,3-DIETHYLUREA IN FATTY ACIDS

$k \times 10^2$ (min.$^{-1}$), t(°C).

Fatty acid \ Urea	1.3-Dibenzylurea	1-Isopropyl-3,3-diethylurea
n-Butyric acid	1.27 (139.6)	3.15 (139.45)
n-Caproic acid	2.68 (155.0)	6.2 (155.0)
n-Capric acid	2.70 (155.0)	3.19 (155.0)
Phenylacetic acid	3.85 (154.9)	very fast (154.9)
Benzoic acid	0.418 (155.0)	1.60 (155.1)

It can be said that these two ureas dissociate more easily in fatty acids than in alcohols. Even in benzoic acid, in which the rates of dissociation of ureas are one-third or one-fourth of those in the other acids, the dissociation proceeds more easily than in alcohols.

This shows that in the process of dissociation of urea the ability of solvents to donate a proton to a urea molecule is an important factor. As the alcohol is a very weak acid, the ability to donate a proton to a urea molecule is so small that the rates in alcohols are slower than in fatty acids.

As the basicities of alcohols are nearly the same as those of ureas, in the case of dissociation in alcohols, alcohols would act as a base to accept a proton. Together with the facts above mentioned that the stronger the

basicity of alcohol the faster the dissociation, it can be said that in the process of dissociation of ureas in alcohols the deprotonation by the solvent alcohols plays an important role in determining reaction rate.

As to the effect of substituents, it is shown by the present experiment that 1-isopropyl-3,3-diethylurea dissociates more readily than 1,3-dibenzylurea in all alcohols used. Similar results were also found in the case of dissociation in fatty acids.

The facts show that the ability of one nitrogen atom in urea to accept a proton and that of the other to donate a proton are important factors of the dissociation. In these two ureas, the basicities of the nitrogen atoms in 1-isopropyl-3,3-diethylurea are stronger than those in 1,3-dibenzylurea. If the solvent alcohol acts only as a base, the order of the reactivities of the two ureas must be reversed. The experimental fact means that the process of protonation of urea by solvent alcohol also controls the rate of dissociation.

These facts will be explained by considering the intermediate complex containing two alcohol and one urea molecules as has been mentioned above. The mechanism is identical with that proposed in the dissociation of ureas in fatty acids[4]. One alcohol in the complex (I) acts as a base to accept a proton and the other alcohol acts as an acid to donate a proton at the same time.

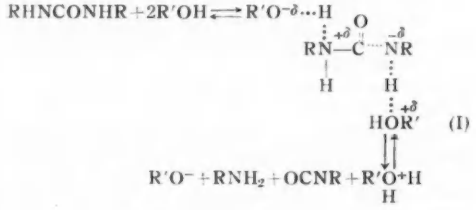

The consideration on the experimental results of the thermal dissociation of ureas in fatty acids and in alcohols leads to the conclusion that the dissociation proceeds very rapidly in a solvent which can acts as a base and as a strong acid at the same time. The basicity of the solvent may be suitable when it is a slightly stronger base than urea and the acidity of it may be favorable when it is a very strong acid. Thus, when the dissociation of ureas in such a solvent as aminophenylacetic acid is measured, the rate of dissociation would be very fast.

Summary

The rate constants of the thermal dissociation of 1,3-dibenzylurea and 1-isopropyl-3,3-diethylurea in alcohols were determined.

The rates of dissociation in fatty acids are faster than those in alcohols and it can be said that the process of protonation of ureas by solvents plays an important role in the dissociation.

In the case of dissociation in alcohols, the reaction seems to proceed by a base catalysis. And the intermediate complex containing two alcohol and one urea molecules was considered. The experimental results were reasonably explained by the proposed mechanism.

The author is indebted to Dr. T. Hoshino for his helpful discussion and Mr. Y. Fujita, Mr. T. Kurachi and Mr. H. Yoshizawa for their help during the course of this experiment.

Department of Physics and Chemistry,
Gakushuin University,
Tokyo

Heats of Combustion and Formation of Some Methoxy-polysilanes and -polysiloxanes: Si-O *Bond Energy**

By Toshio TANAKA and Takeo WATASE

(Received December 15, 1954)

In the preceding paper[1], data on the heats of combustion and formation of some organosilicon compounds, containing alkyl or phenyl group, were presented. The compounds measured therein have such a large number of C-C and C-H bonds, etc., that the bond energies between silicon and other elements calculated from the results turn out to be small differences between large quantities, and may be unreliable. In order to derive the bond energies between silicon and other elements, it is desirable to measure the heat of combustion of organosilicon compounds having the least possible number of C-C and C-H bonds, etc., in the molecule. In the present work the heats of combustion of some methoxy-polysilanes and -polysiloxanes have been measured, and the heats of formations of them and Si-O bond energy have been calculated therefrom.

Experimental

Materials. — Hexamethoxy disilane $(CH_3O)_3Si\cdot Si(OCH_3)_3$ was synthesized by methanolysis of hexachlorodisilane.[2] Tetramethoxysilane $Si(OCH_3)_4$, hexamethoxydisiloxane $(CH_3O)_3Si\cdot O\cdot Si(OCH_3)_3$ and octamethoxytrisiloxane $(CH_3O)_3Si\cdot O\cdot Si(OCH_3)_2\cdot O\cdot Si(OCH_3)_3$ were prepared by methanolysis of the corresponding polychloro-silane and -siloxanes, respectively. These hexachlorodisiloxane and octachlorotrisiloxane were obtained from the distillation residue of industrial tetrachlorosilane with careful fractionation through a helices packed-column of about 20 plates. (Si_2OCl_6 b. p. 137°C, Cl % calcd. 74.7, found 74.6; $Si_3O_2Cl_8$ b. p. 73°C/13 mm, Cl % calcd. 70.9, found 70.8.). These compounds prepared by methanolysis could not be freed from a trace of chlorine by the fractional distillation, so careful dehydrochlorination using dry ammonia[2] or sodium carbonate[3] was carried out. After that these products were carefully distilled through a Stedman column of about 30 theoretical plates. Physical constants and analytical data on these samples are shown in Table I.

TABLE I

DATA ON THE SAMPLES USED FOR COMBUSTION MEASUREMENTS

Formula	b. p. °C/mm Hg	d_4^{20}	n_D^{20}	Si % Found	Si % Calcd.
$Si(OCH_3)_4$	122/760	1.034	1.3688	18.48	18.45
$Si_2O(OCH_3)_6$	118.5/30	1.122	1.3818	21.77	21.74
$Si_3O_2(OCH_3)_8$	95–6/2	—	—	23.17	23.12
$Si_2(OCH_3)_6$	98/20	1.095	1.4070	22.99	23.18

Calorimetry.—The apparatus was the Nenken-type adiabatic bomb calorimeter, incorporating a 300 ml. stainless steel-made bomb and Beckmann thermometers. The temperatures in the calorimeter vessel and water jacket were observed with an accuracy of 0.001°C as described previously[1].

For the complete burning of liquid organosilicon compounds containing alkyl or phenyl group, we previously described the technique using a glass ampoule and promotor.[1] However, the poly-silanes and -siloxanes containing only methoxy group are readily burnt completely by themselves without ampoule, by the ignition of the liquid pool in the crucible.

The procedure used in the combustion experiments was the same as previously described.[1] The calibration experiments of the calorimeter were carried out at a temperature of 20°C. (based on the heat of combustion of benzoic acid at 20°C=6319.0 cal./g.[4], and its water equivalent value was determined to be 2494 cal./degree (relative mean deviation ±0.1%).

By the complete burning of the organosilicon compounds, gaseous carbon dioxide, liquid water and silicon dioxide were involved as the end products. The completeness of combustion was ascertained by visual inspection of the bomb contents for traces of black or yellow materials, and sometimes by the chemical analysis. Four to six combustion measurements were made with each liquid sample, the results of which are recorded in Table II.

TABLE II

Formula	Heat of combustion at constant volume, cal./g.						Mean
$Si(OCH_3)_4$	4548	4560	4556	4548	4553	4554	4553
$Si_2O(OCH_3)_6$	4086	4084	4086	4085	—	—	4085
$Si_3O_2(OCH_3)_8$	3836	3832	3840	3838	3833	—	3836
$Si_2(OCH_3)_6$	4731	4743	4738	4735	4740	—	4737

Each deviation from the mean is somewhat high compared with modern precision techniques, but

* A part of this paper was published in Letter section of *J. Chem. Phys.*, 22, 1268 (1954).

1) T. Tanaka U. Takahashi, R. Ōkawara and T. Watase, This Bulletin, 28, 15 (1954).

2) R. Ōkawara and T. Tanaka, This Bulletin, 27, 119 (1954).

3) R. Ōkawara, T. Tanaka and I. Ishimaru, This Bulletin, 27, 45 (1954).

4) Calculated from the results of Prosen and Rossini, *J. Research NBS.*, 33, 439 (1944).

of sufficient precision for bond energy term purpose in view of the other uncertainties involved.

Results and Discussion

Table III contains the summary of the data for the heats of combustion of four organosilicon compounds with some important thermal data calculated therefrom.

The value of the bomb process was calculated per mole and corrected to the standard constant-volume process where the reactants were at 1 atm. pressure by means of Washburn's equation.[5] The energies evolved in this hypothetical standard process were denoted in Table III by the symbol $-\Delta U_R$. From this quantity the heat evolved in the isobaric process at 1 atm. pressure, $-\Delta H_c$, was obtained by addition of the proper work term. The heats of formation, $-\Delta H_f$, of these compounds from the standard elements (gaseous H_2 and O_2, graphitic C and metallic Si) were calculated from $-\Delta H_c$ by using data -68.32,[6] -94.05[5] and -208.14[7] kcal./mol. for the heats of formation of water, carbon dioxide and amorphous silica, respectively.

Values of 52.1 and 59.2 kcal./g. atom are now generally accepted for the heats of atomization of hydrogen and oxygen, respectively.[8] The corresponding value for carbon may still be regarded as a matter of some controversy. Direct and various indirect measurements give varying values which fall into three main groups centering around 124,[9] 140[10] and 170[11,12] kcal./g. atom, later evidence tending strongly toward the latter two values rather than the former. Here the actual value 171.7 kcal./g. atom[8,12] was adopted. The heat of atomization of silicon is more dubious. In the present work the value 89.9 kcal./g. atom presented by Baughan[13] was adopted. The heats of formation in the gaseous state from monoatomic gases, ΔE, were obtained from ΔH_f of these compounds of formula $Si_aC_bH_cO_d$ by use of the formula:

$$\Delta E = \Delta H_f - 89.9a - 171.7b - 52.1c - 59.2d - H_v$$

The heats of vaporization of these compounds, H_v, were estimated from Trouton's rule. The values ΔE of the four compounds are listed in Table III.

Si-O bond energy.—The value ΔE may be shown by the following formula:

$$\Delta E = pE_{Si-O} + qE_{Si-Si} + rE_{C-O} + sE_{C-H}$$

In this equation E represents the energy value of bond corresponding to each suffix and the factors p, q, r and s the number of bonds in the molecules coming into question. As the energy terms of C-O and C-H bonds are well known, Si-O bond energy can be evaluated. In the case of hexamethoxydisilane, Si-Si bond energy was considered as equal to the negative value of half of atomization heat for silicon. The Si-O bond energy computed in this manner is shown in Table III, using 98.9[14] and 84.1[15] kcal./mol. for C-H and C-O bond energies, respectively.

The earlier energy term value for the Si-O bond, derived from the heat of formation of silica, was given by Pauling as 89.3[16], by Syrkin and Dyatkina as 89[17], by Paul as 104[18] and by Gilman and Dunn as 104[19] kcal./mol. From the consideration of repulsive interactions of the bonding orbital of one with the inner shell of the other, Pitzer[20] estimated for Si-O bond energy to be 106 kcal./mol., using the value 90 kcal./g.

TABLE III

HEAT OF COMBUSTION AND FORMATION AND Si-O BOND ENERGY (kcal./mol.)

Formula	Mole. wt.	$-\Delta U_R$	$-\Delta H_c$	$-\Delta H_f$	$-\Delta E$	$-E_{Si-O}$
$Si(OCH_3)_4$	152.23	693	694	300	1929	102
$Si_2O(OCH_3)_7$	258.38	1054	1056	539	3090	101
$Si_3O_2(OCH_3)_8$	364.54	1397	1399	798	4271	102
$Si_2(OCH_3)_5$	242.38	1148	1150	445	2937	101

5) E. W. Washburn, *Bur. Standards J. Research*, **10**, 525 (1933).
6) Wagman, Kilpatrick, Taylor, Pitzer and Rossini, *J. Research NBS.*, **34**, 143 (1945).
7) R. Thompson, *J. Chem. Soc.*, **1953**, 1908.
8) "Selected Values of Chemical Thermodynamics Properties", Nat. Bur. Stand., Washington, (1950).
9) G. Herzberg, *J. Chem. Phys.*, **10**, 306 (1942); L.H. Long and R.G.W. Norrish, *Proc. Roy. Soc.* (*London*), **A187**, 337 (1951).
10) F.H. Field, *J. Chem. Phys.*, **19**, 793 (1951); Th. Doehard, P. Goldfinger and F. Waelbroeck, ibid., **20**, 757 (1952).
11) G. Glockler, ibid., **19**, 124 (1951).
12) Brewer, Gilles and Jenkins, ibid., **16**, 797 (1948).
13) E.C. Baughan, *Quart. Rev.*, **7**, 103 (1953).
14) Calculated by the method of least squares from the heats of for mation of lower members (from thanee to hexane) in paraffin series, other than methane; E. J. Prosen, W. E. Johnson and F. D. Rossini, *J. Research NBS.*, **37**, 51 (1946), and their preceding papers.
15) Calculated from the heat of formation of dimethyl ether (H.A. Skinner, *Trans. Farad. Soc.*, **41**, 645 (1945).) using above C-H bond energy.
16) L. Pauling, "The Nature of the Chemical Bonds", Cornell Univ. Press, Ithaca, New York, (1940).
17) J. K. Syrkin and M. E. Dyatkina, "Structure of Molecules", Butterworth, (1950).
18) Paul, "Principle of Chemical Thermodynamics", McGraw-Hill, (1951).
19) H. Gilman and G.E. Dunn, *Chem. Revs.*, **52**, 77 (1953).
20) K.S. Pitzer, *J. Am. Chem. Soc.*, **70**, 2140 (1948).

atom for the heat of atomization of silicon and Pauling's electronegativity formula. The value 104 kcal./mol. was also calculated by Thompson[7] from ΔH_f for amorphous silica. The only Si-O bond energy derived from the heats of formation of organosilicon compounds was proposed by Thompson[7] as 117 kcal./mol. However, his combustion experiments contain considerable deviations, so we are not satisfied with that energy value. Also, from the molecular orbital calculation of ionic resonance energy the energy value of 118 kcal./mol. was obtained by Pearson.[21]

The Si-O bond energy term derived here from four organosilicon compounds is in good agreement and slightly lower than the value of 104 kcal./mol. for that bond energy in amorphous silica, calculated from the following data: $\Delta H_{atom.}$ for Si=89.9, $\Delta H_{atom.}$ for O=59.2 and ΔH_f for amorphous silica= −208.14 kcal./mol. There is also such an example between the C—C bond energies for diamond structure and paraffin series compounds.[16]

21) P.G. Pearson, *J. Chem. Phys.*, **17**, 969 (1949).

Summary

1. The heats of combustion of the following four compounds have been measured at 20°C and at constant volume: Tetramethoxysilane, hexamethoxydisiloxane, octamethoxytrisiloxane and hexamethoxydisilane.

2. From these combustion results the corresponding heats of combustion and formation at constant pressure and Si-O bond energy have been calculated, and it has been found that the Si-O bond energy in methoxy-polysilanes and -polysiloxanes was slightly lower than that in amorphous silica.

The authors wish to express their sincere thanks to Mr. R. Okawara for his helpful advice in the preparation of samples. The cost of this research was partly defrayed from the Ministry of Education, to which the authors' thanks are due.

Department of Applied Chemistry, Faculty of Engineering, Osaka University, Osaka

The Ultra-violet Absorption Spectrum of Pyridine N-oxide

By Mitsuo ITO and Norisuke HATA*

(Received December 21, 1954)

Introduction

Organo-chemical properties of pyridine N-oxide have been investigated by Ochiai and his coworkers[1]. Recently, the ultra-violet absorption spectra of these compounds in solutions have been measured by Hirayama and Kubota[2,3]. Generally, in the absorption spectra of π-conjugated compounds containing the heteroatoms, e.g., pyridine and diazines etc., there occur n-π^* electronic transitions as well as π-π^* transitions[4,5]. In the present investigation, the absorption bands due to these two electronic transitions are observed with pyridine N-oxide both in solution of non-polar solvent and in vapor, and the effects of proton donors on these absorption bands are discussed.

Experimental

Solution Spectrum.—The spectrum of pyridine N-oxide in various solutions was measured with a Beckman quartz spectrophotometer model DU, using a fused quartz cell of 1 cm. path. N-hexane, ethyl alcohol and water were used as solvents. Measurements were limited to the region of wavelength shorter than 350 mμ.

Vapor Spectrum.—Ultra-violet absorption spectra of pure pyridine N-oxide vapor and of a mixture with ethyl alcohol in the vapor phase were photographed with a medium quartz spectrograph having a linear dispersion of about 16 Å per mm. at 3,100 Å. The absorption cell was a quartz tube 40 cm. in length, and 3 cm. in diameter, to which a side recess was attached at the middle part. The sample sealed in a thin-walled glass ampoule was inserted in the side recess, and then the cell was evacuated to the pressure of about 10^{-3} mm Hg. After sealing off the cell, the ampoule was broken, the vapor filling the cell at pressures corresponding to the temperatures of the sample.

* Present address: Department of Pharmacy, Nagasaki University, Nagasaki.

1) E. Ochiai, *J. Org. Chem.*, **18**, 534 (1953).
2) H. Hirayama and T. Kubota, *Annual Reports of Shionogi Research Laboratory*, **2**, 47 (1952).
3) T. Kubota, *J. Pharm. Soc. Japan*, **74**, 831 (1954).
4) M. Kasha, *Discus. Farad. Soc.*, **9**, 14 (1951).
5) F. Halverson and R.C. Hirt, *J. Chem. Phys.*, **19**, 711 (1951).

In the case of mixed vapor, conc. alcohol solution of pyridine N-oxide (mole fraction, about 0.25) was used as the sample. Exposures were made against the hydrogen continium, varying the temperature of the sample from 0° to 110°C for the pure vapor, and from 10° to 120°C for the vapor mixture.

Results and Discussion

Solution Spectrum.—The absorption curves for various solutions are shown in Fig. 1.

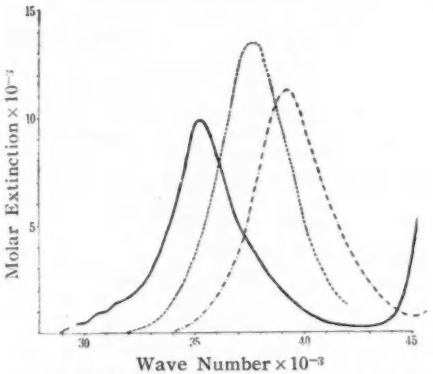

Fig. 1. Absorption spectrum of pyridine N-oxide.
——— *n*-hexane solution
------ ethyl alcohol solution
—·—·— water solution

As to the absorption of *n*-hexane solution, it appears that there are two absorption regions between 28,000 and 44,000 cm^{-1}; one of which is weak, accompanying a fine structure on longer wave-length end, and the other stronger having the maximum at 35,200 cm^{-1} (280 $m\mu$).

When either alcohol or water is used as the solvent, the absorption in the long wave-length region is not observed and the maximum shifts toward shorter wave-length side. Such a spectral behavior in pyridine N-oxide, supporting the assignment that weak long wave-length absorption is an n-π^* transition and the strong shorter wave-length absorption a π-π^* transition, may be explained as follows.

Pyridine N-oxide molecule has two pairs of 2p non-bonding electrons on the oxygen atom, one of which is considered to be in conjugation with the π-electron system of pyridine ring and the other to remain as a non-bonding pair. Generally, since the energy level of the non-bonding orbital lies above the highest π-level in the ground state, the n-π^* transition appears weakly in a longer wave-length region than the π-π^* transition. When proton donor such as alcohol or water is used as the solvent, the oxygen non-bonding orbital is largely stabilized in energy as a result of the formation of hydrogen bond[3]. Consequently, the n-π^* absorption disappears completely. At the same time, since the π-electron configuration will be perturbed by the formation of such a hydrogen bond, the π-π^* absorption shifts considerably to shorter wave-length, which is in agreement with our observation.

In order to estimate each absorption contribution from the n-π^* or π-π^* transition the peak analysis was made for the absorption of *n*-hexane solution according to the procedure given by Stephenson[6]. According to the well known equation,

$$f = 4.32 \times 10^9 \int \epsilon d\nu,$$

the oscillator strengths of the n-π^* and π-π^* transitions are calculated from the areas under the curves (a) and (b) in Fig. 2 respectively, their values being shown in Table I together with those for the other compounds[3,7]. As found from the table, while

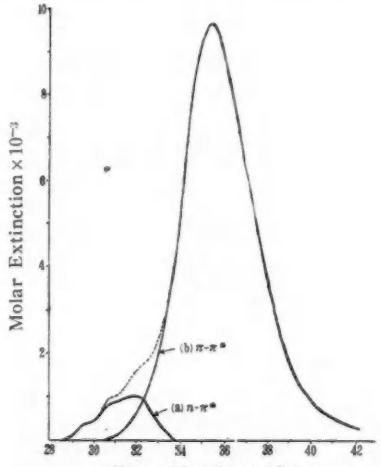

Fig. 2. Peak analysis of the absorption of *n*-hexane solution.

TABLE I
OSCILLATOR STRENGTH OF n-π^* AND π-π^* TRANSITIONS

Compound	$f(n\text{-}\pi^*)$	$f(\pi\text{-}\pi^*)$	$f(n\text{-}\pi^*)/f(\pi\text{-}\pi^*)$
Pyridine N-oxide	0.012	0.173	0.079
Pyridine[3]	0.003	0.041	0.073
Benzaldehyde[7]	0.0006	0.02	0.030
Acetophenone[7]	0.0006	0.014	0.043
P-benzoquinone[7]	0.0003	0.008	0.038

the f values for the n-π^* and π-π^* transitions are of considerably different orders for the

6) H.P. Stephenson, *J. Chem. Phys.*, 22, 1077 (1954).
7) H.L. McMurry, *J. Chem. Phys.*, 9, 241 (1941).

different compounds, their ratio is in the same order of 10^{-2} for pyridine N-oxide as for the other compounds. This also gives supporting evidence for the assignment with respect to the n-π^* and π-π^* transitions mentioned above.

Vapor Spectrum.—The absorption spectra at different temperatures for pure and mixed vapors are sketched in Fig. 3 and Fig. 4, respectively. In the figures the lines show the main absorption bands and their heights the relative intensities, the shaded portions indicating regions of continuous absorption. The calculated vapor pressure values of pyridine N-oxide are given for the various temperatures in the last columns of Fig. 3 and Fig. 4.

In the region 29,000 cm^{-1}~48,000 cm^{-1} there are four absorption regions (I, II, III and IV regions in Fig. 3 or Fig. 4). The longest

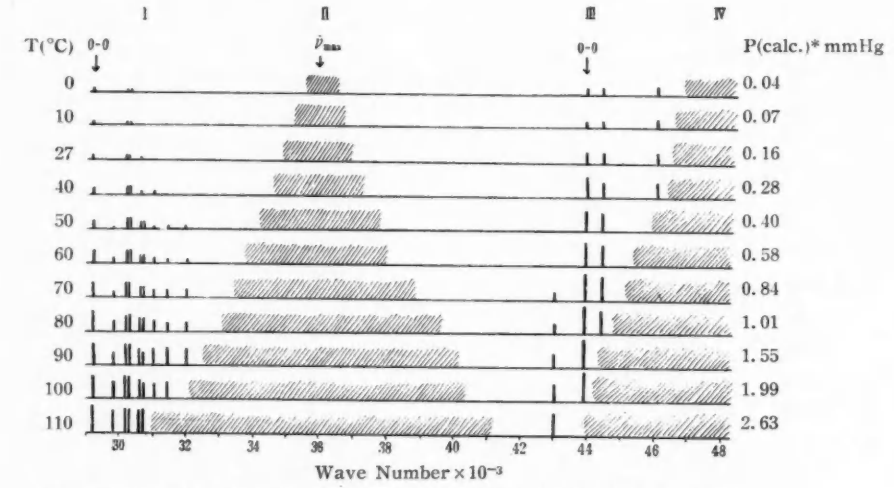

Fig. 3. Schematic absorption spectrum of pyridine N-oxide in pure vapor.
* Calculated by using the relation log P∝1/T and the boiling points of pyridine N-oxide (135° at 5 mm Hg, 113°C at 3mm Hg).

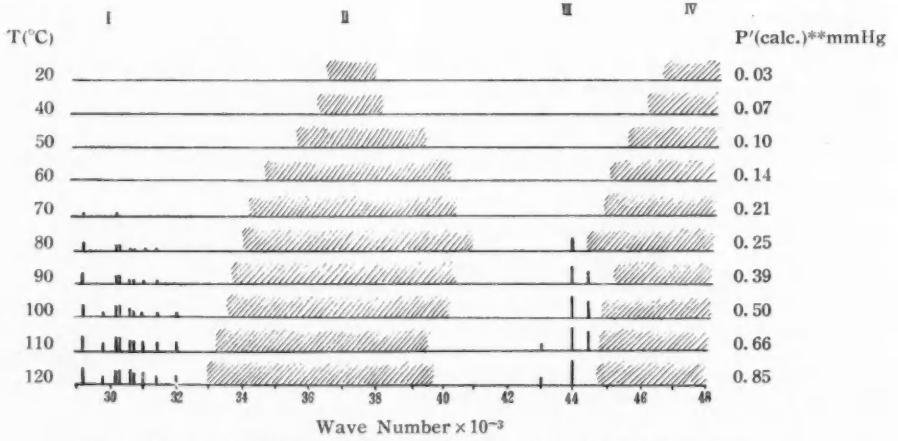

Fig. 4. Schematic absorption spectrum of pyridine N-oxide in vapor mixture with alcohol.
** The partial vapor pressure of pyridine N-oxide P′ is approximately given by $P' = G \times P$, where G is the mol fraction of pyridine N-oxide in alcohol solution and P the vapor pressure of pyridine N-oxide.

wave-length region I is of a very sharp vibrational structure having the O-O band at 29,291 cm^{-1} [8], corresponding to the n-π^* absorption of n-hexane solution. The next, region II is continuous having its absorption maximum at about 35,960 cm^{-1}, corresponding to the π-π^* absorption of n-hexane solution. These spectral features fit in with Kasha's distinguishing criteria[4] that in vapor spectrum n-π^* absorption generally consists of very sharp bands and π-π^* absorption moderately broad or continuous bands. Thus, in accordance with the assignment for the solution spectrum, we confirm that the region I is an n-π^* transition and the region II a π-π^* transition.

Similarly, the region III is accompained by an extremely sharp vibrational structure having the O-O band at 43,884 cm^{-1} [8] and the region IV is continuous. These spectral appearances suggest that the former is an n-π^{**} transition and the latter is a π-π^{**} transition, where π^{**} is a π-level lying above the π^*-level related to the regions I and II.

Comparing the spectra of the pure vapor and the vapor mixture, we may notice that: (1) at low temperatures the n-π^* and n-π^{**} absorptions appear evidently in the former, but they are not observed in the latter, and (2) the π-π^* absorption in vapor mixture, lying at a little shorter wave-length than that for pure vapor at low temperatures, approaches to the position for pure vapor with increasing temperature. This spectral behavior is almost the same as in the case of solution spectrum and shows that, even in the state of vapor, pyridine N-oxide molecule forms hydrogen bond with alcohol molecule at low temperatures[3]. With increasing temperature, the hydrogen bond is broken due to thermal motion, and then the spectral feature of vapor mixture becomes identical with that of pure vapor.

8) The detailed virbrational analysis is to be reported shortly.

Summary

The near ultra-violet absorption spectrum of pyridine N-oxide was measured in solution and vapor, and we concluded from the considerations of solvent effect, oscillator strength and the feature of vapor spectrum that the two of the four absorption regions are due to the excitation of the non-bonding electron, the others due to the excitation of π-electron. From the spectral behavior of pyridine N-oxide, it is also concluded that the pyridine N-oxide molecule forms hydrogen bond with alcohol or water molecule in vapor and solution state.

The authors wish to express their hearty thanks to Prof. S. Imanishi for his kind guidance and valuable suggestions in this research. They are also indebted to Prof. G. Kobayashi of Nagasaki University for his helpful advice and to Mr. H. Umezu for his assistance in the experimental part of this research.

Department of Chemistry, Faculty of Science, Kyushu University, Fukuoka

On the Electro-Osmotic Water Transport Through Cation-Exchange Resin Membranes

By Yoshio ODA and Tadashi YAWATAYA

(Received December 13, 1954)

Introduction

When ion-exchange resin membranes are used as the ionic permselective diaphragms of electrochemical operations, the movement of water takes place through the membranes simultaneously with the ionic migration. This phenomenon seems important from the practical point of view, since it governs the maximum concentration of the electrolyte solution attainable by means of electrolysis, using the membrane. Also, as it concerns the transport number and electric conductivity of the membrane, the study of the phenomenon is expected to supply valuable clues for clarifying the fundamental properties of the ion-exchange resins.

There are three ways of transference of a solvent through a membrane, according to the driving forces which cause it. They are classified as follows.

(a) Transference due to osmotic pressure.

(b) Transference due to the electric potential difference between the two surfaces of the membrane.

(c) Transference due to the difference of hydrostatic pressure, if present.

The item (a), which takes place in the case where the solutions of both sides of the membrane differ in concentration, was previously studied by the authors and reported elsewhere[1].

As the item (b) seems to be especially important in the ordinary applications, the present work is devoted to its study.

The water transference through a membrane caused by electric potential difference has been known as the electro-osmotic phenomenon and already explored to a considerable extent[2]. These previous works were, however, undertaken using mostly very dilute solutions, and lack the data for the range of comparatively high concentration, up to several normals, despite the fact that the range is expected to be the most prosperous field of applying ion-exchange resin membranes.

Although the electro-osmosis in the case where a membrane is inserted between solutions of different concentrations is important for practical purposes, the present study deals with, as the most simple ones, the cation-exchange resin membranes placed between solutions of the same kind and equal concentration.

Experimental

Ion-exchange Resin Membranes.—The cation-exchange resin membranes used in the experiments are mainly of sulfonated phenol resin type and prepared by Dr. M. Sekino and K. Kōno in the Research Laboratory of Asahi Glass Co. In addition to these a cation-exchange resin membrane of a similar type, Nepton CR-51, which had been furnished by Ionics Inc., U.S.A., was used.

The thickness of the membranes varied from 0.9 to 1.2 mm when swollen.

These membranes were thoroughly equilibrated with the solutions, to be used for measurements at least for 24 hours by repeatedly changing the solution.

Apparatus.—A glass cell composed of two half cells as shown in Fig. 1 was used, and a sample membrane was mounted between the flanges, the effective area of the membrane being 5.0 cm^2. The half cell at the right hand side was provided with a capillary tube which served to indicate the movement of the meniscus due to the liquid transportation from the left half cell to the right one. The inner diameter of the capillary was chosen so as to indicate the volume change as sensitively as possible, and it was calibrated with mercury.

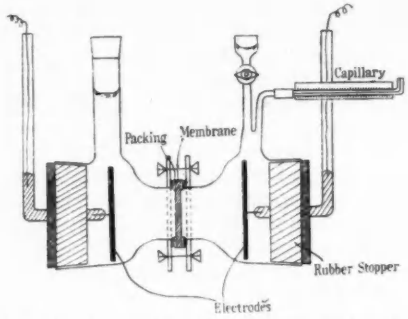

Fig. 1. Apparatus for measurement of electro-osmosis.

The electrodes were Ag and Ag-AgCl for the measurements in chloride solutions, and Pb and Pb-$PbSO_4$ for sulfate solution. Special care was taken for the use of electrodes of ample capacity in order to ensure reversibility of the electrodes.

During the experiments the main part of the cell was dipped into a water thermostat, and the temperature was kept at 25±0.2°C.

Results

It has been known[3] that the volume of electro-osmosis is proportional to the quantity of electricity flowed, namely the product of current intensity, I, and time, t.

$$v=\beta \cdot I \cdot t \qquad (1)$$

In the above equation β is the amount of electro-osmosis caused by the flowing of the unit quantity of electricity.

The present work was started by examining the above relation when using the cation-exchange resin membranes.

(1) Liquid Transference in Relation to Time of Electrolysis.—When the electrical circuit was closed in the apparatus shown in Fig. 1, it was observed that the meniscus in the capillary begins to move, and afterwards showed various tendencies as seen in Fig. 2. In the cases of curve I (Fig. 2) the meniscus retreats at first to the left for a little while and then turns to proceed to the right. On the contrary, in the case of the curve II the meniscus begins to proceed from the start.

Circuit breaking after the current has flowed for some duration causes in the former case a somewhat rapid shift of the

1) Reports of the Research Laboratory, Asahi Glass Co., Vol. III, No. 2, 180 (1953).

2) G. Schmid, *Z. Elektrochem.*, **55**, 229 (1951). K.S. Spiegler, *J. Electrochem.*, **100**, 303C (1953).

3) E. Manegold and K. Solf, *Kolloid Z.*, **55**, 273 (1931).

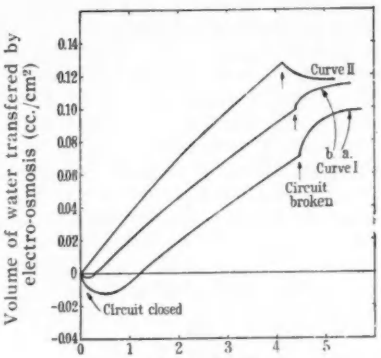

Curve I { a. PV-51, 2A/dm², 0.5N NaCl-soln.
b. Nepton CR-51, 2A/dm², 1N NaCl-soln.
Curve II Nepton CR-51, 2A/dm², 0.5 N $MgCl_2$-soln.

Fig. 2.

meniscus toward the right to come to a standstill. In the latter case it causes the retreat of the meniscus toward the left for a short time.

The mode of the initial meniscus movement, the type of curve I being more frequently met and curve II rather rarely, appeared to vary according to the stiffness of the membrane, kind and concentration of the equilibrating solution, and other unknown factors. The main cause of this initial anomaly seemed to be attributed to the bending of the membrane due to the applied electric field. But further study will be necessary to explain it in detail.

For the present purpose, however, it is sufficient to find the inclination of the linear part of the curves showing water transference.

(2) **Current Density and Rate of Electro-osmosis.**—The rate of electro-osmosis was calculated from the inclination of the linear part of the curves such as shown in Fig. 2, for several typical cation-exchange resin membranes in sodium chloride solution. The samples employed are of sulfonated phenol resin type, P-4, PV-51, and CR-51, the thickness being 0.10, 0.12 and 0.09 cm. respectively. The latter two are backed by a plastic screen to increase mechanical strength.

As shown in Fig. 3, the rate of electro-osmosis appears to be approximately proportional to the current density except within the region of high current density in case of P-4 membrane.

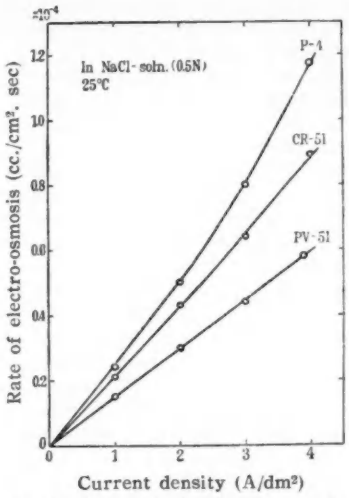

Fig. 3. Current density vs. rate of electro-osmosis.

Since the equation (1) has thus been confirmed to be applicable for the cation-exchange resin membranes, β in the equation will be employed hereafter to compare the characteristics of the membranes.

(3) **Electro-osmosis in Relation to the Concentration of the Solution.**—The relations between β and the concentration of the equilibrating sodium chloride solution were derived for the three sorts of membrane as shown in Fig. 4.

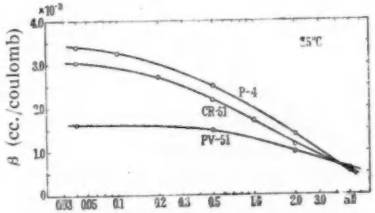

Fig. 4.

In the part of low concentration β rises gradually with the decrease in the concentration and approaches a characteristic value, β_0. There are remarkable differences among β_0 of the three membranes. As the concentration increases β for three membranes converge gradually to come to a nearly equal value at about 5 N.

(4) **β and pH of the Solution.**—The change of β with varying pH of the sodium chloride solution was measured, keeping the concen-

tration of chlorine ion constant at 0.5 N. The sample employed is PV-51. The result is plotted in Fig. 5.

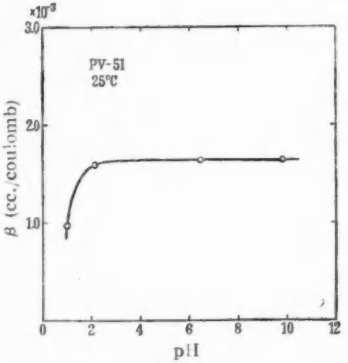

Fig. 5.

From pH 10 to pH 2, β remains approximately constant. The influence of pH seems to become remarkable as the concentration of hydrogen ion comes near that of sodium ion.

(5) Species of Electrolyte and β.—Although the present experiments have been carried out using mainly sodium chloride solution, and the cases in other electrolyte solutions will be dealt with in the future, the measurement of β in two other electrolyte solutions, i.e., magnesium chloride and sodium sulfate solution, are shown in Fig. 6

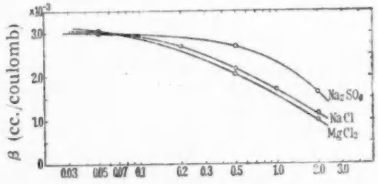

Fig. 6.

in comparison with those in sodium chloride solution. The two electrolytes were chosen in view of the fact that they possess anion or cation in common with sodium chloride.

As shown in the figures, the curves for NaCl- and $MgCl_2$- solution which have a common anion lie very close to each other, while the curve for Na_2SO_4 is separated.

Discussion

Although experimental data are not yet sufficient to allow fully quantitative discussion for the membrane equilibrated with the concentrated solution like those employed in this study, some analyses will be made to interpret the results obtained.

The cation-exchange resins as used in this experiment have as the active groups $-SO_3H$ and -OH radicals fixed on the matrix of hydrocarbon, and the former alone is considered to display cation-exchange action in the neutral solutions. The resin equilibrated with a salt solution, swollen to a degree depending on the concentration of the solution and the degree of cross-linkage of the resin matrix, contains cations (exchangeable ions or counter ions), equivalent to the exchangeable polyanionic groups and an equivalent number of cations and anions (non-exchangeable ions). As the concentration of outside solution increases, more salt molecules penetrate into the resin and non-exchangeable ions increase, and at the same time more water within the resin goes out.

Although the cations corresponding to the penetrating neutral salt are called non-exchangeable cations, apparently discriminating them from the exchangeable ones, it will be assumed in the following discussion that there is essentially no distinction between these two kinds of cation in the resin. This assumption does not appear unreasonable, because the cations mix thoroughly with each other due to the thermal motion in such narrow pores[4] as are found within an ordinary ion-exchange resins.

If an electric field is applied to these ion-exchange resin membranes, all the mobile ions migrate to transport electricity in the direction determined by their charges. Water surrounding these ions seems to accompany the migrating ions.

Transport Number of the Membrane and Electroosmosis.—If the cationic transport number of a cation-exchange resin membrane is denoted by n_+, the volume of the water which moves with a mol of a cation v_+ (including the volume of the cations), and the respective values for the anions in the same membrane by n_- and v_-, then the volume of the water flow caused by electricity of one Faraday is,

$$v = F\cdot\beta = n_+\cdot v_+ - n_-\cdot v_- = (v_+ + v_-)n_+ - v_- \qquad (2)^*$$

From the equation (2), β would change linearly with the cationic transport number n_+, if v_+ and v_- are assumed constant.

In order to compare the equation with the experimental results, the data of β in the preceding chapter are plotted in Fig. 7 against the transport number in the membranes cal-

4) R. Griessbach, *Z. Elektrochem.*, **57**, 147 (1953).

* $n_+ + n_- = 1$.

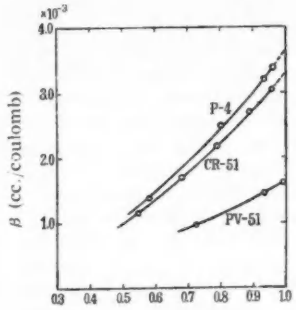

Cationic transport number (n_+).

Fig. 7.

culated** from the data reported elsewhere[1].

As shown in the figure, the linear relationship between β and n_+ appears to hold approximately. But as for the value of β corresponding to $n_+=1$, namely β_0, there is a remarkable discrepancy between the experiment and the theory. Although it is required from the equation (2) that β comes to have a constant value, β_0, regardless of the species of the membrane when n_+ approaches 1, the experimental result reveals a very different situation. Also, a constant inclination of the lines which is suggested by the equation (2) is not realized.

The reason for these discrepancies seems to be attributed to the incorrectness of the assumption that v_+ as well as v_- is constant.

As a matter of fact, from the experimental results the values of (v_++v_-) for the membranes, P-4, CR-51 and PV-51 are found to be 480, 415 and 230 cc./mol. NaCl respectively in the sodium chloride solution (1 N). It is noteworthy that these amounts of water accompanied with the ionic migration through the membrane are decidedly greater than the hydration water of sodium chloride.

The electro-osmosis seems to depend on the water content of the resin rather than on the hydration water of the migrating ions. The situation can be shown in Fig. 8 in which β is plotted against the water content of the resin (P-4).

Therefore in order to discuss the phenomenon further, it will be helpful to compare the concentrations of cation in the solution within the resin and of that in the membrane-permeating solution.

Concentrations of Cation in the Solution within Cation-exchange Resine Membranes and of that in the Membrane-permeating Solution.—Molarities of sodium ion in the solution within the cation-exchange resin membrane PV-51, and of that in the solution which passes through the membrane due to electro-osmosis were calculated from the experimental data and compared in Fig. 9.

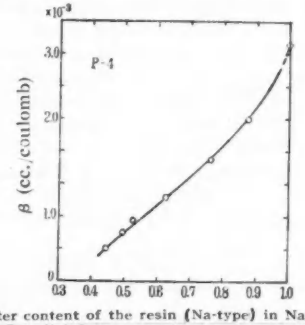

water content of the resin (Na-type) in NaCl-soln.
water content of the resin (Na-type) in distilled water

Fig. 8.

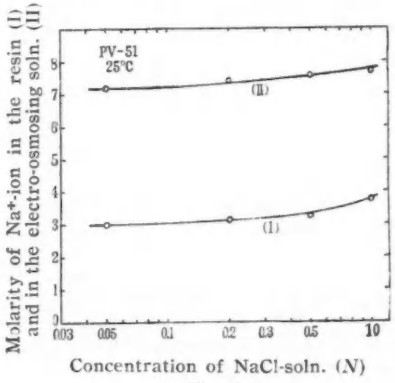

Concentration of NaCl-soln. (N)

Fig. 9.

The former is plotted on the curve (I) and the latter on the curve (II).

Here the procedures of the measurement and the calculation are as follows.

First, in order to measure the water content, small pieces of the cation-exchange resin membrane which have been equilibrated with the solutions of various concentrations are wiped out with filter paper, weighed, dried by means of an Abderhalden's dryer under reduced pressure for 3 hours at 100°C and then weighed again. Second, the cation content of the membranes is determined by

** Generally the transport numbers in an ion-exchange membrane are measured by inserting the membrane between the two solutions of different concentrations. The data of transport number plotted in Fig. 7 were obtained by extrapolating such data to the case where the concentrations of the two sides are made equal.

*** It is assumed that the transport number is not affected by the electro-osmosis.

The membrane-permeating solution due to electro-osmosis contains an unbalanced number of cation and anion, dependent on the transport number of the membrane, and is neutralized with the anion coming from the cathode.

measuring the cation-exchange capacity and the amount of non-exchangeable cation which may be taken out by leaching the membrane with a large volume of distilled water. Combining the above measurements, the molarity of the cation based on the water in the resin can be calculated.

On the other hand, the molarity of cation in the membrane-permeating solution can be calculated from the volume of electro-osmosis and the transport numbers of the membrane[***].

As shown in Fig. 9, two curves, (I) and

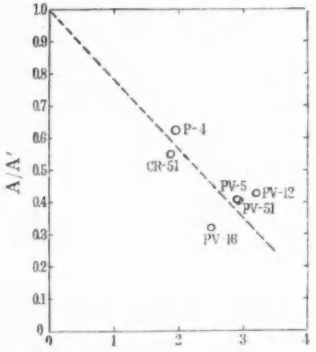

Molarity of fixed charge (A).
Fig. 10.

(II), are alike in the tendency that they decrease gradually with the lowering of the equilibrating concentration, and approach constant values respectively. There are, however, always a distinct difference between them, namely the electro-osmosing solution appears to be more concentrated in cation than that in the resin.

To explain the result, an idea of mobile water and fixed water in the resin membrane will be introduced.

Mobile Water and Fixed Water in the Resin Membrane.—As described in the early part of this chapter, there are fixed polyanions, exchangeable cations and non-exchangeable cations and anions in the pores of cation-exchange resin, and all of these ions are supposed to be hydrated. Besides those occupied by these hydrated ions, the pores of the resin have still remaining rooms which is to be filled with water. And its amount depends on the characteristics of the resin and concentration of the equilibrating solution.

Then it will be reasonable to assume that the hydration water of the fixed polyanionic group and the water at the immediate neighborhood of it are fixed and other water moves with ions when an electric field is applied. The former may be called fixed water and the latter mobile water.

Thus considered, the difference between the two curves (I) and (II) in Fig. 9 is readily explained. Since the electro-osmosing solution comes out from the membrane leaving the fixed water in the resin structure, it must necessarily be more concentrated in cation than the solution within the resin.

Now, as the most simple case, the electro-osmosis through a cation-exchange resin membrane containing no non-exchangeable ions will be considered. Such a state can be attained by equilibrating the membrane with a salt solution and then leaching it with a large volume of distilled water.

If we denote the amount of the fixed water in the resin membrane by α (g./meq. fixed ion), the molarity of the fixed charge by A, and the molarity of the cation in the membrane-permeating solution by A', the following relationship must exist among them.

$$A=\frac{1}{F\cdot\beta_0+\alpha}=\frac{1}{1/A'+\alpha} \tag{3}$$

Therefore,

$$A/A'=1-\alpha\cdot A \tag{4}$$

It is seen in the equation (4) that A/A' plotted against A should be linear, if α is independent of the structure of the resin and the concentration of the equilibrating solution.

The A/A' derived by extrapolation of the curves like those in Fig. 7 to zero concentration are plotted in Fig. 10 for the several membranes of similar type. The results are not yet enough to prove satisfactorily the constancy of α, but if we admit the linear relationship in the figure, the amount of the fixed water in the membrane can readily be estimated from the inclination of the line.

In this way α is found to be 10~15 mol./(eq. fixed ion) in the case of sulfonated phenol resin type in distilled water.

Thus considered, it becomes evident that neither v_+ or v_- in equation (2) is constant and is dependent on the properties of the resins.

Summary

The water transference due to electro-osmosis was studied for several cation-exchange resin membranes of sulfonated phenol resin type, mainly in sodium chloride solution. It was shown that (1) the electro-osmosis depended on the transport number of the membrane and the amount of water

contained in the resin, and (2) the experimental results could be explained by introducing the idea of fixed water and mobile water in the membrane. The fixed water is supposed to be composed mainly of the hydration water attached to the polar groups of the resin.

The writers would like to thank Dr. M. Sekino and Mr. K. Kono for their kind supply of the cation-exchange resin membranes employed in this study. Also they are indebted to Dr. S. Uemura and Mr. M. Funaoka for helpful suggestions.

Research Laboratory,
Asahi Glass Co. Ltd.,
Benten-cho, Tsurumi-ku,
Yokohama

Studies on Hydration by Ultrasonic Interferometer. V. The Change of Hydration of Inorganic Electrolytes with Temperature

By Tunetaka SASAKI* and Tatuya YASUNAGA

(Received January 17, 1955)

Introduction

We have already calculated the amount of hydration of ions from the compressibility of their solution, on the assumption that the hydration shells together with the ions themselves are incompressible under the pressure of an ultrasonic wave[1], and confirmed that the results obtained were satisfactory, since they were in accord with the other known facts on hydration[2].

As the reaction of ionic hydration is exothermic, temperature rise is supposed to cause the dehydration of ions. This is always true for a salt crystal having water of crystalization and we can expect that this also applies for the ionic hydration in the aqueous solution. The present study was undertaken to confirm this for several simple electrolytes in solution, using an ultrasonic interferometer for the measurement of the hydration.

Experimental Method

The ultrasonic interferometer used to measure the sound velocity and the method of calculation of hydration from the sound velocity was the same as in the first report[1]. The ultrasonic frequency used was 406.927 kc./sec.

Experimental Results and Discussions

The samples used were the aqueous solutions of 1N NaCl. The sound velocity was measured at the temperature ranging from 0°C to 60°C for water and the aqueous solution of NaCl. The curves obtained for water and NaCl solution ran parallel to each other as shown in Fig. 1.

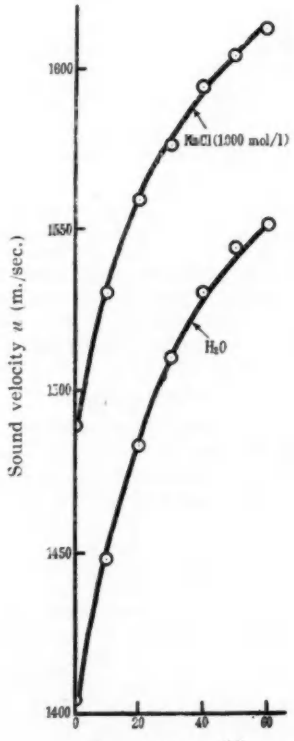

Fig. 1. Change of sound velocity with temperature.

* Present address: Department of Chemistry, Faculty of Science, Tokyo Metropolitan University, Setagayaku, Tokyo.

1) T. Yasunaga and T. Sasaki, *J. Chem. Soc. Japan*, 72, 87 (1951).

2) T. Yasunaga and T. Sasaki, *J. Chem. Soc. Japan*, 72, 89, 366 (1951); T. Sasaki, T. Yasunaga and H. Hujiwara, *J. Chem. Soc. Japan*, 73, 181 (1952).

TABLE I

Temperature °C	0	10	20	30	40	50	60
U (m./sec.)	1489.9	1528.0	1558.5	1576.6	1594.3	1604.0	1613.5
d (g./cc.)	1.0458	1.0441	1.0413	1.0396	1.0378	1.0338	1.0292
β (10^{-7} cgs)	43.08	41.02	39.54	38.70	37.91	37.60	37.33
V (cc./mol.)	137.8	125.9	116.7	106.6	106.5	99.6	103.5

We then calculated the compressibility from the sound velocity and density, and computed the amount of hydration of ions as the volume of incompressible water which was shown in Table I.

The amount of hydration decreases with increasing temperature as shown in Fig. 2.

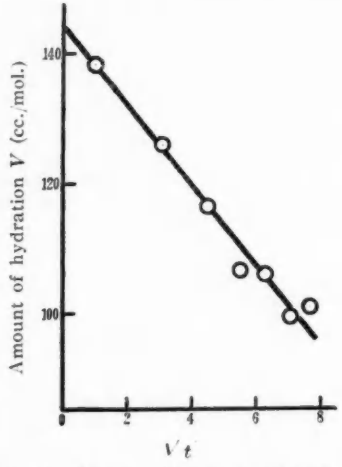

Fig. 2. Change of amount of hydration with temperature (1 N NaCl solution).

As the hydration reaction is exothermic, being caused by the mutual interaction between the ion and water dipoles, this temperature dependence is just what we expect. The relation is best expressed by

$$V_t = V_o - 6\sqrt{t}, \qquad (1)$$

where V_t is the volume of hydration water per mole solute at t°C and V_o, the value of V at 0°C. In this connection, we have already obtained a similar empirical formula for the change of the amount of hydration with concentration in a previous report[3], namely,

$$V_c = V_o - 36\sqrt{C}, \qquad (2)$$

where V_c denotes the volume of hydration water per mole solute at the concentration C and V_o, the value of V_c at the infinite dilution. We can see that temperature and concentration affect the hydration in exactly the same manner. Further, we calculated so called electrostriction, namely, the volume change due to the dissolution of salt in water at various temperatures as we did in a previous paper[4]. Fig. 3 shows the result.

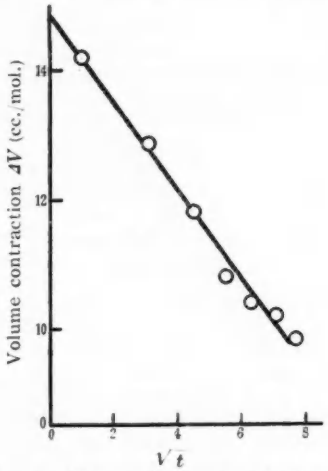

Fig. 3. Change of volume contraction with temperature (1 N NaCl solution).

In a previous paper[5] we have already confirmed a proportionality between the amount of hydration and the volume change at constant temperature and concentration for various electrolytes. From Figs. 2 and 3 we

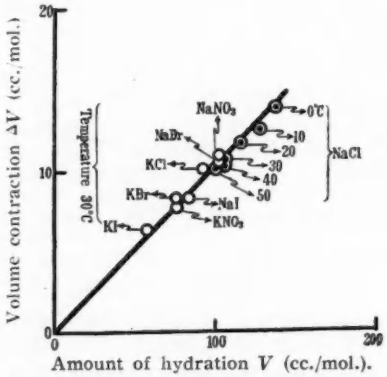

Fig. 4. Relation between amount of hydration and volume contraction.

3) T. Yasunaga and T. Sasaki, *J. Chem. Soc. Japan*, **72**, 89 (1951).

4) T. Yasunaga and T. Sasaki, *J. Chem. Soc. Japan*, **70**, 379 (1949).

5) T. Sasaki, T. Yasunaga and H. Hujiwara, *J. Chem. Soc. Japan*, **73**, 181 (1952).

can also obtain a proportionality between them even for the change of temperature at constant concentration. They are shown in Fig. 4.

It is confirmed that these two straight lines coincide with each other. In other words, the amounts of hydration and volume contraction show a unique proportionality irrespective of whether it is produced by the change of the temperature or the nature of electrolyte, and is expressed by

$$\Delta V/V=0.10.$$

Again, this fact shows, as reported in a previous paper[3], that ΔV and V are closely related to each other and are reasonably assumed to be the measure of hydration. If we assume that water of volume V is compressed by ΔV due to hydration, the mean pressure of hydration of about 4000 atmospheres is obtained, which is necessary to produce this volume contraction. The theoretical calculation for the relation between V and ΔV will be given in the next paper.

Summary

Sound velocity was measured at the temperature ranging from 0° to 60°C for water and the aqueous solutions of NaCl.

The amount of hydration was calculated from the sound velocity data for NaCl, which was shown to change linearly with the square root of temperature.

Volume contraction due to the dissolution of NaCl was also calculated at various temperatures which was found to change proportionally with the amount of hydration. The proportionality constant (0.10) was the same as obtained when the nature of the salt was changed. The mean hydration pressure was estimated to be about 4000 atmospheres.

A part of the cost of this study has been defrayed from the Scientific Research Expenditure of the Ministry of Education, given to one of the authors.

Department of Chemistry, Faculty of Science, Kyushu University, Fukuoka

Studies on the Electronic Structures of 2,5-Dichloroaniline and 2,5-Dichloronitrobenzene by Their Pure Quadrupole Spectra

By Hisao Negita, Hitoshi Yamamura and Haruo Shiba

(Received January 27, 1955)

Since Dehmelt and Krüger[1] succeeded in observing the pure quadrupole spectrum due to Cl^{35} and Cl^{37} of *trans*-1,2-dichloroethylene, many workers have reported spectra of various chlorine compounds, a few of them, however, from chemical viewpoints.

Among them, Meal[2] has pointed out that there is a rough linearity between Hammett's σ[3] of substituents and the resonance absorption frequencies in the spectra of several monosubstituted chlorobenzenes. But, as the absorption frequencies of *p*-nitrochlorobenzene and *o*- and *m*-chloroaniline have not so far been observed, i. e., data of the corresponding isomers of the two series have been missed, the electronic behaviors of amino- and nitro-groups in the benzene ring can not be compared with each other by the spectra of monosubstituted chlorobenzenes.

So we studied those of 2,5-dichloroaniline and 2,5-dichloronitrobenzene, each of which was observed at 77°K independently by Weatherly et al.[4], and by Bray et al.[5], and both of which were observed at 292°K by us.

Experimental

As pointed out by several workers,[1,6] the absorption frequency ν of chlorine compounds is expressed as follows, provided that the electronic distribution around the chlorine nucleus is axially symmetric:

$$\nu=|eqQ|/2h,$$

where e is the proton charge, q the electric field gradient at the nucleus, Q the nuclear quadrupole moment of the atom, which is negative,[7] and h Planck's constant. As the moment Q is regarded as constant in each compound, ν may be con-

1) H. G. Dehmelt and H. Krüger, *Z. f. Physik*, **129**, 401 (1951).
2) H. C. Meal, *J. Am. Chem. Soc.*, **74**, 6121 (1952).
3) L. P. Hammett, "Physical Organic Chemistry", McGraw-Hill Book Co. Inc., New York, N. Y. (1940), p. 188.
4) T. L. Weatherly and Q. Williams, *J. Chem. Phys.*, **21**, 2073 (1953).
5) P. J. Bray and P. J. Ring, *J. Chem. Phys.*, **21**, 2226 (1953).
6) H. C. Allen, *J. Phys. Chem.*, **57**, 501 (1953).
7) C. H. Townes and S. Geschwind, *Phys. Rev.*, **74**, 626 (1948).

sidered to be proportional to q, which, by its definition, has a maximum value in the pure covalent bond and is zero in the pure ionic. Accordingly, it is only necessary to determine ν in order to have an insight into the electronic structures of the chlorine compounds.

Apparatus.—To find the absorption frequencies, we used the frequency-modulated super-regenerative spectrometer,[1] its main oscillator being shown in Fig. 1. The frequencies generated were between about 25 Mc. and 38 Mc., for the absorption frequencies of the most organic chlorine compounds are known to lie in this range.

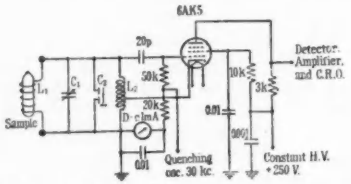

Fig. 1. Main oscillator of the spectrometer.
L_1; removable, ca. 1μH., L_2; fixed, ca. 1μH., tap being variable, C_1; variable, max. 50 pF., C_2; vibrating for freq. modulation.

For the frequency measurement, both the heterodyne frequency meter and the crystal oscillator of 1 Mc. were used. The experimental error was several kc., which was not serious in the following considerations.

Samples.—2,5-Dichloronitrobenzene and 2,5-dichloroaniline were prepared by nitration and successive reduction of *p*-dichlorobenzene[8]. These compounds were recrystallized to the constant melting points, 54°–55° and 50°C respectively.

The *p*-dichlorobenzene used as the reference material was commercial pure grade.

Results and Considerations

Results obtained are shown in Table I. The absorption lines of the two *p*-dichlorobenzene derivatives are more feeble than that of *p*-dichlorobenzene itself, the reason for which is not evident.

TABLE I

RESONANCE ABSORPTION FREQUENCIES DUE TO Cl^{35} OF *p*-DICHLOROBENZENE AND ITS DERIVATIVES (292°K)

Compounds			
Resonance freq. (Mc.)	33.927 (2) 34.044 (5)	34.286 (1,4)	35.545 (5) 37.290 (2)

In this Table, the numbers in the brackets stand for ordinal numbers of chlorine atoms in the benzene ring. These numbers were assigned in reference to the data of absorption frequencis of Cl^{35} in *o*- and *m*-nitrochlorobenzene (37.260 and 35.457 Mc. respectively[2]) and Br^{81} in *o*- and *m*-bromoaniline (220.255 and 222.614 Mc. respectively[9]) at 77°K; there were no available data of *o*- and *m*-chloroaniline to identify the lines of 2,5-dichloroaniline.

The lower values of frequencies of 2,5-dichloroaniline compared with that of *p*-dichlorobenzene indicate that the amino-group in the benzene ring releases elctrons, and more powerfully towards the *o*-position than towards the *m*-position. On the contrary, the greater values of 2,5-dichloronitrobenzene indicate that the nitro-group attracts electrons, and preferentially from the *o*-position; while the unique value of *p*-dichlorobenzene results from the fact that the state of the two chlorine atoms in this compound are equivalent, which is different from the cases of the other two derivatives.

These facts are in good agreement with the views of the "Electronic Theory of Organic Chemistry" by Robinson and Ingold and the results obtained from data of the dipole moments of amino- and nitro-groups[10]. Though the former is rather qualitative and the latter indirect, the quadrupole data show explicitly the state of electron shift.

Meal[3] suggested that there was a linear relation between resonance absorption frequency ν due to Cl^{35} and Hammett's σ of a substituent in monosubstituted chlorobenzene. We examined whether this relation existed or not in the *p*-dichlorobenzene derivatives, and found that there was a more excellent linearity between them, although the value of Hammett's σ for Cl (2) in the 2,5-dichloroaniline was not seen. These results are shown in Table II and Fig. 2.

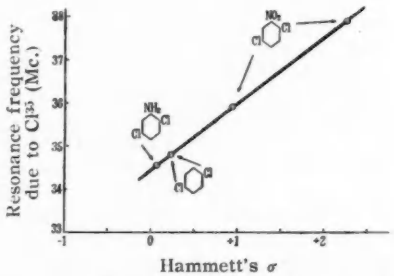

Fig. 2. Relation between the resonance absorption frequencies due to Cl^{35} and Hammett's σ of the substituents in *p*-dichlorobenzene and its derivatives.

8) E. Jungfleisch, *Ann. chim.*, [4], **15**, 257, 259 (1868).

9) P. J. Bray, *J. Chem. Phys.*, **22**, 950 (1954).

10) L. F. Fieser and M. Fieser, "Textbook of Organic Chemistry", Maruzen Publishing Co. Ltd., Tokyo, (1952), p. 449.

TABLE II

RESONANCE ABSORPTION FREQUENCIES AT 0°K AND HAMMETT'S σ OF *p*-DICHLOROBENZENE AND ITS DERIVATIVES

Compounds	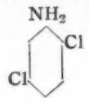		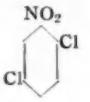		
Positon of Cl	Cl (2)	Cl (5)	Cl (1,4)	Cl (2)	Cl (5)
Hammett's σ	*o*-NH_2 ? *p*-Cl +0.227 ?	*m*-NH_2 −0.161 *p*-Cl +0.227 +0.066	*p*-Cl +0.227 +0.227	*o*-NO_2 +2.03 *p*-Cl +0.227 +2.257	*m*-NO_2 +0.710 *p*-Cl +0.227 +0.937
Resonance freq. at 0°K (Mc.)	34.42	34.55	34.80	37.92	35.92

In Table II, the value of Hammett's σ of *o*-nitro-group was taken from Meal's data and the resonance absorption frequencies at 0°K were obtained to ignore effects of lattice vibrations, by extrapolating the data[4,5] at 77°K and our data at 292°K, referring to the curve of *p*-dichlorobenzene. Assuming the linearity between ν and σ, we may compute σ of *o*-amino-group as −0.26 from Fig. 2.

Summary

The pure quadrupole spectra of 2,5-dichloroaniline and 2,5-dichloronitrobenzene were observed at room temperature (292°K), and the effects of electron releasing or attracting power of amino- and nitro-group in the benzene ring were compared with each other. On the other hand, a linear relation between resonance absorption frequencies due to Cl^{35} and Hammett's σ of the substituents in these compounds was found, and Hammett's σ of *o*-amino-group was assumed to be −0.26.

We are indebted to Prof. T. Ichikawa and Prof. D. Nakae for their generarity in granting us the use of their facilities, and to Prof. T. Kawano for the loan of the frequency meter.

Chemical Department, Faculty of Science, and Chemical Laboratory, Faculty of Engineering, Hiroshima University, Hiroshima

Synthetic Studies on the Benzofuran Derivatives. Part I. A New Synthesis of Karanjin

By Yoshiyuki KAWASE, Takashi MATSUMOTO and Kenji FUKUI

(Received February 4, 1955)

Karanjin, a kind of flavonol, was isolated in colorless needle crystals, $C_{18}H_{12}O_4$, m.p. 158.5°C as an unsaponifiable matter from the seed oil of a leguminous plant *Pongamia glabra Vent.* karanjia by Limaye[1] and by Beal and Katti[2].

The chemical structure of this substance was studied by Limaye[3] and Manjunath, Seetharamiah and Siddappa[4], and was proved to have a constitutional formula (I). The

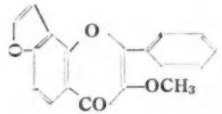

(I)

total synthesis of this karanjin (I) was reported by Seshadri and Venkateswarlu[5] and Row and Seshadri[6], but the yields were not so good. We also have been studying the synthesis of this substance independently and have obtained karanjin more easily and in higher yield.

Starting from 7-hydroxy-3-methoxyflavone-

1) D.B. Limaye, *Proc. Indian Sci. Congr.*, 1925, 118; 1926, 151.
2) Beal and Katti, *J. Am. Pharm. Assoc.*, 14, 1086 (1926).
3) D.B. Limaye, *Rasayanam*, I, 1 (1936); I, 119 (1937).
4) B.L. Manjunath, A. Seetharamiah and S. Siddappa, *Ber.*, 72B, 93 (1939).
5) T.R. Seshadri and V. Venkateswarlu, *Proc. Indian Acad. Sci.*, 13A, 404 (1941).
6) L.R. Row and T.R. Seshadri, ibid, 33, 168 (1951).

8-aldehyde (II) as Seshadri[7] and Limaye[8] did, 3-methoxyflavone-7,8-furan-α-carboxylic acid (IV) was synthesised in a good yield by the method of Tanaka[9] for benzofuran synthesis;—that is, the aldehyde (II) and ethyl bromomalonate were made to react in acetone in the presence of potassium carbonate, and the condensation product was hydrolysed to the acid (IV), m.p. 283°C (decomp.), yield 88.2%. As the intermediate product of this reaction, the colorless needle crystals, m.p. 183°C, were obtained and were found to be identical with the ethyl ester (IIIa) of the above mentioned acid (IV); therefore, it is clear that the ethyl ester of furan-α-carboxylic acid was produced in this reaction as the intermediate product.

Then, this acid (IV) was decarboxylated in quinoline in a stream of nitrogen gas with copper powder into colorless needle crystals, m.p. 159°C, yield 26.5%, the melting point of which was not depressed by admixture with natural karanjin (I). Further, this synthetic karanjin was derived to 3-hydroxy and 3-acetoxy derivatives and was decomposed into benzoic acid, methoxymethylkaranjketone (VI) and karanjic acid (VII) by alkaline hydrolysis. The melting points of these substances (I, Va, Vb, VI and VII) coincided well with those of the natural products, as shown in the following Table.

We are grateful to the Institute of Organic Chemistry, Osaka City University for carrying out microanalyses and to Prof. T. R. Seshadri for giving us the sample of natural Karanjin.

Experimental[10]

7-Hydroxy-3-methoxyflavone-8-aldehyde (II).—This aldehyde (II) was prepared from 7-hydroxy-3-methoxyflavone by the methods of Seshadri[7] and Limaye[8].

3-Methoxyflavone-7,8-furan-α-carboxylic acid (IV).—A Mixture of 7.5 g. of 7-hydroxy-3-methoxyflavone-8-aldehyde (II), 8 g. of ethyl bromomalonate, 30 g. of anhydrous potassium carbonate in 620 cc. of absolute acetone was refluxed under stirring for 10.5 hours on a steambath. After distilling off the acetone, the residue was mixed with a solution of 5 g. of potassium hydroxide in 50 cc. of water and heated on a steambath for one hour, then diluted with water, decolorised, filtered and acidified with dilute sulfuric acid. The precipitate was collected and dissolved in sodium bicarbonate solution, followed by filtering and acidifying with dilute sulfuric acid. The precipitates were collected, washed with water and recrystallised from alcohol in colorless plates of

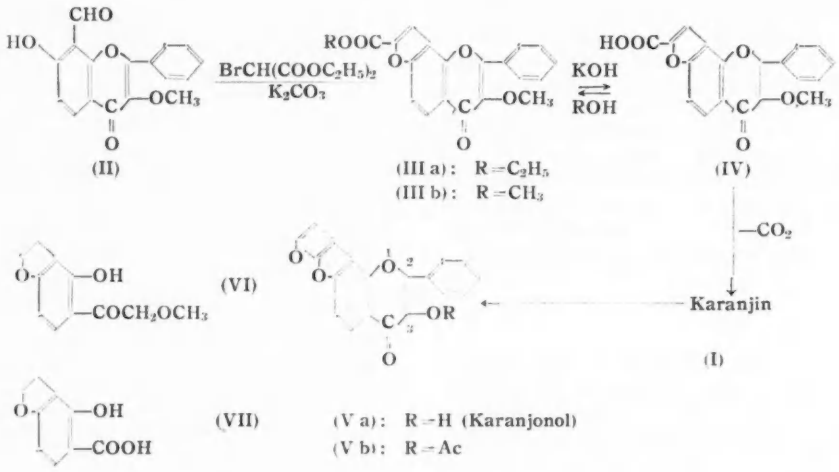

TABLE

THE MELTING POINTS OF KARANJIN AND ITS DERIVATIVES (°C)

Products	Karanjin (I)	3-OH (Va)	3-OAc (Vb)	Alkaline dec. prod. (VI)	Alkaline dec. prod. (VII)
Natural products[4]	158.5	199–200	177	96	218 (dec.)
Synthetic products	159	200	177	95.5	215–6 (dec.)

7) S. Rangaswami and T.R. Seshadri, *Proc. Indian Acad. Sci.*, **9A**, 7, 259 (1939).
8) S.D. Limaye and Limaye, *Rasayanam*, I, 161 (1939).
9) S. Tanaka, *J. Am. Chem. Soc.*, **73**, 872 (1951).
10) All melting points were not corrected.

m.p. 283°C (decomp.); yield 7.5 g. (88.2%). Found: C, 67.40; H, 3.83. Calculated for $C_{19}H_{12}O_6$: C, 67.86; H, 3.57%.

Esters (IIIa, IIIb) of the Acid (IV) and the Intermediate Substance of the above Reaction.—This acid (IV) was esterified with methanol or ethanol and sulfuric acid by the usual method. These esters were recrystallised from methanol or ethanol in colorless needles. *Methyl ester*, m.p. 194.5°C (IIIb). Found: C, 68.58; H, 3.96. Calculated for $C_{20}H_{14}O_6$: C, 68.57; H, 4.00%. *Ethyl ester*, m.p. 182°C (IIIa). Found: C, 69.38; H, 4.53. Calculated for $C_{21}H_{18}O_6$: C, 69.23; H, 4.39%.

A part of the residue after distilling off the acetone in the above procedure was recrystallised from alcohol in colorless needles, m.p. 183°C. Found: C, 69.22; H, 4.53. Calculated for $C_{21}H_{18}O_6$: C, 69.23; H, 4.39%. The melting point of this intermediate substance was not depressed by admixture with the ethyl ester (IIIa), m.p. 182°C.

Karanjin (I).—A mixture of 10 g. of 3-methoxyflavone-7,8-furan-α-carboxylic acid (IV), 4 g. of copper powder in 140 cc. of quinoline was heated under stirring in an atomosphere of nitrogen gas for about 40 minutes at 180–190°C until evolution of carbon dioxide ceased. It seems to be important that attention be paid to duration of time and temperature in this decarboxylation. After cooling, a little alcohol was added and the mixture was filtered from copper and was acidified with dilute hydrochloric acid. The brown precipitates thus formed were collected. The mother liquid was made alkaline with sodium hydroxyde and quinoline was distilled off by means of steam distillation. The residue was acidified after cooling and crude precipitates were collected. The crude karanjin thus obtained was recrystallised three times from ethyl acetate with the aid of charcoal in colorless needles, m.p. 159°C; yield 2.3 g. (26.5%). The melting point of this substance was not depressed by admixture with the natural karanjin. Found: C, 74.01; H, 4.04. Calculated for $C_{18}H_{12}O_4$: C, 73.97; H, 4.11%.

3-Hydroxyflavone-7,8-furan (Va) and 3-acetoxyflavone-7,8-furan (Vb).—These compounds (Va and Vb) were prepared according to the directions of Seshadri et al.[11].

A mixture of karanjin and anhydrous aluminium chloride in nitrobenzene was heated for one hour. After the product was worked up in the usual manner, the substance was recrystallised from dilute alcohol in colorless crystals, m.p. 200°C, which gave violet reaction with ferric chloride. This compound (Va) was acetylated to the 3-acetoxy derivate (Vb), m.p. 177°C with acetic anhydride in pyridine.

Alkaline Decomposition of Synthetic Karanjin.—According to the directions of Manjunath et al.,[4] a mixture of 1 g. of synthetic karanjin in alcohol and saturated methanolic potash was refluxed four hours. After distilling off the solvent, the residual solution was acidified and extracted with ether. The ethereal solution was first extracted with aqueous sodium bicarbonate solution and then with aqueous potassium hydroxide solution. Benzoic acid (0.2 g.) m.p. 121°C, and karanjic acid (0.02 g.) (VII), m.p. 215–6°C (decomp.) were obtained from bicarbonate solution; and methoxymethylkaranjketone (0.35 g.) (VI), m.p. 95.5°C, was obtained from potassium hydroxide solution.

Summary

Starting from 7-hydroxy-3-methoxyflavone-8-aldehyde (II), 3-methoxyflavone-7,8-furan-α-carboxylic acid (IV) was synthesised in good yield by the method of Tanaka for benzofuran synthesis and was decarboxylated in quinoline with copper powder into karanjin (I).

Faculty of Liberal Arts and Science, Toyama University, Toyama

11) T. R. Seshadri and V. Venkateswarlu, *Proc. Indian Acad. Sci.*, **17A**, 16 (1943).

A Semi-empirical Approach to the SCF Molecular Orbitals

By Hideo Kon

(Received January 27, 1955)

Introduction

The semi-empirical ASMO method recently proposed by Pariser and Parr[1] presents a way to calculate the transition energies and oscillator strengths of a variety of π-electron systems without much labour, in such a quantitative conformity with experiments as is rarely found in this kind of calculation. One of the essential points of their method is to alter the values of Coulomb repulsion integrals over atomic orbitals by introducing semi-empirical elements on a similar ground as in the method of "atoms in molecules" of Moffit[2]. The reasonable nature of such revision of integral values is illustrated by

1) R. Pariser and R.G. Parr, *J. Chem. Phys.*, **21**, 466, 767 (1953).

2) W. Moffit, *Proc. Roy. Soc.*, **A210**, 245 (1951).

the improvements in the results of their calculations. Nothing is known, however, of the improvements in the form of MO's which might be brought about by introducing the revised integrals, and one has to be content with the naive Hückel method or to resort to the elaborate, laborious, self-consistent field method of Roothaan[3].

In this preparatory note, a trial is given to incorporate the Pariser and Parr's semi-empirical method into the iterative procedure of Roothaan in order to reflect their reasonable revision of the integral values on the form of molecular orbitals. In the course of this calculation, the author found that Pople's treatment of unsaturated hydrocarbon[4] was based on a similar idea, but there, the Coulomb repulsion integrals were approximated by the Coulomb energy between two point charges instead of the charged sphere model of Pariser and Parr, and the details were somewhat different from the present treatment.

Modification of Roothaan's SCF Equation

A molecular orbital (ϕ_i) of a π-electron system is expressed as a linear combination of atomic orbitals (χ_p),

$$\phi_i = \sum_{\mu} c_{ip}\chi_p.$$

The coefficients c_{ip} are determined by a homogeneous set of equations derived by Roothaan.

$$\sum_q c_{ip}(L_{pq} - S_{pq}\varepsilon_i = 0,$$

$$L_{pq} = G_{pq} + I_{pq},$$

$$G_{pq} = \sum_i^{occ}[2J_{i,pq} - K_{i,pq}],$$

$$I_{pq} = \int \chi_p(\nu) H_{core} \chi_q(\nu) d\tau_\nu$$
$$= \int \chi_p(\nu)[T(\nu) + \sum_r U_r(\nu)]\chi_q(\nu) d\tau_\nu .$$

$U_r(\nu)$ is the potential on the electron ν due to the atom r stripped of its π-electron. $J_{i,pq}$ and $K_{i,pq}$ are defined as follows:

$$J_{i,pq} = \int\int \phi^*_i(\mu)\phi_i(\mu)[e^2/r_{\mu\nu}]$$
$$\chi^*_p(\nu)\chi_q(\nu) d\tau_\nu\, d\tau_\mu,$$
$$K_{i,pq} = \int\int \phi_i{}^*(\mu)\phi_i(\nu)[e^2/r_{\mu\nu}]$$
$$\chi^*_q(\mu)\chi_q(\nu) d\tau_\mu d\tau_\nu .$$

The simplifying assumptions of Pariser and Parr such as; 1) zero differential overlap, $\chi_p\chi_q = 0$, 2) neglect of non-neighbour core integral I_{pq}, are taken into account here, so that $J_{i,pq}$ and $K_{i,pq}$ are rewritten in terms only of atomic Coulomb repulsion integrals as follows,

$$J_{i,pq} = 0, \quad p \neq q,$$
$$J_{i,pp} = \sum_q c^2_{iq} \int \chi^*_q(\mu)\chi_q(\mu)[e^2/r_{\mu\nu}]\chi^*_p(\nu)\chi_p$$
$$(\nu) d\tau_\mu d\tau_\nu = \sum_q c^2_{iq}(qq \mid pp)$$
$$= c^2_{ip}\,(pp \mid pp) + \sum_{q\neq p} c^2_{iq}(qq \mid pp),$$
$$K_{i,pq} = c_{ip}c_{iq}\,(pp \mid qq).$$

Similarly, the core integrals reduce to two integrals:

$$I_{pq} = \alpha_p, \quad p = q,$$
$$= \beta_{pq}, \quad p \neq q, \text{ atom } p \text{ being linked directly to atom } q,$$
$$= 0, \quad \text{otherwise.}$$

Thus the expression for the quantity L_{pq} is replaced by

$$L_{pp} = \alpha_p + \sum_i 2c^2_{ip}(pp \mid pp) + \sum_i \sum_{q\neq p} 2c^2_{iq}(pp \mid qq)$$
$$- \sum_i c^2_{ip}\,(pp \mid pp)$$
$$= \alpha_p + \frac{1}{2} Q_p(pp \mid pp) + \sum_{q\neq p} Q_q(qq \mid pp),$$
$$L_{pq} = \beta_{pq} - \sum_i c_{ip}c_{iq}(pp \mid qq)$$
$$= \beta_{pq} - \frac{1}{2} P_{pq}(pp \mid qq), \quad p \neq q.$$

Here Q_p is the π-electron density on p-atom and P_{pq} reduces to the mobile bond order, if atoms p and q are the neighbouring atoms, but if not, it has not any definite physical meaning. In addition to these simplifications, the following assumptions are made in this paper in dealing with the core integrals α_p and β_{pq}.

1) The Coulomb integral α_p can be approximated as the valence state ionization potential (W_{2p}) of a $2p$ electron on a free atom, less the sum only of the Coulomb repulsion integrals (pp qq), summation being carried out over all the other atoms q involved in the π-electron system. This neglect of Coulomb penetration integrals is found to reduce the labour without having a significant influence on the good numerical performance of Pariser and Parr's original work. 2) The resonance integral β_{pq} which as in ref. 1, is one of the empirical parameters and is carried from molecule to molecule, is assumed, apart from Pariser and Parr, to be proportional to the inverse sixth-power of the bond distance r_{pq} and the proportionality constants are so chosen as to reproduce the observed first transition energy of a particular molecule as closely as possible. As the reference molecule, ethylene, formaldehyde and pyrazine

3) C.C.J. Roothaan, *Rev. Mod. Phys.*, 23, 69 (1951); R. G. Parr and R.S. Mulliken, *J. Chem. Phys.*, 18, 1338 (1950).

4) J.A. Pople, *Trans. Farad. Soc.*, 49, 1375 (1953).

are chosen for the bond C=C, C=O and C=N, respectively. In ref. 1, it is postulated that β_{pq} can be expressed as, $\beta_{pq}=a\exp(-br_{pq})$. Two experimental data being needed to fix the parameters a and b, it is not easy to extend it to other cases than C=C bonds. Whether or not the inverse sixth-power equation is appropriate will be tested by applying it to a variety of compounds and by comparing the results with observations. Taking these assumptions into account, the matrix element L_{pp} can be written down as,

$$L_{pp}=W_{2p}+\frac{1}{2}Q_p(pp\,|\,pp)+\sum_{q\neq p}(Q_q-1)(qq\,|\,pp).$$

If we put, $Q_p=Q_q=1$, then L_{pp} becomes a constant. As L_{pp} in the present treatment plays an analogous role to the Coulomb integral in the simple molecular orbital method, the constant L_{pp} will bring about a uniform distribution of π-electrons as in the alternant hydrocarbons treated by the simple molecular orbital method. For non-alternant hydrocarbons and hetero-molecules, Q_p, $Q_q\neq1$ and L_{pp} depends in a complicated manner on the geometrical configuration of the molecule, that is L_{pp} is a function not only of the charge density of p-atom and q-atoms. In Wheland and Mann's iterative method, the Coulomb integral on an atom p is dependent only on Q_p[5]. The above mentioned functional relation, however, is a more satisfactory one and is in harmony with the Coulson and Longuet-Higgins' theory[6], where the charge density on an atom and the Coulomb integral of other atoms are connected to each other by their mutual polarizability (π_{pq}).

Roothaan's iterative procedure to find the self-consistent set of c_{ip}'s is then followed, making at each step a guess at a better set of c_{ip} values to attain a rapid convergence. The symmetry coordinates are fully made use of in order to reduce the order of secular equations. Of the molecules calculated in this paper, ethylene and benzene have geometrical symmetry sufficient for finding the self-consistent set of c_{ip}'s only through the symmetry requirements, and so the iteration is unnecessary.

Numerical Values of the Basic Quantities

Following Pariser and Parr, the Coulomb repulsion integrals $(pp\,|\,qq)$ are computed by making use of their uniformly charged sphere model for bond distances longer than 2.80 Å and proper quadratic extrapolation formulae are used for bonds shorter than 2.80 Å. The resonance integral β_{pq} is computed as mentioned above from the formula, $\beta_{pq}=k/r^3_{pq}$, k being the proportionality constant, to which numerical values -17.464, -13.983 and -8.8086 are assigned for C=C, C=N and C=O bond, respectively. In Fig. 1 are shown the geometricals and designations for the calculated eight molecules. Except for s-triazine, geometricals are all based on the experimental data.

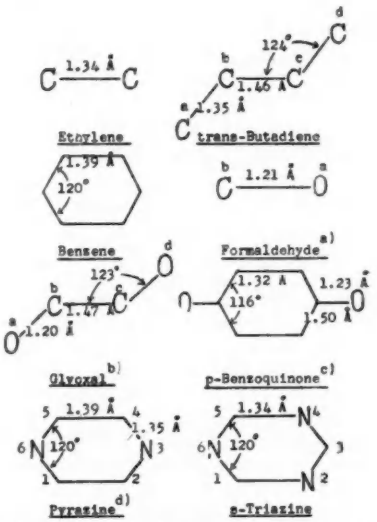

Fig. 1. Geometricals and designations of the calculated molecules.

a) D. P. Stevenson, J. E. LuValle and V. Schomaker, *J. Am. Chem. Soc.*, **61**, 2508 (1939).
b) J. E. LuValle and V. Schomaker, ibid., **61**, 3520 (1939).
c) S.M. Swingle, ibid., **76**, 1409 (1954).
d) V. Schomaker and L. Pauling, ibid., **61**, 1769 (1939).

Results of Calculation

After the iterative processes have come to convergence, the electronic transition energies are calculated by use of the following formula, no configuration interaction being allowed for, except in the symmetry degenerate cases of benzene and s-triazine.

$$\left.\begin{matrix}E_{V(ij)}\\E_{T(ij)}\end{matrix}\right\}-E_N=(\epsilon_j-\epsilon_i)-(J_{ij}-K_{ij})\pm K_{ij}.$$

Here, E_N, E_V and E_T designate the energy of the ground, excited singlet and excited triplet configuration, respectively, electronic excitation being from orbital i to j. J and K are the Coulomb repulsion and exchange

5) G.W. Wheland and D.E. Mann, *J. Chem. Phys.*, **17**, 264 (1949).
6) C. A. Coulson and H. C. Longuet-Higgins, *Proc. Roy. Soc.*, **A191**, 39; **A192**, 16 (1947).

repulsion integrals in terms of molecular orbitals.

$$J_{ij}=\int\int\phi^*_i(\mu)\phi_i(\mu)[e^2/r]\phi^*_j(\nu)\phi_i(\nu)d\tau_\mu d\tau_\nu\,,$$
$$K_{ij}=\int\int\phi^*_i(\mu)\phi^*_j(\mu)[e^2/r]\phi_i(\nu)\phi_j(\nu)d\tau_\mu d\tau_\nu\,.$$

The calculated results are compared in Tables I-III with the observed values and with those by Pariser and Parr.

TABLE I

CALCULATED TRANSITION ENERGIES VS. EXPERIMENTAL VALUES OF HYDROCARBONS

Molecule	State	Calculated energy above the ground state (ev)		Obs.*) (ev)
		This paper	Pariser-Parr	
Ethylene	$^1B_{1u}$	(7.60)	(7.60)	7.60
	$^3B_{1u}$	4.47	4.5	3.1—5.6
trans-Butadiene	^1B_u	6.19	6.21	6.0
	^1A_g	7.72	7.87	7.2(?)
	^3B_u	4.10	3.92	—
	^3A_g	6.17	4.61	—
Benzene	$^1B_{2u}$	4.96	4.9	4.9
	$^1B_{1u}$	5.37	5.3	6.0
	$^1E_{1u}$	7.01	7.0	7.0
	$^3B_{1u}$	3.62	4.0	3.8
	$^3E_{1u}$	4.52	4.45	—
	$^3B_{2u}$	4.96	4.9	—

*) See ref. 1 and those cited there.

It can be seen there that, in spite of the neglect of the Coulomb penetration integrals, the calculated values agree well with those observed, almost to the same extent as do the Pariser and Parr's values. It must, also, be noted that these agreements are obtained without taking account of the configuration interactions, except in benzene and triazine. This may be accepted as a good reason for neglecting the Coulomb penetration integrals and for the availability of the simple inverse sixth-power formula to compute β_{pq}, at least in hydrocarbons.

TABLE II

CALCULATED TRANSITION ENERGIES VS. EXPERIMENTAL VALUES FOR PYRAZINE AND *s*-TRIAZINE

Molecule	State	Calculated energy above the ground state (ev)		Obs. (ev)
		This paper	Pariser-Parr	
Pyrazine	$^1B_{3u}$	4.74	4.71	4.77
	$^3B_{3u}$	3.03	3.85	3.35
s-Triazine	$^1A'_2$, $^3A'_2$	5.43	5.29	5.62*)
	$^1A'_1$	6.17	—	—
	$^1E'_1$	7.41	—	—
	$^3A'_1$	4.97	4.26	—

*) R.C. Hirt, F. Halverson and R.G. Schmitt, *J. Chem. Phys.*, **22**, 1148 (1954).

The calculation of *s*-triazine is based on the assumed bond length shown in Fig. 1, because it was non-existent. A slightly shorter C=N bond distance (1.34 Å) than in pyrazine is presumed for *s*-triazine, taking into account that the C=N bond in cyanuric triazide is shorter than 1.35 Å. As shown in Table II, the calculated result for N→V transition in *s*-triazine is improved, compared with Pariser-Parr's value. Recently it is reported that the existence of this molecule was shown by Grundmann and Kreutzberger. The experimental data of ultraviolet and infrared absorption spectra are published, and the detailed x-ray analysis is reported in progress, by which the present calculation might be revised so as to allow for the experimentally determined bond lengths.

TABLE III

CALCULATED TRANSITION ENERGIES VS. EXPERIMENTAL VALUES FOR OXYGEN CONTAINING MOLECULES

Molecule	State	Calculated energy above the ground state (ev)	Obs. (ev)
Form-aldehyde*)	$^1A_1$	7.80	7.95
	$^3A_1$	4.49	—
Glyoxal	^1B_u	7.47	7.51**)
	^3B_u	5.09	—
p-Benzo-quinone	$^1B_{2u}$	6.08	5.21***)
	$^3B_{2u}$	4.37	—

* Slight differences in calculated results between the present and the previous communication (This Bulletin, 27, 565 (1954).) are due to the different bond lengths adopted.

** Estimated value; see the previous communication (This Bulletin, loc. cit.)

*** G. Scheibe et al., *Ber.*, **59**, 2617 (1926).

A comment on the calculated results of *p*-benzoquinone will be given in Sec. V.

The self-consistent molecular orbitals finally obtained are tabulated in Tables IV-V. Unfortunately, none of the molecules treated in this paper has definite dipole moment and there seems to be no means of crucial test for the quality of the molecular orbitals obtained. A few points are still to be noted. 1) The bond lengths r_{ab} and r_{bc} of *trans*-butadiene calculated from the theoretical bond orders through the bond order-bond length relation of Coulson are 1.35 Å and 1.49 Å, while the assumed values are 1.35 Å and 1.46 Å, respectively, a situation satisfactorily self-consistent. For other molecules containing hetero-atoms, the existence of excess charge prevents one from setting up a simple relation between bond orders and bond lengths. However, the bond length r_{12} of pyrazine, where the net positive charge on carbon atoms is comparatively small, the

computed and assumed (experimental) bond lengths are in complete agreement, 1.39 Å.

2) The π-electron density on nitrogen atoms of pyrazine is computed by the simple molecular orbital method using the set of correction parameter for nitrogen atom which was found by Lowdin[7] to result in satisfactory agreements between the computed and observed values of dipole moment in diazines. It is 1.155 in units of electronic charge, while the present method gives only a little higher value, 1. 238.

These together with the fact that the present method applied to fulvene[8], yields the value of dipole moment in satisfactory agreement with the estimated value, might be helpful for judging the quality of the molecular orbitals obtained here.

TABLE IV

SELF-CONSISTENT MOLECULAR ORBITALS*)

Molecule	ε (ev)	Molecular Orbital	
trans-Butadiene	− 2.480	$\phi_1=0.4397\ (\chi_a+\chi_d)+0.5538\ (\chi_b+\chi_c)$	$q_a=1$
	− 0.296	$\phi_2=0.5538\ (\chi_a-\chi_d)+0.4397\ (\chi_b-\chi_c)$	$q_b=1$
	10.826	$\phi_3=0.5538\ (\chi_a+\chi_d)-0.4397\ (\chi_b+\chi_c)$	$p_{ab}=0.974$
	13.010	$\phi_4=0.4397\ (\chi_a-\chi_d)-0.5538\ (\chi_b-\chi_c)$	$p_{bc}=0.227$
Formaldehyde	− 3.701	$\phi_1=0.5472\ \chi_a+0.8370\ \chi_b$	$q_a=1.401$
	10.916	$\phi_2=0.8370\ \chi_a-0.5472\ \chi_b$, $q_b=0.599$	$p_{ab}=0.916$
Glyoxal	− 5.140	$\phi_1=0.5541\ (\chi_a+\chi_d)+0.4393\ (\chi_b+\chi_c)$	$q_a=1.384$
	− 3.853	$\phi_2=0.6205\ (\chi_a-\chi_d)+0.3390\ (\chi_b-\chi_c)$	$q_b=0.616$
	9.202	$\phi_3=0.4393\ (\chi_a+\chi_d)-0.5541\ (\chi_b+\chi_c)$	$p_{ab}=0.908$
	11.847	$\phi_4=0.3390\ (\chi_a-\chi_d)-0.6205\ (\chi_b-\chi_c)$	$p_{bc}=0.156$

*) q: π-electron density in units of e; p: mobile bond order

Criticism of the Assumption-1

Now it seems necessary to make a remark on the validity of assumption-1, made in sec. II. According to the approximation of zero-differential overlap adopted throughout the present calculation, the Coulomb integral (α_p) of an electron in the potential field due to the atomic cores in a molecule is expressed in terms of the Coulomb repulsion integrals as well as of the Coulomb penetration integrals as follows:

$$\alpha_p=W_{2p}-\sum_q[(pp\,|\,qq)+(q:\,pp)]\,,$$

Of the integrals in this equation, the Coulomb penetration integrals $(q:\,pp)$ can not be computed easily, in cases where the atoms p and q are of different species. As, in addition, the order of magnitude of $(q:\,pp)$ is supposed to be relatively small, they are left out, as a first approximation, in the calculations in the preceding sections. In order to see how much the results would be affected by this simplification, *trans*-butadiene is treated by use of the Coulomb integrals computed without leaving out the Coulomb penetration integrals. Instead of computing $(q:\,pp)$ exactly, corrections are made for L's by subtracting 1.0 and 1.5 ev, respectively, from the L_{pp}(atom p being a methylene carbon)

TABLE V

SELF-CONSISTENT MOLECULAR ORBITALS

Molecule	ε (ev)	Molecular Orbital	
Pyrazine	− 4.507	$\phi_1=0.3646\ (\chi_1+\chi_2+\chi_4+\chi_5)+0.4838\ (\chi_3+\chi_6)$	$q_1=0.881$
	− 2.107	$\phi_2=0.2397\ (\chi_1-\chi_2-\chi_4+\chi_5)-0.6205\ (\chi_3-\chi_6)$	$q_3=1.238$
	− 0.316	$\phi_3=0.5000\ (\chi_1+\chi_2-\chi_4-\chi_5)$	$p_{12}=0.651$
	9.572	$\phi_4=0.3421\ (\chi_1+\chi_2+\chi_4+\chi_5)-0.5157\ (\chi_3+\chi_6)$	$p_{23}=0.650$
	11.013	$\phi_5=0.5000\ (\chi_1-\chi_2+\chi_4-\chi_5)$	
	13.506	$\phi_6=0.4388\ (\chi_1-\chi_2-\chi_4+\chi_5)+0.3390\ (\chi_3-\chi_6)$	
s-Triazine	− 4.965	$\phi_1=0.3569\ (\chi_1+\chi_3+\chi_5)+0.4538\ (\chi_2+\chi_4+\chi_6)$	$q_1=0.620$
	− 1.940	$\phi_2=0.2138\ (\chi_1-2\chi_3+\chi_5)-0.3478\ (\chi_2+\chi_4-2\chi_6)$	$q_2=1.380$
	− 1.940	$\phi_3=0.3703\ (\chi_1-\chi_5)\quad+0.6024\ (\chi_2-\chi_4)$	$p_{12}=0.621$
	10.402	$\phi_4=0.6024\ (\chi_1-\chi_5)\quad-0.3703\ (\chi_2-\chi_4)$	
	10.402	$\phi_5=0.3478\ (\chi_1-2\chi_3+\chi_5)+0.2138\ (\chi_2+\chi_4-2\chi_6)$	
	13.448	$\phi_6=0.4538\ (\chi_1+\chi_3+\chi_5)-0.3569\ (\chi_2+\chi_4+\chi_6)$	

7) P.O. Lowdin, *J. Chem. Phys.*, **19**, 1323 (1951).
8) H. Kon, to be published soon.
9) R.G. Parr and B.L. Crawford, Jr., *J. Chem. Phys.*, **16**, 1049 (1948).

and L_{qq} (atom q being a methine carbon). This manner of correction comes from the following consideration: The values of Coulomb penetration integrals (p: qq), where atom p and q are both carbon, can be obtained through the formula derived by Parr and Crawford[9] using the Slater type atomic orbitals. They are 0.91 and 0.58 ev for the interatomic distances 1.35 Å and 1.46 Å, respectively. The methylene carbon atoms in butadiene have one formal double bond (1.35 Å), while the methine carbons have one formal single (1.46 Å) and double bond. Assuming the contributions from the other atoms than those linked together directly to be small, the corrections to be made for L's of a methylene and methine carbon atoms are 0.91 and 1.49 ev, respectively, which are rounded to 1.0 and 1.50 ev as given above. This correction, though it is only approximate because of ignoring the effect of the hydrogen atom and the non-neighbouring carbon atoms, would be sufficient for the qualitative purpose.

TABLE VI
COMPARISON OF CALCULATED RESULTS WITH AND WITHOUT CORRECTION

	Correction	
	with	without
Orbital energy (ev)	− 2.730	− 2.480
	− 0.434	− 0.296
	10.689	10.826
	12.777	13.010
Excit. energy (ev)		
^1B_u	6.20	6.19
^3B_u	4.10	4.10
Coeff. of AO		
c_{1a}	0.4258	0.4397
c_{2a}	0.5645	0.5538
π-elec. density		
q_a	0.953	1.000
q_b	1.046	1.000
Bond order		
p_{ab}	0.972	0.974
p_{bc}	0.228	0.227

The calculated results of transition energy, coefficients of AO, π-electron densities and mobile bond orders, with and without correction are compared in Table VI. As can be seen there, the overall alteration brought about by introducing the correction is a minor one. And though the orbital energies are changed a little after correction, the transition energies are almost unchanged. The same holds for the relation between the AO coefficients and the bond orders derived from the former.

Conspicuous among the results may be the fact that the uniformity of π-electron distribution in butadiene (or, the hydrocarbons in general), which is assured in the Hückel method is broken down by the correction. At any rate the results in Table VI, together with the good agreements between the calculated and the observed transition energies show that one can safely dispense with Coulomb penetration integrals at least in computing the transition energies of hydrocarbons (and those hetero-molecules where the perturbation due to the hetero-atoms are not so serious), and that the wave functions so obtained would be fairly good approximations to the best possible ones.

The numerical agreement between the computed and experimental transition energy of p-benzoquinone is shown to be inferior to other cases. (Table III) The situation may probably be improved by making such a correction as mentioned above, especially for the tertiary carbon atoms (p) where, owing to the adjacent electronegative oxygen atoms, the amount to be subtracted from L_{pp} is considered too great to be ignored. It can also be understood from the similar point of view that the π-electron densities on nitrogen atoms listed in Table V appear a little higher than desirable.

The author expresses his deep thanks to Professor H. Tominaga for his interest and encouragement throughout the course of this work.

Department of Chemistry, Faculty of Science, Tôhoku University, Sendai

Sorption of Gases on Evaporated Nickel Films. II. Adsorption and Decomposition of Carbon Monoxide at Low Pressures. Part 1

By Zenjirō Oda

(Received October 19, 1954)

Introduction

The adsorption of carbon monoxide by evaporated metallic films has already been investigated by several authors[1,2,3] it being known that carbon monoxide is chemisorbed without dissociation. However, some discrepancies are found among their views on the mechanism of adsorption. On the other hand, while a number of works[4,5,6,7] have been reported on the decomposition of this gas by reduced nickel catalysts, no attempt has been made on an evaporated nickel film. Since previous works have been carried out at higher pressures and on reduced nickel, elementary processes involved in the reaction have not yet been clarified.

The present work was undertaken to investigate the behavior of carbon monoxide molecules on a clean nickel surface at room temperature as well as at high temperatures above 100°C, which permitted one to discuss the special features of evaporated nickel film in catalytic activity. Part 1 of this series is confined to the adsorption at room temperature and the decomposition at high temperatures will be described in part 2.

Experimental

The apparatus and procedures used were essentially the same as in the previous papers[8,9], except that the films deposited on the wall of a glass bulb at 0°C were pre-sintered at 90°C for about ten minutes.

Carbon monoxide, made by dropping 85% formic acid on concentrated sulfuric acid in a flask which was heated at about 110°C and well evacuated before the generation of the gas, was purified by passing it through the following train; (1) 55% potassium hydroxide solution, (2) the same solution containing 4% pyrogallol, (3) concentrated sulfuric acid, (4) phosphoric acid anhydride, and (5) a liquid-oxygen trap.

Results and Considerations

1) **Adsorption Rate.**—Admitting the gas to the nickel film within the temperature range of −78 to 100°C, it is taken up in a similar way irrespective of the film temperature, and these uptakes shall be called *room-temperature-adsorption* and distinguished from *high-temperature-decomposition* which will be mentioned in part 2 of this series.

As shown in Fig. 1, the adsorption of carbon monoxide comprises two stages, i.e., an initial rapid stage and a later slow one. At the initial stage, the pressure change was too rapid to be followed by the Pirani gauge in the first one minute after admission of gas, but the rate appeared to be substantially constant irrespective of the adsorbed amount. At the later stage, on the other hand, the rate becomes slow with the amount of successive adsorption.

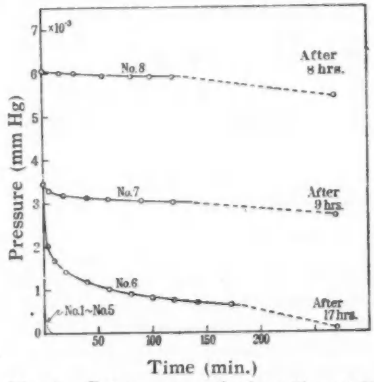

Fig. 1. Rate curves of adsorption at 0°C.

Setting the apparent rate of pressure decrease in the later stage $-\frac{dp}{dt}$ equal to the rate of adsorption r_a, we can plot $\log r_a$ against the adsorbed amount v for curve 6 in Fig. 1, in which the rate begins to decrease with v appreciably. Then a linear

1) (a) O. Beeck, A. E. Smith and A. Wheeler, *Proc. Roy. Soc.* (*London*), *A*, 177, 62 (1940); (b) O. Beeck, "Advances in Catalysis" Vol II, Academic Press Inc. New York, 1950, p. 151.
2) E. K. Rideal and B. M. W. Trapnell, *Proc. Roy. Soc.* (*London*), *A*, 205, 409 (1951).
3) A. S. Porter and F. C. Tompkins, ibid., A, 217, 529. 544 (1953).
4) H. A. Bahr and Th. Bahr. *Ber.*, 61, 2177 (1928).
5) S. Horiba and T. Ri, *Rev. Phys. Chem. Japan*, 4, 73 (1930); T. Ri, ibid., 5, 41 (1931).
6) H. Tsuchiya, *Bull. Inst. Phys and Chem. Research*, 10, 951 (1931).
7) T. Kwan and T. Izu, *Catalyst*, no. 6, 43 (1949).
8) Z. Oda, *Oyobutsuri* (*J. Appl. Phys. Japan*), 22, 142 (1953).
9) Z. Oda, This Bulletin, 27, 467 (1954).

relation is obtained as shown in Fig. 2, from which the rate is represented as a function of v by

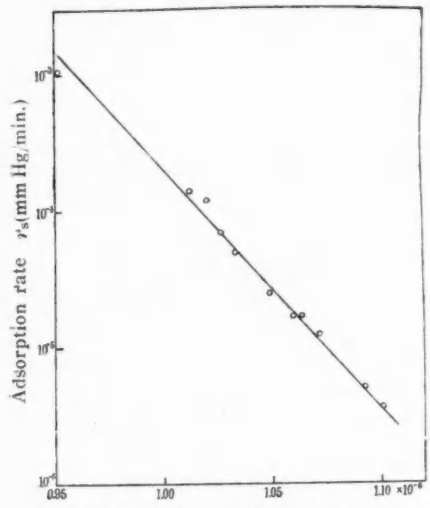

Fig. 2. The rate of adsorption as a function of adsorbed amount.

$$\ln r_a = \ln a - \alpha v, \tag{1}$$

The Elovich equation[10] is thus derived.

$$r_a = a e^{-\alpha v}. \tag{2}$$

As $r_a = \frac{dv}{dt}$, integration of Eq. (2) gives

$$v = 1/\alpha\{\ln(t+k) - \ln t_0\}, \tag{3}$$

where $k = \exp(av_0)/a\alpha$, $t_0 = 1/a\alpha$ and v_0 is the amount already taken up before $t=0$. Using p instead of v and plotting p against $\log(t+k)$ for the result shown in Fig. 2, the validity of Eq. (3) is tested in Fig. 3, where the value of k is selected to smooth the plot. The slope of this line gives $2.3/\alpha$. Values of α thus calculated from Figs. 2 and 3 are 4.09×10^{7} mol.$^{-1}$ and 4.42×10^{7} mol.$^{-1}$, respectively, showing a good agreement with each other. Furthermore, if one assumes $v_0=0$ at $t=0$, it is given from Eq. (3) that $t_0=k=1.3$ min. and so the initial rate a is calculated to be about 1.8×10^{-8} mol./min. from the relation $t_0=1/a\alpha$. This value shows a good coincidence with the observed one 5.6×10^{-8} mol./min. obtained from Fig. 2. This fact indicates the assumption $v_0=0$ at $t_0=0$ to be probable, i. e., the rapid adsorption preceding the slow one is not included in Eq. (2).

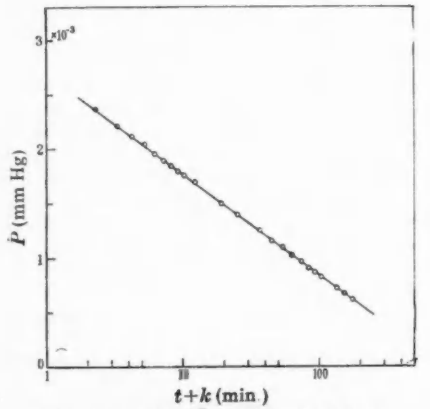

Fig. 3. $p-\log(t+k)$ plot $k=1.3$ min.

When the adsorption increases still more, the rate is expressed by

$$r_a = \beta(p - p_e), \tag{4}$$

where β is a rate constant and p_e is an equilibrium pressure.

2) Adsorption Equilibrium. — The initial stage where the adsorption rate was very rapid gave equilibrium pressures of 10^{-6} to 10^{-5} mmHg, but at the later stage, the equilibrium was not readily attained. After measuring a rough adsorption isotherm up to a pressure of about 5×10^{-2} mmHg, the system was evacuated to high vacuum. On admitting a dose of gas again, the rapid uptake was not observed but the slow one alone took place. Therefore, it is reasonable to consider that the initial stage is an irreversible adsorption and the later stage includes a reversible one; hence the calculation of isothermal heat of adsorption is not possible at the initial stage.

Now the Langmuir adsorption isotherm may be written in the form

$$p/v = 1/v_m b + p/v_m, \tag{5}$$

where b is an adsorption coefficient and v_m the amount adsorbed at saturation. Thus, as shown in Fig. 4a, plotting p/v against p for an isotherm, two straight lines intersecting at about 1×10^{-4} mm Hg are obtained. Fig. 4b shows the data below this pressure on enlarged scales. From the slopes and intercepts at p/v -axes in Figs. 4a and 4b, v_m and b can be calculated for both pressure ranges. For lower pressure range $v_{m1}=1.15\times10^{-6}$ mol. and $b_1=4.97\times10^{5}$ mm Hg^{-1}; for higher range $v_{m2}=1.29\times10^{-6}$ mol. and $b_2=3.87\times10^{3}$ mm Hg^{-1}. These results suggest that there exist two sites with different adsorption coefficients on the surface of the nickel film. In such a case, the adsorption isotherm is generally expressed by[11]

10) S. Yu. Elovich and G. M. Zhabrova, *Zhur. fiz Khim.*, **13**, 1761, 1775 (1939).

11) S. Brunauer, "Adsorption of Gases and Vapors, Physical Adsorption", Princeton Univ. Press, Princeton, 1945, p. 74.

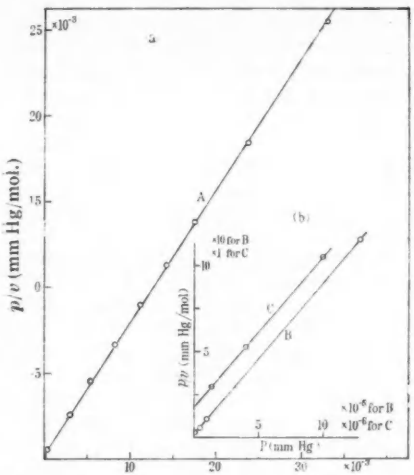

Fig. 4. Adsorption isotherms at 0°C plotted according to the Langmuir equation
(a) high-pressure range.
(b) low pressure range.

$$v=\frac{v_1b_1p}{1+b_1p}+\frac{v_2b_2p}{1+b_2p} \tag{6}$$

In the present case, we can set $v_1=v_{m1}$, $v_2=v_{m2}-v_{m1}$ and $b_1\gg b_2$. If p is small, the second term of the right-hand becomes negligible compared with the first term. So that

$$v\simeq\frac{v_1b_1p}{1+b_1p}, \tag{7}$$

which indicates that the adsorption takes place exclusively on the sites with larger adsorption coefficient. On the other hand, if p becomes large, it follows $b_1p\gg1$, so that

$$v\simeq v_1+\frac{v_2b_2p}{1+b_2p} \tag{8}$$

which shows that the subsequent adsorption occurs on the remaining sites with smaller adsorption coefficient.

The amounts of rapid adsorption and the total one measured with several films at 0°C are summarized in Table I. The ratio of the rapid adsorption to the total one is about 80% and the average value of the latter is 3.92×10^{-6} mol./10 mg. Ni.

Discussions

Porter and Tompkins[3] have found the Elovich equation to be applicable to the rate of uptake of hydrogen and of carbon monoxide by evaporated iron films between 78 and 140°K. In order to interpret these results they have considered the total process involving the initial rapid process to be a united process, by assuming that the iron film has a heterogeneous surface with sites of different adsorption potential and activation energy required for adsorbed molecules to migrate, so that the sticking of gas molecules must proceed from sites of lower activation energy to sites of higher. However, as mentioned above, in the adsorption of carbon monoxide as well as in the case of oxygen[9], the rate of uptake in the initial stage is very rapid and substantially constant, independent of the adsorbed amount; in the case of the former this rapid adsorption amounts to about 80% of the total adsorption, after which the rate falls with the increase in adsorption. Furthermore, Eq. (2) has been proved to be applicable to the beginning of the later stage only.

From these facts, another interpretation for Eq. (2) than that of the above authors is desirable. Davis[12] has shown that in the chemisorption of nitrogen on tungsten the activation energy E increases with surface coverage θ. Recently Zwietering and Roukens[13] have also observed the same relation in the chemisorption of nitrogen on iron. If such a relation is assumed to exist in the present system, we may write

$$E(\theta)=E_0+\gamma\theta, \tag{9}$$

12) R. Davis, *J. Am. Chem. Soc.*, **68**, 1395 (1946).
13) P. Zwietering and J. J. Roukens, *Trans. Farad. Soc.*, **50**, 178 (1954).

TABLE I
INITIAL ADSORPTION AND TOTAL ADSORPTION OF CO AT 0°C

Equil. pressure	Evaporated amount	Rapid adsorption	Total adsorption (obs.)	Total adsorption (per 10mg. Ni)	Rapid adsorption / Total adsorption
$\times10^{-2}$ mm Hg	mg.	$\times10^{-6}$ mol.	$\times10^{-6}$ mol.	$\times10^{-6}$ mol.	%
3.5	3.3	1.12	1.38	4.18	81.3
3.5	3.3	1.10	1.34	4.06	82.1
4.3	3.2	0.99	1.21	3.78	81.8
8.5	3.4	1.00	1.25	3.68	79.9
			(average)	3.92	81.3

where E_0 is the activation energy at the initial stage.

It is well known that carbon monoxide is adsorbed on evaporated metallic films as molecules[1,2,3]. Hence, the rate is generally given by the following equation

$$r_a = kp(1-\theta)e^{-E(\theta)/RT}. \quad (10)$$

Substituting for $E(\theta)$ from Eq. (9),

$$r_a = kp\, e^{-E_0/RT}(1-\theta)\, e^{-(\gamma/RT)\theta}. \quad (11)$$

In the isothermal adsorption, if p is constant or its change is small, it is possible to set $kp\, e^{-E_0/RT} = a_0$ and $\gamma/RT = \alpha_0$. Then Eq. (11) reduces to

$$r_a = a_0(1-\theta)\, e^{-\alpha_0\theta}. \quad (12)$$

When α_0 is so large that the change of $(1-\theta)$ can be negligible compared with that of $e^{-\alpha_0\theta}$, Eq. (12) may be approximately represented by the expression

$$r_a = a\, e^{-\alpha_0\theta}, \quad (13)$$

which is formally identical with Eq. (2).

In terms convenient for application to the data shown in Fig. 2, Eq. (9) can be written in the form

$$E(v) = E_0 + \gamma' v.$$

Since $\alpha = 4\times10^7$ mol.$^{-1}$ and $RT = 2\times273 = 546$ cal./mol., we obtain $\gamma' = \alpha RT = 2.2\times10^{10}$ cal./mol.[2] In addition, since the amount adsorbed in this run is $v = 1.5\times10^{-7}$ mol., the activation energy for the final part of this run is given by

$$E = E_0 + 3.3 \text{ kcal./mol.},$$

i.e., the activation energy increases by 3.3 kcal./mol. during this adsorption.

On the other hand, it is found from the adsorption isotherms that the surface of nickel film comprises two areas with sites differing in their adsorption coefficients and these areas correspond to the rapid and slow adsorption, respectively. According to Beeck[1], the heat of adsorption of carbon monoxide on nickel film is 35 kcal./mol. and constant over 85% of the surface coverage, after which it falls abruptly to a very low value. Hence, it is reasonable to consider the heat of adsorption at the initial stage equal to 35 kcal./mol. and that at the later stage corresponding to a very low value.

For the explanation of the over-all process of adsorption in connection with the surface character of the films, we assume the surface to comprise two areas A and B. Area A has sites of high heat of adsorption Q_A and the adsorption on these requires a small activation energy E_A; area B has sites of low heat of adsorption Q_B and for these the corresponding energy E_B is large: between these quantities we have the relation $Q_A > Q_B$ and $E_A < E_B$. On admitting an amount of gas to a fresh film, gas molecules colliding at random against the surface will be adsorbed exclusively by A at the initial stage. After A has been completely covered with gas molecules, the adsorption on B will begin. However, E_B is so large compared with E_A, that this process can be expected to be slow. These deductions would lead to a view that the initial and later stages correspond to A and B, respectively, i.e., the ratio of A to the total area is about 80% and the remainder corresponds to area B. However, it may be assumed that there exist some adsorption sites with various intermediate values of Q and E between those for A and B. Hence Eq. (2) is interpreted to represent the adsorption rate on these sites. On the other hand, when the remaining area becomes B alone, it is possible to set $\gamma = 0$, $E_0 = E_B$ and $\theta = \theta_B$ the coverage fraction of B. Then Eq. (11) becomes

$$r_a = kp(1-\theta_B)\, e^{-E_B/RT}. \quad (14)$$

At constant temperature and if p is nearly constant or its change is small, Eq. (14) reduces to

$$r_a = \beta_0(1-\theta_B), \quad (15)$$

with $\beta_0 = kp\, e^{-E_B/RT}$. This equation is equivalent to Eq. (4). Thus the adsorption of carbon monoxide on nickel films may be satisfactorily interpreted in terms of the non-uniformity of the surface throughout its over-all process.

In conclusion, the auther wishes to thank Mr. Y. Mizushima for valuable discussion and Mr. T. Ichimiya for his interest and encouragement.

The Electrical Communication Laboratory, Nippon Telegraph and Telephone Public Corporation, Musashino-shi, Tokyo

Sorption of Gases on Evaporated Nickel Films. III. Adsorption and Decomposition of Carbon Monoxide at Low Pressures. Part 2

By Zenjirō Oda

(Received October 29, 1954)

Introduction

As mentioned in part 1[1] of this series, carbon monoxide was merely chemisorbed by nickel films under 100°C. However, with the rise of temperature above 130°C., carbon monoxide was found to be decomposed to carbon dioxide and atomic carbon which reacted with nickel atoms to give nickel carbide. In this report the kinetics of decomposition is discussed on the basis of the non-uniformity of the surface.

Experimental

In order to determine the quantity of carbon dioxide produced by the decomposition of carbon monoxide, the apparatus used was partially modified as shown in Fig. 1. The reaction bulb

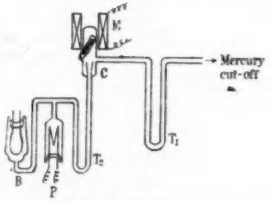

Fig. 1. The reaction apparatus.
B. Evaporation bulb; T_1, T_2. Cold traps
P. Pirani gange; C. Greaseless cock;
M. Electro-magnet.

was connected to the gas handling system through two cold traps T_1, T_2 and a "greaseless cock" C. During the reaction these traps were cooled with liquid-oxygen. The carbon dioxide produced was condensed onto the inside wall of T_2. Closing the "greaseless cock" C by means of an electro-magnet and removing the liquid-oxygen from T_2, the increase in pressure in the volume of BPT_2 could be measured by the Pirani gauge P. As will be mentioned below, since carbon dioxide was not adsorbed by nickel films covered with the carbon monoxide layer of rapid adsorption, the amount of carbon dioxide liberated was evaluated[2] from the rise in pressure.

In order to study the changes of the film structure after reaction, a small piece of cover glass for the microscope slide was previously set in the bulb, on which the nickel film was also deposited. When the reaction was finished, this piece was taken out as a sample for electron diffraction study. The films used in this experiment were pre-sintered for about thirty minutes at the same temperatures as those of the reaction.

Results and Considerations

1) Production of Carbon Dioxide. — Changing the reaction temperature in turn from 100° to 250°C for each gas admission, the pressure change was followed. Fig. 2

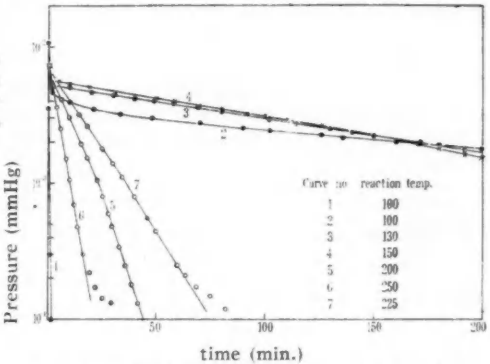

Fig. 2. Reaction rate curves at various temperatures.

shows the rate curves in log P vs t plots. We see that at the later stage the plots at 100°C are slightly convex, linear at 130°C and slightly concave towards t-axis at 150[3] and 200°C, whereas at 250°C the plot yields a straight line except below the pressure of 3×10^{-1} mmHg. With the "greaseless cock" closed and liquid-oxygen removed from T_2, a remarkable rise in pressure was observed above 130°C. Even if the trap was cooled again by dry ice, pressure change was hardly observed. Furthermore, mass-spectrometric analysis[4] proved this condensable gas to be carbon dioxide. Hence, it became evident

1) Z. Oda, This Bulletin, 28, 281 (1955).
2) Allowance were made for the difference in temperature of each part and the leak of the "greaseless cock". The accuracy was about ±5%.
3) In this case, since the amount of carbon produced before this run was very small, it was considered that the diffusion of carbon took place readily, and the behavior was similar to that at 200°C.
4) A small gas reservoir with a "magnetic-slug-break-off" was previously inserted ahead of trap T_2. After reaction the gases condensed in trap T_2 were collected in this reservoir by transferring liquid-oxygen from T_2 to it, and then it was sealed off and analysed.

that carbon monoxide was decomposed on nickel film above 130°C.

On admitting the gas to a fresh film at a constant temperature, the rate of pressure change and the amount of carbon dioxide produced in each run was measured. These results obtained at 200 and 150°C are given in Figs. 3a, 3b, 4a and 4b. As shown in Figs. 3a and 3b, at the initial stage, carbon dioxide was not observed immediately after the reaction had ceased. This was also the case, even if the film was kept for several hours

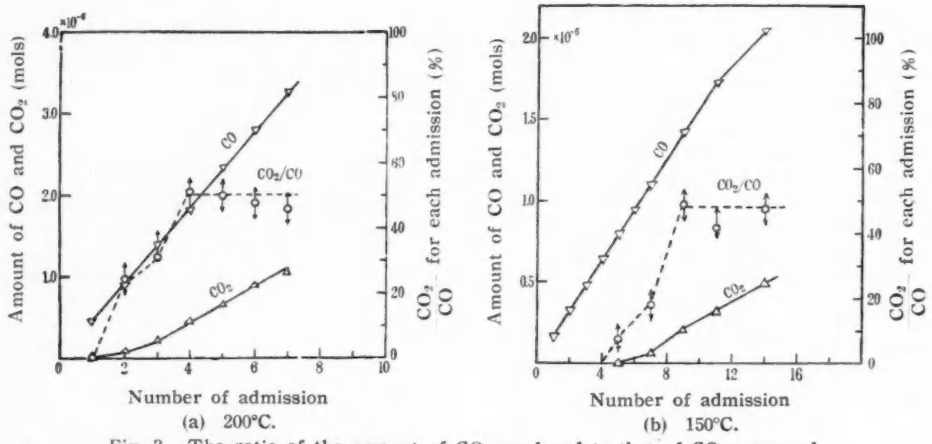

Fig. 3. The ratio of the amount of CO_2 produced to that of CO consumed.

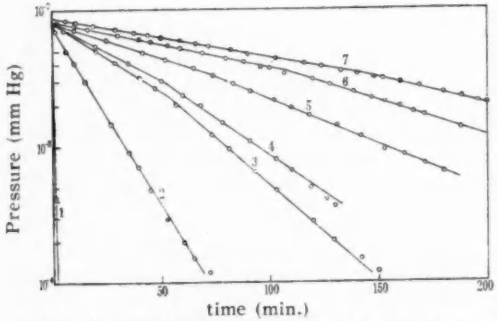

Fig. 4a. Reaction rate curves at constant temperature. (T=200°C)

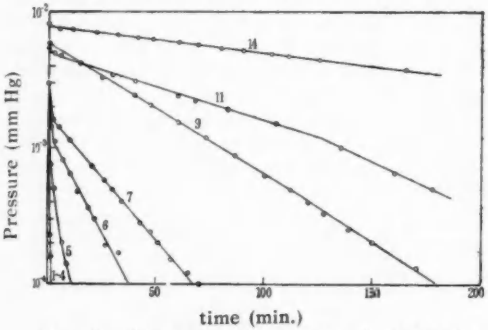

Fig. 4b. Reaction rate curves at constant temperature. (T=150°C)

at that temperature. With repetitions of reaction, the ratio of the amount of carbon dioxide to that of carbon monoxide consumed in one run (denoted by CO_2/CO) increases to 40~50%, which suggests that the reaction $2CO=CO_2+C$ occurs quantitatively on nickel films. Comparing these behaviors with the rate curves at 200°C shown in Fig. 4a, it is seen that run 1 represents the curve of adsorption, runs 2 and 3 the rate curves comprising the adsorption and decomposition, and the runs after 4 are regarded as being of decomposition itself. In a example at 150°C shown in Fig. 4b, a similar state of affairs occurs, i.e., the runs after 9 are the rate curves of decomposition. However, the log P vs t plots show linear relation at pressures above 10^{-4} mm Hg in order. At 250°C, on the other hand, while the ratio CO_2/CO changes in a manner similar to that at 200°C, the rate curves are linear between 1×10^{-2} and 3×10^{-4} mm Hg and slightly concave towards t-axis in higher pressure range than 1×10^{-2} mm Hg.

2) The Initial Stage.—Prior to considerations of the rate of decomposition, we shall first compare the initial rapid adsorption with the total adsorption at high temperatures. The total adsorption[5] 3.92×10^{-6} mol./10 mg

5) This is defined as the amount taken up at 0°C and $P\simeq5\times10^{-3}$ mm Hg as mentioned in part 1.

Ni shown in part 1 of this series is the average value for several films pre-sintered at 90°C for ten minutes. In the present case, however, since the films have been pre-sintered at higher temperatures, their available areas should be decreased. Fig. 5

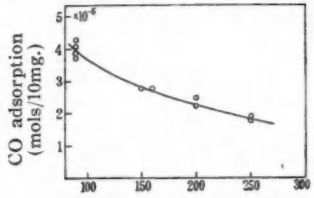

Fig. 5. Variation of total adsorption with pre-sintering temperature.

shows the variation of the total adsorption with pre-sintering temperature when the films have suffered pre-sintering for thirty minutes. These results are listed in Table 1, from which the initial adsorption is found to occupy 70~80% of the available area and to be almost independent of the reaction temperature.

However, it was not evident whether carbon monoxide was adsorbed with or without decomposition at the initial stage. While it was noted by previous authors that at high temperatures carbon dioxide was hardly adsorbed[6,7] on a nickel surface or slightly adsorbed[8] with dissociation even at 30°C, their experimental conditions differed substantially from the present author's. Hence, an attempt was made to make sure whether carbon dioxide was adsorbed on nickel film or not. After cooling only the trap T_2 with dry ice instead of liquid-oxygen, a dose of carbon dioxide was admitted to the film at 150 and/or 250°C. When the surface was clean or partially covered with carbon monoxide, rapid adsorption was observed. However, no adsorption was found after the rapid adsorption of carbon monoxide had been completed. This fact suggests that in the initial stage, if any carbon dioxide is formed, it is also adsorbed on nickel film and does not condense in the trap cooled with liquid-oxygen. Hence, it is impossible to decide the adsorbed state of carbon monoxide on nickel film. However, it may be possible to conclude that carbon monoxide and or its degradation products are strongly bounded by film surface and not readily desorbed until the surface is covered to 70~80% of its available area.

TABLE I

INITIAL RAPID ADSORPTION OF CO AT HIGH TEMPERATURES BEFORE DECOMPOSITION

React. temp.	Evaporated amount	Rapid adsorption (obs.) (per 10 mg. Ni)		Total adsorption* (per 10 mg. Ni)	(Rapid adsorption / Total adsorption)
°C	mg.	10^{-3} mol.	10^{-6} mol.	10^{-3} mol.	%
150	3.3	0.65	1.97		
	3.5	0.71	2.03		
	2.8	0.78	2.78		
(average)			2.33	2.9	80.3
200	3.2	0.52	1.62		
	2.3	0.39	1.69		
	3.0	0.49	1.65		
	3.6	0.56	1.56		
	2.8	0.46	1.64		
	3.6	0.57	1.58		
(average)			1.62	2.25	73.2
250	3.0	0.41	1.37		
	3.5	0.48	1.37		
(average)			1.37	1.8	76.1

*) Average values obtained from Fig. 5.

3) **The Later Stage.**—As mentioned above, the amount of carbon monoxide consumed in one run is wholly converted to carbon dioxide after the reaction has been repeated many times, and thus considerations will be made in such a case.

Now we start on the assumption that the decomposition of carbon monoxide on the

6) N. Nikitin, *Z. anorg. Chem.*, **154**, 130 (1926).

7) S. Horiba and T. Ri, *Rev. Phys. Chem. Japan*, **4**, 41 (1930).

8) J. A. Dillon and H. E. Farnsworth, *Phys. Rev.*, **94**, 753 (1954); *J. Chem. Phys.*, **22**, 1601 (1954).

surface of nickel film proceeds through the following elementary processes:

1) $CO\ (g) \rightleftarrows CO\ (ads)$,
2) $CO\ (ads) \rightarrow (C-O)^*$,
3) $CO\ (g)+(C-O)^* \rightarrow CO_2(g)+C\ (atom)$,
4) $C\ (atom)+Ni \rightarrow Ni_3C$,

where $(C-O)^*$ represents the activated state of a carbon monoxide molecule. Assuming the reaction 2) to be the rate-determining step, the reaction will be of the first order with respect to the adsorbed amount of carbon monoxide v. Hence the rate is given by

$$-dP/dt=k_1v \qquad (1)$$

Let θ_{co} and θ_c denote the fraction of the adsorption sites covered by carbon monoxide and carbon[9], respectively, then $(1-\theta_{co}-\theta_c)$ gives the fraction still bare at a given time. The corresponding adsorption isotherm is given by

$$\frac{\theta_{co}}{1-\theta_{co}-\theta_c}=bP. \qquad (2)$$

Hence

$$\theta_{co}=\frac{(1-\theta_c)\,bP}{1+bP},$$

or, using v instead of θ_{co},

$$v=\frac{(1-\theta_c)v_m bP}{1+bP}, \qquad (3)$$

where v_m is the amount of carbon monoxide corresponding to the total adsorption sites. Upon substituting this value for v in Eq. (1), we obtain

$$-dP/dt=k_1(1-\theta_c)v_m bP/1+bP. \qquad (4)$$

Since the rate curves obtained is apparently of different form depending on temperature, we shall consider each case.

i) 200°C.

In this case, since carbon formed on the surface is considered to diffuse rapidly to interior, the rates of its production and disappearance from the surface balance with each other at a given θ_c. Hence, θ_c may be taken as nearly constant during the reaction period of one admission, and thus Eq. (4) can be reduced to

$$-dP/dt=k_2P/1+bP, \qquad (5)$$

where

$$k_2=k_1(1-\theta_c)bv_m. \qquad (6)$$

Intergation of Eq. (5) gives

$$\ln P+bP=C-k_2t, \qquad (7)$$

or

$$\log P+(b/2{,}3)P=C'-(k_2/2{,}3)t. \qquad (8)$$

This means that if b is sufficiently large the log P vs t plot should be concave towards t-axis (cf. Fig, 4a). In order to apply Eq. (8) to the experimental data, it is necessary to obtain the value of b. By assuming that as the reaction time increases the term $(b/2.3)P$ becomes negligible compared with the absolute value of log P in the pressure range studied, Eq. (8) will be reduced to

$$\log P=C'-(k_2/2{,}3)t. \qquad (9)$$

Therefore, in Fig. 4a, by extrapolating the curve at large t towards a smaller one and setting the extrapolated value at any time t to be G, a plot of $G-\log P$ vs P is obtained as shown in Fig. 6. The slope of this line

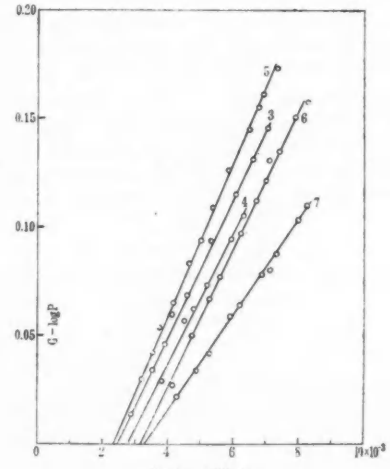

Fig. 6. $G-\log P$ vs P plots.

gives $b/2.3$. Thus, plotting $\log P+(b/2.3)P$ against t for the data shown in Fig. 4a, good straight lines are obtained as shown in Fig. 7. Although the value of b is nearly constant, independent of the repetition of reaction, the slope of lines, i.e., k_2 decreases with reaction. According to the relation (6) this is attributed to the increase of θ_c, i.e., a blocking effect by the carbon produced.

ii) 150°C.

From the definition of b it is anticipated that the bends in the log P vs t plots at this temperature must appear in a lower pressure range than at 200°C. This is evident by comparing Fig. 4b with Fig. 4a.

On the other hand, since the diffusion of carbon seems to be slower than at 200°C k_2 should not be constant but should decrease with time even in one run. Therefore, it is probable that the tendency to become concave towards t-axis due to the neglet of $(b/2.3)P$ term is just compensated by the decrease of k_2, and thus the plots yield straight lines

9) This includes atomic carbon and nickel carbide (Ni_3C) remaining on the surface.

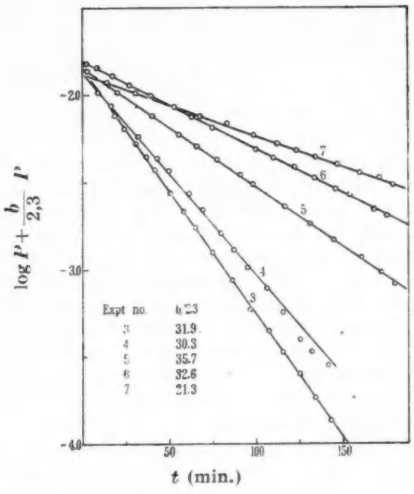

Fig. 7. $\log P+\frac{b}{2,3}P$ vs t plots.

above 1×10^{-3} mm Hg pressure. Consequently the plots of $G-\log P$ vs P are not represented by straight lines giving the value of $b/2.3$. Although it is impossible to analyse the reaction rate more precisely, Eq. (4) seems to hold for this case also.

ii) 250°C.

In this case, b is so small that the bend due to $(b/2.3)P$ term is not observed below 1×10^{-2} mm Hg. For example, a value of b derived from a rate curve above this pressure is 15 $(\text{mm Hg})^{-1}$, from which it follows $bP=0.075$ at $P=5\times10^{-3}$ mm Hg. Thus neglecting bP compared to 1 in Eq. (5), we find

$$-dP/dt=k_2P, \qquad (10)$$

i.e., the reaction becomes of the first order type in agreement with experimental results.

4) Heat of Adsorption and Activation Energy of Decomposition.—Let Q and E_2 be the heat of adsorption and the apparent activation energy of the reaction, respectively, the temperature dependencies of b and k_2 are given by

$$b=b_0e^{Q/RT} \quad \text{and} \quad k_2=k_{20}e^{-E_2/RT}. \qquad (11)$$

Therefore, at two temperatures, for example 200 and 225°C, the rates of decomposition were measured on the same film and b was evaluated by the procedure noted above. From plots of $\log b$ vs $1/T$ and $\log k_2$ vs $1/T$ for two films, the average values of Q and E_2 were found to be about 20.5±1.4 and 14.6±0.7 kcal/mol., respectively.

In addition, the temperature dependency of k_1 is given by

$$k_1=k_{10}e^{-E_1/RT}. \qquad (12)$$

Hence, from Eqs. (6), (11) and (12) we can obtain a relation

$$E_2=E_1-Q. \qquad (13)$$

With the values of Q and E_2 obtained above, it follows $E_1=35.1\pm2.1$ kcal/mol., which may be regarded as the potential energy difference between the activated state and the adsorbed state of the reactant. It is interesting to note that this energy is nearly equal to the heat of adsorption[10] at the initial stage where the decomposition cannot be detected.

5) Electron Diffraction Study.—After the reaction had been carried out under various conditions, electron diffraction photographs were taken with six films. If the ratio of the number of reactant molecules consumed to that of nickel atoms deposited was less than about 20%, the nickel pattern alone was observed, but if this ratio reached to about 40%, nickel carbide (Ni_3C) pattern[11] was also revealed in addition to that of nickel. The electron diffraction photographs before and after reaction are shown in Fig. 8.

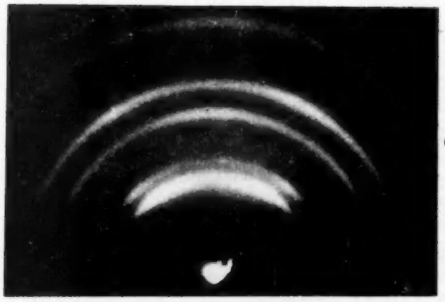

(a)

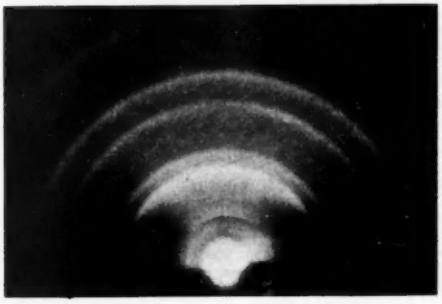

(b)

10) See part 1.

11) This was analysed by X-ray diffraction data given by A. Cimino and G. Parravano, *J. Phys. Chem.*, **56**, 706 (1952).

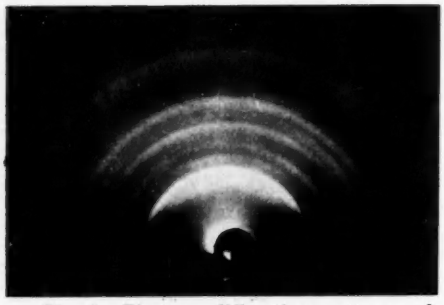

(c)

Fig. 8. Electron diffraction patterns of evaporated nickel films before and after reaction. (a) Pre-sintered at 100°C. for 1 hr. (b) After reaction at 200°C.; CO molecules consumed $=1.98\times10^{18}$, Ni atoms of film $=2.9\times10^{19}$. (c) After reaction at 250°C.; CO molecules consumed $=1.29\times10^{19}$, Ni atoms of film $=3\times10^{19}$.

It has been pointed out by several authors[12,13,14] that in the carburization of nickel by carbon monoxide, carbide is initially formed and then graphitic carbon is produced, which increases with the rise in reaction temperature[15]. When the extent of decomposition is small no pattern of nickel carbide is detected. This fact may be interpreted as the insufficient intensity of diffraction by carbide of a small amount, even though it exists. We can conclude, therefore, that carbon monoxide is converted to carbon dioxide and nickel carbide instead of graphitic carbon on the surface of evaporated nickel films under our experimental conditions.

Discussion

As has been mentioned in part 1, the surface is assumed to be non-uniform and consisted of two areas A and B with different activity. From the fact that the decomposition at high temperatures occurs after the initial rapid adsorption which covers a fraction of surface similar to that at *room-temperature-adsorption*, it is surely expected that carbon monoxide molecules adsorbed on B would participate in the reaction. Furthermore, the fact that the heat of adsorption obtained from the temperature dependency of b is smaller than that on A (=35 kcal/mol.) also suggests that the molecules adsorbed on B with lower heat of adsorption would be activated and undergo decomposition. That is, in the decomposition of carbon monoxide, sites with high heat of adsorption are not active but those with low heat are rather active because of the ease of desorption. Similar observation has been made by Beeck[16] in the catalytic hydrogenation of ethylene with various evaporated metallic films. He has pointed out that the metals with higher activity possess lower heat of adsorption for ethylene and explained this finding by the reasoning that metals with higher heat of adsorption for ethylene are poisoned more seriously by adsorbed ethylene and its degradation products because of the difficulty of desorption.

In the previous investigations[7,17] on the decomposition of carbon monoxide by reduced nickel catalysts, such a phenomenon as that rapid adsorption precedes decomposition has not been observed. This difference may be attributed to the difference in the cleanliness of the surface. That is, under any conditions for the preparation of reduced catalysts generally adopted, it seems to be very difficult or impossible to drive out some impure gases which adhere firmly to the surface and produce such a clean surface as evaporated film. The catalytic reactions on these reduced catalysts have been well interpreted in terms of the intrinsic heterogeneity of the surface. In this work also, to explain the results obtained, it has been necessary to assume the surface heterogeneity on the evaporated nickel films, in spite of their cleanliness. However, it is uncertain whether this heterogeneity is due to the intrinsic difference in surface energy or the interaction of adsorbed molecules or both.

In conclusion, the author wishes to express his thanks to Messrs. Y. Mizushima and T. Ichimiya for their interest in this investigation and for valuable discussion; to Mr. K. Ono for the electron diffraction study, and to Mr. K. Nakagawa for mass-spectrometric analysis.

The Electrical Communication Laboratory, Nippon Telegraph and Telephone Public Corporation, Musashino-shi, Tokyo

12) H. A. Bahr and Th. Bahr, *Ber.*, **61**, 2177 (1928).
13) H. Tsuchiya, *Bull. Inst. Phys. and Chem. Research*, **10**, 951 (1931).
14) S. Oketani, S. Nagakura and K. Tsuchiya, *J. Japan Inst. Metals*, **18**, 325, 329 (1954).
15) The critical temperature where the process $Ni_3C \rightarrow C+Ni$ (or Ni_xC) begins to occur has been variously reported, for example 270,[15] 420 [13] or 500°C[14].
16) O. Beeck, *Disc. Farad. Soc.*, No 8, 118 (1950).
17) T. Kwan and T. Izu, *Catalyst*, No 6, 43 (1949).

On the Electronic Structures of Butadiene

By Yuji MORI

(Received December 20, 1954)

Introduction

The interpretation of the ultraviolet absorption spectra of molecules is approached by two methods in principle. The first is the molecular orbital[1] method, and the second is the valence bond method[2]. The hybridized method between these two, which was developed by London and was used in the calculation of the ultraviolet absorption spectra of diphenyl[3], has been employed in the present study. The outline of this method is as follows*. The molecule under consideration is divided into some parts in such a way that they have simple forms of molecular orbitals. Then the wave function of the entire molecule is approximated by the products of antisymmetrized molecular orbitals of these parts. For instance, styrene is divided into two parts, i. e., the phenyl radical and the vinyl radical. Then the wave functions of the π-electron system of styrene are expressed by the antisymmetrized products of molecular orbitals of the benzene ring and of the vinyl radical.

The important character of this treatment is that the electronic states of the entire molecule are expressed by those of the simple parts included in it. So this method may be thought of as the valence bond method which has the local molecular orbitals taking the place of the atomic orbitals.

In this treatment, polar structure which means charge transfer from one part to another is important for the excited state. Previously the absorption spectra[4] of styrene was studied by this treatment including polar structures, and it was shown that polar structures are important for excited states.

In the present paper, polar and bonding structures between π-electron systems of the two vinyl radicals of butadiene are introduced, and for convenience the semi-empirical treatment investigated by Parizer and Parr[5] is applied in the later section.

Wave Functions and Computations

The "*trans*-form" model is chosen for butadiene in the present calculation, and the bond distances and the bond angle of skeleton are equal to those of the model in the calculation of Parr and Mulliken[6] (Fig. 1).

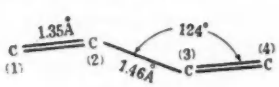

Fig. 1.

The wave functions of the π-electron system of butadiene are expressed by the π-electron wave functions of two vinyl radicals having the molecular orbitals as

$$\varphi_1=\frac{1}{\sqrt{2\sigma_1}}(\chi_1+\chi_2),\quad \varphi_3=\frac{1}{\sqrt{2\sigma_3}}(\chi_3+\chi_4),$$

$$\varphi_2=\frac{-1}{\sqrt{2\sigma_2}}(\chi_1-\chi_2),\quad \varphi_4=\frac{1}{\sqrt{2\sigma_4}}(\chi_3-\chi_4),$$

where χ_i is the atomic orbital, and σ_i is the normalization factor.

Thus the unperturbed wave functions of butadiene are

$$(^1A_g),\ \psi_1=\frac{1}{\sqrt{4!}\sqrt{N_1}}\sum_P(-1)^P P\varphi_1(1)\bar{\varphi}_1(2)\varphi_3(3)\bar{\varphi}_3(4),$$

$$(^1A_g),\ \psi_2=\frac{1}{\sqrt{4!}\sqrt{N_2}}\sum_P(-1)^P P\frac{1}{2}\{\varphi_1(1)\bar{\varphi}_2(2)\varphi_3(3)\bar{\varphi}_3(4)$$
$$-\bar{\varphi}_1(1)\varphi_2(2)\varphi_3(3)\bar{\varphi}_3(4)+\varphi_1(1)\bar{\varphi}_1(2)\varphi_3(3)\bar{\varphi}_4(4)$$
$$-\varphi_1(1)\bar{\varphi}_1(2)\bar{\varphi}_3(3)\varphi_4(4)\},$$

$$(^1B_u),\ \psi_3=\frac{1}{\sqrt{4!}\sqrt{N_3}}\sum_P(-1)^P P\frac{1}{2}\{\varphi_1(1)\bar{\varphi}_2(2)\varphi_3(3)\bar{\varphi}_3(4)$$
$$-\bar{\varphi}_1(1)\varphi_2(2)\varphi_3(3)\bar{\varphi}_3(4)-\varphi_1(1)\bar{\varphi}_1(2)\varphi_3(3)\bar{\varphi}_4(4)$$
$$+\varphi_1(1)\bar{\varphi}_1(2)\bar{\varphi}_3(3)\varphi_4(4)\},$$

$$(^1A_g),\ \psi_4=\frac{1}{\sqrt{4!}\sqrt{N_4}}\sum_P(-1)^P P\frac{1}{2}\{\varphi_1(1)\bar{\varphi}_4(2)\varphi_3(3)\bar{\varphi}_3(4)$$
$$-\bar{\varphi}_1(1)\varphi_4(2)\varphi_3(3)\bar{\varphi}_3(4)+\varphi_1(1)\bar{\varphi}_1(2)\varphi_3(3)\bar{\varphi}_2(4)$$
$$-\varphi_1(1)\bar{\varphi}_1(2)\bar{\varphi}_3(3)\varphi_2(4)\},$$

1) Concerning the simple MO method, Eyring, "Quantum Chemistry", (1949), p. 192, 254. Concerning the ASMO method, M. Goeppert-Mayer and A. L. Sklar, *J. Chem. Phys.*, **6**, 645 (1938); D. P. Craig, *Proc. Roy. Soc.*, **A200**, 474 (1950). Concerning the LCAOSCF method, C. C. J. Roothaan, *Rev. Mod. Phys.*, **23**, 69 (1951).

2) L. Pauling, *J. Chem. Phys.*, **1**, 280 (1933); Eyring "Quantum Chemistry," (1949) p 243.

3) A. London, *J. Chem. Phys.*, **13**, 364 (1945).

* Reference 3).

4) Unpublished, presented at the Annual Meeting of the Chemical Society of Japan, Tokyo, April, 1951.

5) R. Pariser and R. G. Parr, *J. Chem. Phys.*, **21**, 466, 767 (1953).

6) R. G. Parr and R. S. Mulliken, *J. Chem. Phys.*, **18**, 1338 (1950).

$$(^1B_u),\ \psi_5=\frac{1}{\sqrt{4!}\sqrt{N_5}}\sum_P(-1)^P P\frac{1}{2}\Big\{\varphi_1(1)\bar{\varphi}_4(2)\varphi_3(3)\bar{\varphi}_3(4)$$
$$-\bar{\varphi}_1(1)\varphi_4(2)\varphi_3(3)\bar{\varphi}_3(4)-\varphi_1(1)\bar{\varphi}_1(2)\varphi_3(3)\bar{\varphi}_2(4)$$
$$+\varphi_1(1)\bar{\varphi}_1(2)\bar{\varphi}_3(3)\varphi_2(4)\Big\},$$

$$(^1A_g),\ \psi_6=\frac{1}{\sqrt{4!}\sqrt{N_6}}\sum_P(-1)^P P\frac{1}{2}\Big\{\varphi_1(1)\bar{\varphi}_2(2)\varphi_3(3)\bar{\varphi}_4(4)$$
$$-\bar{\varphi}_1(1)\varphi_2(2)\varphi_3(3)\bar{\varphi}_4(4)-\varphi_1(1)\bar{\varphi}_2(2)\bar{\varphi}_3(3)\varphi_4(4)$$
$$+\bar{\varphi}_1(1)\varphi_2(2)\bar{\varphi}_3(3)\varphi_4(4)\Big\},$$

$$(^1A_g),\ \psi_7=\frac{1}{\sqrt{4!}\sqrt{N_7}}\sum_P(-1)^P P\frac{1}{2}\Big\{\varphi_1(1)\bar{\varphi}_2(2)\varphi_3(3)\bar{\varphi}_4(4)$$
$$-\bar{\varphi}_1(1)\bar{\varphi}_2(2)\varphi_3(3)\varphi_4(4)-\varphi_1(1)\varphi_2(2)\bar{\varphi}_3(3)\bar{\varphi}_4(4)$$
$$+\bar{\varphi}_1(1)\varphi_2(2)\bar{\varphi}_3(3)\varphi_4(4)\Big\},$$

where P means the permutation of electrons, and $(-1)^P$ takes $+1$ or -1 according to even or odd permutation respectively, and N_i is the normalization factor. The wave functions ψ_1, ψ_2, ψ_3 are non-polar, and ψ_4, ψ_5 are polar. ψ_6, ψ_7 represent bonding structures.

The perturbed wave function of butadiene Φ_i is

$$\Phi_i=\sum_j a_{ij}\psi_j.$$

The secular determinant is thus

$$\det|H_{ij}-N_{ij}W|=0,$$

where

$$H_{ij}=\int\psi_i H\psi_j d\tau,\quad N_{ij}=\int\psi_i\psi_j d\tau.$$

The matrix elements are expanded into the integrals over the molecular orbitals φ_i of vinyl radicals. Further these integrals are expanded with the integrals over atomic orbitals χ_i which have already been given by Parr and Mulliken[6]. The numerical values of integrals necessary for the present calculation are listed in Tables I and II.

TABLE I

$s_{12}=0.27854$	(11 : 12) = 3.60741
$s_{13}=0.03371$	(22 : 23) = 2.93264
$s_{14}=0.00218$	(22 : 34) = 1.93346
$s_{23}=0.23281$	(11 : 23) = 1.66096
	(11 : 34) = 1.25870
(1 : 12) = 2.27950 e.v.	(11 : 13) = 0.29845
(2 : 23) = 1.63069	(11 : 24) = 0.18599
(1 : 22) = 0.98620	(22 : 13) = 0.46282
(2 : 33) = 0.67476	(11 : 14) = 0.01730
(1 : 13) = 0.30278	(22 : 14) = 0.03027
(1 : 23) = 0.03460	(12 : 12) = 1.09000
(2 : 34) = 0.03027	(23 : 23) = 0.73099
(2 : 14) = 0.01730	(12 : 23) = 0.63583
(1 : 33) = 0.00865	(12 : 34) = 0.46282
(1 : 14) = 0.00000	(12 : 13) = 0.12543
(1 : 24) = 0.00000	(12 : 24) = 0.06920
(1 : 34) = 0.00000	(13 : 23) = 0.10813
(1 : 44) = 0.00000	(12 : 14) = 0.00432
	(14 : 23) = 0.00865
(11 : 11) = 16.92975	(13 : 13) = 0.01730
(11 : 22) = 9.23913	(13 : 24) = 0.00865
(22 : 33) = 8.69412	(13 : 14) = 0.00000
(11 : 33) = 5.52358	(14 : 14) = 0.00000
(11 : 44) = 3.82801	

TABLE II

$\sigma_1=1.27854$	$E_1=2W_{2p}-12.11931$
$\sigma_2=0.72146$	$E_2=2W_{2p}-1.44338$
$S_{13}=0.11826$	
$S_{14}=0.12007$	[11 : 13] = 1.15565
$S_{24}=0.11613$	[11 : 14] = 1.26194
$\varepsilon_1=W_{2p}-12.60205$ e.v.	[11 : 23] = 1.10343
$\varepsilon_2=W_{2p}-6.01337$	[11 : 24] = 1.16176
$\lambda_1=-12.00831$	[11 : 34] = 1.26546
$\lambda_2=-12.34752$	[22 : 13] = 1.14301
$\lambda_{12}=-2.88461$	[22 : 14] = 1.24381
$\omega_{13}=-5.50703$	[22 : 23] = 1.12520
$\omega_{14}=-5.43695$	[22 : 24] = 1.20289
$\omega_{24}=-5.09605$	[22 : 34] = 1.26878
$K_{11}=13.08479$	[12 : 13] = 0.31791
$K_{12}=13.00330$	[12 : 14] = 0.35521
$K_{22}=13.37096$	[12 : 23] = 0.32708
$K_{13}=5.84053$	[12 : 24] = 0.36362
$K_{14}=5.88618$	[12 : 34] = 0.39976
$K_{24}=6.07678$	[13 : 14] = 0.19285
$J_{12}=4.16874$	[13 : 24] = 0.18874
$J_{13}=0.18853$	[14 : 23] = 0.18874
$J_{14}=0.19812$	[14 : 24] = 0.18571
$J_{24}=0.17659$	
$H_{11}=-93.69588$	$N_1=0.97210$
$H_{22}=-82.05927$	$N_2=0.95815$
$H_{33}=-84.14202$	$N_3=0.98605$
$H_{44}=-85.31311$	$N_4=1.01395$
$H_{55}=-84.44434$	$N_5=0.98605$
$H_{66}=-72.54143$	$N_6=0.97210$
$H_{77}=-85.96205$	$N_7=1.01395$
$H_{12}=+2.24563$	$N_{12}=-0.02890$
$H_{14}=-24.01682$	$N_{14}=+0.24188$
$H_{16}=+2.24209$	$N_{16}=-0.01435$
$H_{17}=+3.48230$	$N_{17}=-0.02810$
$H_{24}=+0.00508$	$N_{24}=-0.00216$
$H_{26}=+2.00350$	$N_{26}=-0.02890$
$H_{27}=+1.04476$	$N_{27}=-0.01415$
$H_{45}=+10.77883$	$N_{45}=-0.12094$
$H_{47}=+22.75446$	$N_{47}=-0.23684$
$H_{67}=-35.53348$	$N_{67}=+0.48956$
$H_{35}=-22.08459$	$N_{35}=+0.23770$

In these tables E_1 and E_2 are the energy levels of the vinyl radical whose wave functions are

$$E_1;\ \sum_P(-1)^P P\varphi_1(1)\bar{\varphi}_1(2),$$

$$E_2;\ \sum_P(-1)^P P\frac{1}{\sqrt{2}}\Big\{\varphi_1(1)\bar{\varphi}_2(2)-\bar{\varphi}_1(1)\varphi_2(2)\Big\},$$

The integral I_i is the core energy of the molecular orbital of vinyl radical and λ_i is the energy of perturbation from another vinyl radical core. Then the next relation is

$$\int\varphi_i(\nu)H_{\text{core}(\nu)}\varphi_i(\nu)d\tau_\nu=I_i+\lambda_i.$$

The other integrals in these tables are

$\lambda_{12}=\int\varphi_1(\nu)H_{\text{core}(\nu)}\varphi_2(\nu)d\tau_\nu$,
$\omega_{ij}=\int\varphi_i(\nu)H_{\text{core}(\nu)}\varphi_j(\nu)d\tau_\nu$(i=1 or 2, j=3 or 4),
$S_{ij}=\int\varphi_i(\nu)\varphi_j(\nu)d\tau_\nu$,

$$K_{ij}=\iint|\varphi_i(\nu)|^2\frac{e^2}{r_{\nu\mu}}|\varphi_j(\mu)|^2 d\tau_\nu d\tau_\mu,$$

$$J_{ij}=\iint\varphi_i(\nu)\varphi_j(\nu)\frac{e^2}{r_{\nu\mu}}\varphi_j(\mu)\varphi_i(\mu)d\tau_\nu d\tau_\mu,$$

$$[jk:lm]=\iint\varphi_j(\nu)\varphi_k(\nu)\frac{e^2}{r_{\nu\mu}}\varphi_l(\mu)\varphi_m(\mu)d\tau_\nu d\tau_\mu,$$

$$(r:st)=\int\chi_s(\nu)\boldsymbol{H}_r(\nu)\chi_t(\nu)d\tau_\nu,\quad s_{rs}=\int\chi_r(\nu)\chi_s(\nu)d\tau_\nu,$$

$$(rs:tu)=\iint\chi_r(\nu)\chi_s(\nu)\frac{e^2}{r_{\nu\mu}}\chi_t(\mu)\chi_u(\mu)d\tau_\nu d\tau_\mu,$$

where

$$H_{core(\nu)}=\sum_{r=1}^{4}H_r(\nu),$$

$$H_r(\nu)=\boldsymbol{H}_r(\nu)-\int\left(\frac{e^2}{r_{\nu\mu}}\right)|\chi_r(\mu)|^2 d\tau_\mu,$$

and $\boldsymbol{H}_r(\nu)$ is the potential due to the neutral carbon atom.

The energy levels of butadiene obtained by the present calculation are shown in Fig. 2 (left column), and those of ASMO SCF CI calculation using the SCF wave functions by Parr and Mulliken[8], and including the same configurations as in Coulson's calculation[7] are also shown in Fig. 2 (second column).

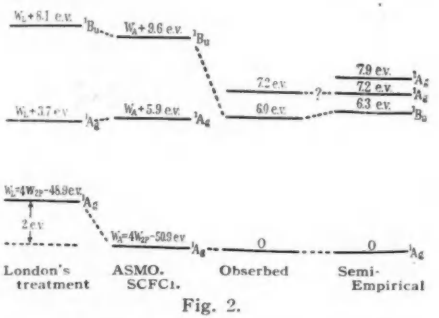

Fig. 2.

The wave functions of the ground state and the lowest ^1B_u state are

(^1A_g)(ground state);

$$\psi_1=0.9326\phi_1+0.0381\phi_2+0.1500\phi_4+0.0491\phi_6-0.1688\phi_7,$$

(^1B_u); $\psi_3=0.6062\phi_3+0.6641\phi_5$,

Discussion

The absorption spectra of butadiene[6] show the strong absorption bands about 2000 Å and 1700 Å. No absorption band has been observed in the wave length region longer than 2000 Å.

The selection rule shows that the ^1A_g—^1B_u transition is allowed and the ^1A_g—^1A_g transition is forbidden. Then, the strong bands of 2000 Å and 1700 Å may correspond to the ^1A_g—^1B_u transitions*.

By this calculation the lowest ^1B_u state exceeds 8.1 e.v. over the ground state and the lowest ^1A_g—^1A_g transition is about 3.7 e.v. The ASMO SCF CI calculation predicts that the lowest ^1A_g—^1B_u excitation energy is about 9.6 e.v. and the lowest ^1A_g—^1A_g excitation energy is about 5.6 e.v. These two calculations agree qualitatively in the next point. The lowest excited ^1A_g state is lower than the lowest ^1B_u state. If this is true there may be a weak absorption band in the wave length longer than 2000 Å, while this weak band has not been observed. The cause of discrepancy may be interpreted as follows. In general the detailed ASMO calculation gives the high excitation energy for the excited singlet state and low excitation energy for the triplet state. This is mainly due to the overestimation of one center repulsion energy as Moffitt[9] mentioned it. This energy integral is important to determine the energies of polar structures. The ASMO wave functions of excited singlet states include more polar structures than that of ground state in most cases, and the contributions of polar structures for the triplet states are less than for the singlet ground state. In the case of ethylene the triplet state includes no polar structure, and the singlet excited $^1B_{1u}$ state is given by the linear combination of the polar structures only in usual estimation. Thus the overestimation of one centre repulsion energy results in the high excitation energy for singlet—singlet transition and results in the low energy for the triplet state. In the case of the lowest excited ^1A_g state of butadiene, however, the contributions of polar structures are slight, as the important configuration of this state is ψ_7, which is the product of the two triplet states of vinyl radicals. So the excitation energy for this ^1A_g state may be low in the non-empirical calculation. Therefore the excitation energy (5.9 e. v.) by ASMO SCF CI calculation may coincide with the experimental value better than that (3.7 e. v.) by this hybridized treatment, because the contributions of polar structures to the ground state are greater in this hybridized calculation than in ASMO SCF CI calculation owing to the neglect of the high energy structures as

$$\sqrt{\frac{1}{4!}}\sum_r(-1)^r P\frac{1}{\sqrt{2}}\{\varphi_2(1)\bar{\varphi}_2(1)\varphi_3(3)\bar{\varphi}_3(4)+\varphi_1(1)\bar{\varphi}_1(1)\varphi_3(3)\bar{\varphi}_3(3)\},\cdots\cdots.$$

7) C. A. Coulson and J. Jacobs, *Proc. Roy. Soc.*, **A206**, 287 (1951).

8) E. P. Carr, L. W. Pickett and H. Stücklen, *Rev. Mod. Phys.*, **14**, 260 (1942).

* For *cis*-butadiene, the $^1A_1$—$^1A_1$ transition (A_g—A_g transition in *trans*-butadiene) is allowed but the intensity of the lowest $^1A_1$—$^1A_1$ transition may not be so strong.

9) W. Moffitt, *Proc. Roy. Soc.*, **A210**, 224, 245 (1951).

Then the weak forbidden band may not be observed, owing to the superposition with the strong allowed transition band.

The electron affinity of carbon atom is negative when the $2p$ and $2s$ orbitals with the usual screening constant for the neutral carbon atom are also used in the calculation of the energy of the negative carbon ion. Further, the electron affinity of vinyl radical which is calculated by the ASMO method is negative. This is an example of the error by the overestimation of the one center repulsion energy. In the negative carbon ion the electron cloud becomes larger on account of the increased electrostatic repulsion. So the consideration for the expansion of the electron cloud will be needed in the calculation of the energy of the negative carbon ion. Then in the valence bond method the variation of the screening constant of the negative carbon ion in polar structures will be the one approach to the energy levels of molecules avoiding this error. More directly the use of semi-empirical value of the one center repulsion integral which is determined by the consideration of the energy of the negative carbon ion was proposed by Moffitt[9] and by Parizer and Parr[5].

In the molecular orbital method the perfect non-empirical treatment may be given by the inclusion of the higher excited Rydberg orbitals and the effect of the σ-electrons. But this treatment will be too complicated to be useful or calculating the energy levels of the complex molecule. For London's treatment in this paper the use of semi-empirical values from the energy levels of the vinyl radical (or ethylene molecule) is interesting.

The energy of the ground state by this calculation exceeds 2 e. v. over the result of ASMO SCF CI calculation. This discrepancy is due to the neglect of the higher energy configurations, for instance the inclusion of the structure mentioned before,

$$\frac{1}{\sqrt{4!}}\sum_{P}(-1)^{P}P\frac{1}{\sqrt{2}}\{\varphi_2(1)\bar{\varphi}_2(2)\varphi_3(3)\bar{\varphi}_3(4)+\varphi_1(1)\bar{\varphi}_1(1)\varphi_4(3)\bar{\varphi}_4(4)\},$$

depresses the ground state by about 2 e. v.. If the energy depression of the ground state by the interaction with the neglected high energy structures is assumed to be 2 e. v. and the depressions of the other states are assumed to be zero, the energy levels by this treatment of London's will be close to those by the ASMO SCF CI calculation. But in order to obtain the same result as that by the ASMO SCF CI calculation one needs more complicated computations by this treatment for the large molecule.

The energy depression of the ground state by the interaction between the two vinyl radicals is about 0.3 e.v. and is mainly contributed by polar structure and by bonding structures. By this result one can expect the small resonance energy of butadiene.

From the wave function of the lowest ${}^1B_u$ state, it can be seen that the weight of polar structure is great, and that in London's treatment polar structures can not be ignored.

Semi-Empirical Calculation

Parizer and Parr[5] presented the semi-empirical method and obtained good results for the lower excited states of conjugated molecules by a simple procedure. They omitted many integrals except the Coulomb repulsion and resonance integrals, and simplified the procedure of calculation. Using their method the energy levels of butadiene are calculated in order to compare them with the results of the last section. The procedure of calculation is the same as that in the second section. The penetration integrals (11 : 3), (11 : 4) and (22 : 3)are assumed to be $-(11:33)$, $-(11:44)$ and $-(22:33)$ respectively. The values of the integrals used in this calculation are shown in Table III, and the other integrals are omitted. Then the matrix elements are easily computed. The result is shown in Fig. 2 (right column).

TABLE III

$(11:11)=10.53$	$H_{11}=W_1$
$(11:22)=7.38$	$H_{22}=W_1+7.46$
$(11:33)=5.35$	$H_{33}=W_1+7.36$
$(11:44)=3.75$	$H_{44}=W_1+7.82$
$(22:33)=7.16$	$H_{55}=W_1+7.82$
	$H_{66}=W_1+14.82$
$\beta_{12}=-2.92$	$H_{77}=W_1+10.11$
$\beta_{23}=-1.68$	$H_{12}=-0.68$
	$H_{14}=-1.68$
$\varepsilon_1=W_{2p}+\alpha-2.92$	$H_{16}=+0.10$
$\varepsilon_2=W_{2p}+\alpha+2.92$	$H_{17}=+0.05$
	$H_{24}=0$
$\lambda_{12}=-2.04$	$H_{25}=-0.68$
$\lambda_i=\alpha'$	$H_{27}=-0.34$
	$H_{46}=+0.84$
$K_{11}=K_{12}=8.95$	$H_{47}=+1.68$
$K_{13}=K_{14}=K_{24}=5.40$	$H_{67}=\frac{1}{2}W_1+7.41$
$J_{12}=1.57$	$H_{35}=-1.68$
$[11:34]=0.85$	
$[12:34]=0.05$	
	$N_i=1$
$\omega_{ij}=-0.84$	$N_{ij}=0$ (except N_{67})
$E_1=2W_{2p}+2\alpha+3.11$ $E_2=E_1+7.41$	$N_{67}=\frac{1}{2}$

The calculation by this treatment predicts the absorption bands at 1950 Å, 1700 Å and 1500 Å. The 1950 Å band is an allowed transition ^1A_g—^1B_u and corresponds to the 2000 Å strong absorption band observed experimentally. The 1700 Å and 1500 Å bands by this calculation are forbidden transitions and may have weak intensities. The important result of this calculation is that the lowest ^1A_g—^1A_g transition is higher than the lowest ^1A_g—^1B_u transition. Then this result supports the possibility that the lowest ^1A_g—^1A_g transition band might overlap with the strong absorption band and be impossible to observe.

The energy depression of the ground state by the interaction between the vinyl radicals is about 0.4 e. v., and is mainly contributed by the polar structures.

Conclusion

The energy levels of butadiene were calculated by London's treatment and by the semi-empirical treatment including polar structurs, and compared to the results by the ASMO SCF CI calculation and to the experimental data. According to this comparison, the non-empirical treatment which is described in this paper shows the same results as those by the ASMO SCF CI method. But for the experimental results, the non-empirical treatment does not show agreement. Most of the error in the excitation energy of the non-empirical treatment is due to the overestimation of the one centre repulsion energy, and this will be clear by the comparison to the result of the semi-empirical treatment. The result of the semi-empirical treatment is fairly good approximation to the experimental data. The effect of polar structures for the excited states is important and can not be ignored.

The author wishes to thank Dr. I. Tanaka and Prof. S. Shida of this laboratory for their kind discussion and encouragement. This research is supported in part by the grant in aid for the miscellaneous scientific researches of the Ministry of Education.

Laboratory of Physical Chemistry,
Tokyo Institute of Technology,
Tokyo

Studies on Molecular Structure by the Measurement of the Dielectric Constant of Gases. II. Dipole Moment and the Molecular Structure of Mono- and sym-Dihalogenomethyl ether

By Takehiko CHIBA

(Received January 24, 1955)

In halogenomethyl ether, CH_3OCH_2X, the two groups CH_3O–and CH_2X–have the possibility of rotating around the central C–O bond. The rotation around C–C bond has been extensively studied hitherto, but the rotation about C–O bond has not been so often subjected to examination. In addition, the group CH_3O– has a dipole moment opposite in its direction to that of the group $-CH_2X$, i.e. the dipole of the former group points towards the oxygen atom, while that of the latter points outward from the central carbon to the halogen atom. This situation is not encountered in the case of dihalogenoethanes. The problem has already been investigated by the measurement of dipole moment in non-polar solution[1], Raman effect[2], and infrared absorption spectrum[3]. The conclusion obtained is that the molecule has a shallow minimum about the equilibrium position so that there exists a wide distribution of molecules from the equilibrium position. The present work is carried out on mono and di-halogenomethyl ethers to investigate the molecular structure in the gaseous state from the standpoint of the dipole moment at various temperatures, for a slight change in the molecular configuration may sensibly be detected by the dipole moment measurement.

Preparation of the Materials

Monochloromethyl Ether CH_2ClOCH_3 was synthesized[4] from methanol, formalin, and hydro-

1) Y. Morino, H. Shiio and I. Miyagawa, *Repts. Radiation Chem. Research Inst.* (Tokyo Univ.), 5, 6 (1950).
2) M. Katayama and Y. Morino, ibid., 4, 1, (1949).
3) S. Mizushima, T. Shimanouchi, T. Miyazawa and M. Hayashi, unpublished.
4) *Org. Synthesis*, vol. 9, p. 59.

gen chloride. Dry air was passed through the crude distilate to exile the dissolved hydrogen chloride and then redistilled, b.p. 55–57°C.

***sym*-Dichloromethyl Ether** CH_2ClOCH_2Cl was synthesized[5] by the reaction of chlorosulfonic acid on polyoxymethylene in conc. sulfuric acid. It was purified as above, b.p. 103°C.

Monobromomethyl Ether CH_2BrOCH_3 was synthesized[6] from polyoxymethylene, methanol, and hydrogen bromide. It was purified as above, and redistilled, b.p. 86–88°C.

***sym*-Dibromomethyl Ether** CH_2BrOCH_2Br was synthesized[7] from polyoxymethylene, red phosphorus, and bromine, b.p. 148–150°C.

Experimental Procedure and Results

The apparatus for the measurement of dielectric constant was reported in the preceding paper[8]. The compounds are all reactive, and particularly, decompose readily in moist air. For monochloro- and monobromo-methyl ether, the usual gas filling method cannot be used on account of their low boiling point. The sample is first introduced in a trap which is connected to the cell, cooled with dry ice during the evacuation of the apparatus, and then evaporated to fill the gas cell by bringing the trap to room temperature. This operation has the disadvantage that the vapor contacts the grease of the cocks.

In the case of monobromoether, the observed polarization increases gradually with the runs of observation, so that the temperature dependence of the moment of this substance is also measured in heptane solution. For dibromoether, the measurement is carried out only in heptane solution because of the instability of this compound. The results of the measurements are summarized in Table I[9].

TABLE I

OBSERVED POLARIZATIONS AND DIPOLE MOMENTS OF MONOCHLORO-, DICHLORO-, MONOBROMO-, AND DIBROMO-METHYL ETHERS

Monochloromethyl ether

nR_D =18.0 cc. $P_E + P_A$ =18.9 cc.

T(°K)	n	p(mm Hg)	P(cc.)	ΔP(cc.)	μ(D)
296.3	6	70–102	82.5	0.6	1.76
337.8	5	83–120	75.1	0.3	1.77
370.4	7	70–103	73.3	0.5	1.82
412.3	7	92–113	68.3	0.4	1.83
467.2	7	81–110	66.2	0.4	1.90

n: number of the observations.
p: pressure range of the observations.
ΔP: average deviations of P.

sym-Dichloromethyl ether

MR_D =22.9 cc. $P_E + P_A$ =24.0 cc.

T	n	p	P	ΔP	μ
338.3	8	48–82	41.4	0.5	0.98
353.0	8	59–76	40.2	0.5	0.97
371.0	7	54–79	40.7	0.4	1.01
412.2	6	62–83	41.6	0.3	1.09
412.5	5	60–82	41.8	0.6	1.10

Monobromomethyl ether*

MR_D =20.8 cc. $P_E + P_A$ =21.8 cc.

T	n	p	P	μ
301.0	7	49–68	106.3–106.5	2.04
338.4	5	51–61	95.2– 98.0	2.03–2.07
338.4	8	61–70	93.5– 94.2	2.00
371.0	6	50–60	89.2– 94.0	2.03–2.10
371.1	6	63–74	89.2– 92.5	2.03–2.08
412.0	9	51–67	82.6– 83.4	2.03–2.08

* Observed polarization changes considerably with the runs of observation, so ΔP is not given in this case.

In heptane solution

T	ε_1	d_1(g./cc.)	α	β	$P_{2\infty}$(cc.)	μ
267	1.9574	0.7076	3.38	0.477	128.2	2.16
298	1.9111	0.6810	2.92	0.458	119.1	2.18
330	1.8648	0.6530	2.43	0.399	109.8	2.18

sym-Dibromomethyl ether

MR_D =28.6 cc. $P_E + P_A$ =30.0 cc.

T	ε_1'**	d_1'**	α	β	$P_{2\infty}$	μ
261	1.971	0.707	5.58	0.506	50.5	0.94
274	1.944	0.697	5.45	0.507	50.9	0.97
297	1.909	0.678	5.16	0.487	50.2	0.99
323	1.874	0.656	4.87	0.460	51.2	1.06

** The prime indicates that these values are extrapolated ones, which differ a little from the values of the pure solvent.

The observed moments of the monochloroether are in good agreement with the values previously reported by Morino, Shiio and Miyagawa in carbon tetrachloride solution[1]. Whereas for dichloroether the discrepancy between the present data and theirs seems fairly large. In the solution method some doubts may exist in the extrapolation to infinite dilution. Indeed, from their data polarization of about 44 cc. is estimated by a more reasonable extrapolation. This is close to the value obtained in the present observation.

Discussion of Results

I) Monochloromethyl Ether.—The result shows a great increase in the moment with temperature. This means that these molecules are a mixture of molecular form of stable, less polar ones and less stable, more polar ones[10]. From the appropriate bond

5) H. Stephen, et al., *J. Chem. Soc.*, **117**, 514 (1920).
6) Karvonen, *Chem. Zentl.*, **1912** II, 1268.
7) W. Tischtschenko, et al., *Chem. Zentl.*, **1915** I, 837.
8) T. Chiba, This Bulletin, **28**, 19 (1955).
9) In the calculation of the moment all the $P_E + P_A$'s are assumed to be 1.05 MR_D.

10) If a single form is assumed for this molecule, from the observed P *vs.* $1/T$ curve, the moment and the atomic polarization of 1.46 D and 20 cc. is obtained. The latter value is unreasonably high for the molecule of this kind, consequently the assumption of one rigid form is completely denied.

moments and bond angles, the moment of the molecule corresponding to the form in which the CH_3 group and Cl atom are in the *cis* position is calculated to be 0.65D, that of the form in which Cl atom is turned from the *cis* position through 60° (*gauche*) is 1.48D and that of the form in which the two are in the *trans* is 2.74D[11] (Fig. 1). The *cis* position is regarded as quite unstable, since at this position the distance between the Cl atom and the CH_3 group is very short. So we can safely ignore the *cis* form.

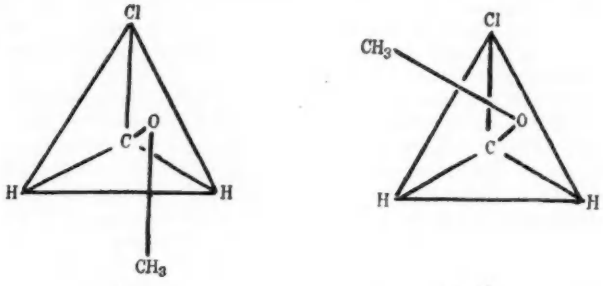

trans *gauche*

Fig. 1. The *trans* and *gauche* forms of monochloromethyl ether

From the results of the infrared and Raman effect spectroscopy[2,3], the existence of definite isomers is not concluded but rather the molecule should be distributed over a wide range of the angle of internal rotation. On the other hand, from the numerical calculation of the potential energy of these molecules as a function of the internal rotational angle by the use of appropriate interatomic potential[12], it was found that the molecule has a shallow potential minimum about the *gauche* position in good accord with the results of the spectra. From the temperature dependence of the dipole moment it cannot be decided whether the potential curve, as a function of the internal rotation angle, has minima at the *trans* and the *gauche* position, or whether it increases monotonously from the *gauche* position to the *trans* one: in other words, in such a curve as *a* or *b* in Fig. 2, the polarization vs. $1/T$ curve may be nearly the same in the temperature range of the present experiment. This means that, even if the potential be of the type *b*, the mean dipole moment may be treated by assuming the potential *a*[13]. Therefore, if we assume tentatively that the molecule is composed of the two isomers, *trans* and *gauche*, then from the observed change of the moment with temperature the energy difference of the two forms, ΔE, that is, the energy of the *trans* form minus the energy of the *gauche* one, is found to be approximately 700 cal./mol.[14].

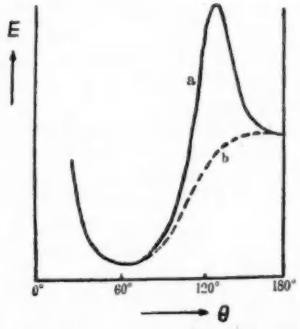

Fig. 2. Two types of intramolecular potential giving, respectively, (a) two separated isomers, and (b) continuous distribution.

With the model in which bond dipoles are located at the middle point of bond radius, the electrostatic energy between the two bond dipoles OCH_3 and CCl which stabilized the *gauche* position against the *trans* is calculated to be 1.3 kcal./mol.[15], so the observed result suggests that the *trans* position is stabilized by 1.3-0.7=0.6 kcal. due to the steric repul-

11) In the calculation the following values of bond moments are assumed: μ_{CCl}=1.8 D, μ_{CO}=1.0 D, μ_{CH_3O}=1.1 D.

12) H. Shiio, unpublished.

13) Strictly speaking, this is not true, but the above consideration may be allowed by taking average moment values in the neighborhood of the *trans* and the *gauche* as μ_t and μ_g. To discuss whether the potential be *a* or *b*, needs more precise molecular parameters, which in this case are unfortunately not known.

14) For the method of estimating ΔE from the observed temperature dependence of the moment, see I. Miyagawa, *J. Chem. Soc. Japan, (Pure Chem. Sect.)* 75, 970 (1954).

15) Assumed bond distances and the bond radii are as follows:

r_{CCl}=1.76Å, r_{CO}=1.42Å, $r_{C\cdot}$=0.77Å, $r_{O\cdot}$=0.65Å.

sion between CH_3 group and Cl atom. Of course, we cannot put too much significance on the individual figures, because the approximation used here is rather crude, but this is a reasonable magnitude when compared with those of haloethane derivatives. It must now be added that if we assume a mixture of *cis* and *trans* or of *cis*, *gauche* and *trans*, instead of *gauche* and *trans*, the moment of the *trans* form must be considerably higher than the calculated one in order to explain the observed data. This account confirms the validity of the neglection of the *cis* form.

II) *sym*-Dichloromethyl Ether.—Extending the consideration I), the following three forms are assumed: *t,t*-form in which the two chlorine atoms are in the *trans* to the opposite $-CH_2Cl$ group, *t,g*-form in which the one is in the *trans* and the other in the *gauche*, and *g,g*-form in which both are in the *gauche* position[15] (Fig. 3). Using the

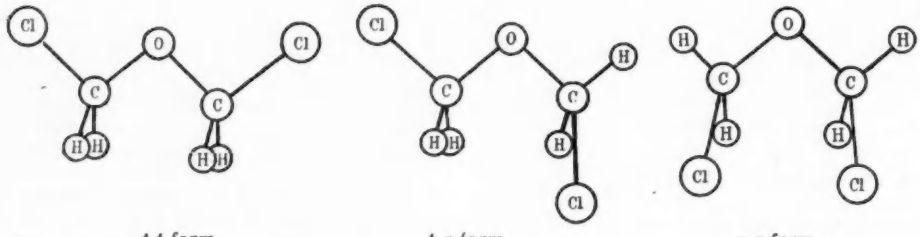

t,t-form *t,g*-form *g,g*-form

Fig. 3. The three forms considered for dichloromethyl ether

observed energy difference between the *trans* and the *gauche* forms of monochloro ether in I), the following relations can be obtained, provided that the interatomic distance and valence angles are the same in the two compounds.

$$E_{tt}-E_{gg}=0.7\text{ kcal.}\times 2+E_{tt}(\mu)-E_{gg}(\mu)$$
$$E_{tg}-E_{gg}=0.7\text{ kcal.}+E_{tg}(\mu)-E_{gg}(\mu)$$

where E's are the energies corresponding to the individual forms, $E(\mu)$'s are the energies of the dipole interaction of two CCl bond dipoles. Calculating in the same way as in I), $E(\mu)$'s are as follows: $E_{tg}(\mu)-E_{gg}(\mu)=0.5$ kcal., and $E_{tt}(\mu)-E_{gg}(\mu)=1.3$ kcal., leading to the total energy difference of $E_{tg}-E_{gg}=1.2$ kcal. and $E_{tt}-E_{gg}=2.7$ kcal. Therefore, if these arguments are valid, the contribution of *t,t*-form to the observed moment may be neglected. Further, the moment value of *g,g*-form is definitely small, so if it is tentatively assumed to be zero, the observed temperature dependence of the moment gives the values of $E_{tg}-E_{gg}=1.3$ kcal., and $\mu_{tg}=2.02$D (calculated moment of $\mu_{tg}=2.37$D).

Thus in view of the order of approximation the agreement between the calculated and the observed values are fairly good, which lead to the conclusion that the energy relation discussed above is essentially correct. It is noted that in this case, too, *t,t*-, *t,g*- and *g, g*-forms need not be definite isomers, but represent mean values about their positions

III) Monobromomethyl Ether.—There is a small difference in the moment value in the gaseous state (average moment 2.04D) and in solution (2.18D), but no temperature dependence of the moment in either case[17]. The same discussion as in I) leads to the energy difference between the *trans* form and the *gauche* one or zero or $\pm\infty$[18]. The moment value of this compound must be nearly the same or at least slightly less than that of the corresponding form of monochloroether. From the assumption of $\Delta E=0$, the calculated average moment is 2.2D, but from the assumption of $\Delta E=\pm\infty$ the calculated moment is 2.7 or 1.5D using the moment of monochloroether. Therefore, ΔE is considered to be equal to zero.

The comparison of this result with the case of monochloroether is interesting. In I) it is seen that the difference in the electrostatic energy between the *trans* and the *gauche* form is partly reduced by the steric energy difference of Cl and CH_3, but in this case ΔE from the steric energy of Br and CH_3 is so great that the electrostatic one is completely

16) The *g,g*-form denotes the configuration in which each CCl bond rotates 120° in opposite direction from the *t,t*-form. The one in which both groups rotate in the same direction is excluded because of the shortness of the Cl, Cl distance: ca. 2.3Å.

17) We have found that in halogenoethane derivatives when the temperature dependence of the moment is measured both in heptane solution and in gaseous state, ΔE derived from both methods are usually in good agreement, although the moment value itself may differ to some extent. (cf. I. Miyagawa, *J. Chem. Soc. Japan (Pure Chem. Sect.)*, 75, 1166 (1954)).

18) The possibility of free rotation is completely ruled out because of the short distance between Br and CH_3 at *cis* position as mentioned in (I).

cancelled leaving ΔE zero. Since ΔE, originated from electrostatic force, does not differ seriously in these two compounds, the steric one is several hundred calories higher in Br.....CH_3 than in Cl.....CH_3. This difference in steric energy is estimated to be 1.3 kcal. according to the Lenard-Jones type intermolecular potential used by Miyagawa for the case of halogenoethane derivatives[19]. As this figure depends greatly upon the molecular parameter, especially upon the valence angle, the agreement between the observed and the calculated figure seems fairly good.

IV) *sym*-Dibromomethyl Ether.—Temperature range of the measurement is narrow because the solution method has to be used. But the tendency of the temperature dependence of the moment is the same as in dichloroether. The same argument as that used in the dichloroether being applied, it is found from the observed value that the energy difference between the *t, g-* and *g, g-*forms is 0.9 kcal./mol. and $\mu_{tg}=1.9$D. Putting the dipole energy of dibromoether equal to that of dichloroether, then it is easily seen from the same discussion as in (II), that the difference in ΔE between dibromo- and dichloro-ether, is the same as that between monobromo- and monochloro-ether, i.e., 0.7 kcal. This value is compared to the observed one, that is, 1.3—0.9=0.4 kcal./mol.. In taking account of the errors in the experiment and the approximate nature of the treatment it can be said that the agreement is rather good.

Concluding the above discussion, the assumption that the dipole-dipole interaction and the steric repulsion are the main factors of the hindering potential of this kind of molecules holds approximately in the mono- and di-halogenomethyl ethers.

19) I. Miyagawa, *J. Chem. Soc. Japan (Pure Chem. Sect.)*, 75, 1177 (1954).

Summary

The temperature dependence of the dipole moment was investigated on monochloromethyl ether (I), *sym*-dichloromethyl ether (II) and monobromomethyl ether (III) in the gaseous state, and (III) and *sym*-dibromomethyl ether (IV) in heptane solution. The moment of (I), (II) and (IV) increases with temperature, while that of (III) does not.

From the observed data the energy difference between the *gauche* and the *trans* position is 0.7 kcal./mol. in (I), and zero in (III). Similarly ΔE's between *t,g-* and *g,g-*form of (II) and (IV) are estimated to be 1.3 kcal. and obtained to be 0.9 kcal./mol. respeetively from the observed results.

These energy values are explained satisfactorily by the electrostatic energy of dipole interaction and the steric energy between non-adjacent groups, which are of reasonable order of magnitudes as compared to the case of haloethane derivatives. The author wishes to express his sincere thanks to Prof. Y. Morino for his kind guidance through this study and to Dr. I. Miyagawa for much valuable advice. The cost of this research has been defrayed from the Grant in Aid for Fundamental Scientific Research from the Ministry of Education, to which the author's thanks are also due.

Department of Chemistry, Faculty of Science, The University of Tokyo, Tokyo

Reactions of Chloromethylpolysiloxanes with Thiourea[1]

By Shunichi NOZAKURA

(Received January 31, 1955)

Concerning the reaction of halogenomethylsilicon compound with thiourea, the synthesis of thiuronium salts from bromomethyltrimethylsilane has been reported.[2] Recently, Noller and Post also carried out the reaction of chloromethyltrimethylsilane[3] with thiourea, and thereby synthesized trimethylsilylmethylmercaptan.

I have reported in a previous paper[4] that the silicon-containing thiuronium salts were obtained from the reaction of the various chloromethylsilicon compounds, $ClCH_2Si(CH_3)_2R$, ($R=CH_3$—, $CH_3(CH_2)_3$—, $CH_3(CH_2)_7$—, C_6H_5— and $ClCH_2(CH_3)_2SiO$—) with thiourea and

1) Paper III in a series on the study of organosilicon compound.
2) D.C. Noller and H.W. Post, *J. Org. Chem.*, 17, 1393 (1952).
3) G.D. Cooper, *J. Am. Chem. Soc.*, 76, 2500 (1954).
4) S. Nozakura, *J. Chem. Soc. Japan (Pure Chem. Sect.)*, 75, 958 (1954).

that no fission of silicon-carbon bonds took place. It was of great interest that the difunctional bischloromethyltetramethyldisiloxane gave only the corresponding dithiuronium salt even when an excess of disiloxane was used.

The present study has been undertaken in order to clarify the nature of the above reaction. Thus we have studied the reactions between the chloromethylpolysiloxanes (I, II, III and IV) and thiourea and the decomposition of thiuronium salts by an aqueous solution of alkali.

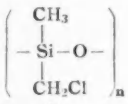

(I)

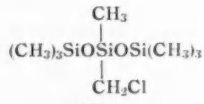

(II)

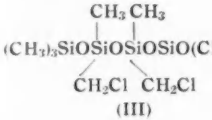

(III)

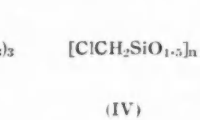

(IV)

Chloromethylmethylpolysiloxanes and Thiourea.—Because of the low solubility of the compound (I) in hot alcohol, the reaction apparently was found to be heterogeneous in the first stage and gradually became homogeneous as the reaction proceeded. The water-soluble polythiuronium chloride (V) was obtained quantitatively as a glassy solid after refluxing for several hours.

(I) (V)

The addition of an excess of aqueous ammonia to an aqueous solution of the compound (V) gave a white amorphous precipitate, methylpolysiloxane, with an evolution of methylmercaptan. Probably the fission of silicon-carbon linkage would take place in the first place, followed by the usual fission of sulfur-carbon bond[5] and the immediate condensation of the newly formed silanol to give a new siloxane linkage, as shown below;

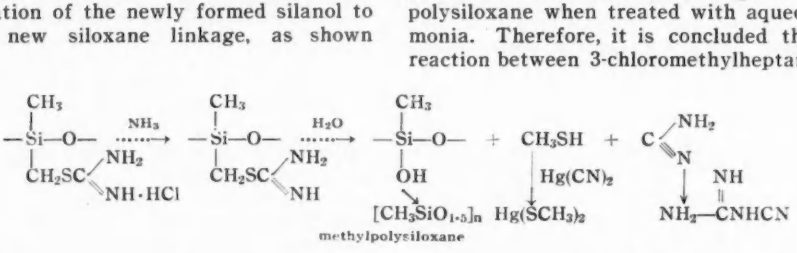

methylpolysiloxane

The chlorine content of the methylpolysiloxane was found to be very low (0.25%). This would suggest that the chlorine of chloromethylpolysiloxane (I) might be quite active in the reaction with thiourea.

When the compound (I) has been used in quantities double that calculated for thiourea, it was found that the ether-soluble part of the reaction product contained the compound (I), the unreacted substance. The decomposition of the water-soluble part by aqueous ammonia gave the precipitation of impure methylpolysiloxane, which contained a small amount of unreacted chloromethyl groups (Cl, 3.35%). These results indicate that nearly one half of the starting polysiloxane (I) reacted with thiourea and the other half remained unreacted. This may be interpreted to be due to the fission and recombination of siloxane bonds. Such an interpretation is confirmed experimentally by the reaction of trimethylsilyl-end-blocked simple chlormethylmethylpolysiloxanes (II) and (III) with thiourea as described below.

When a mixture of an alcoholic solution of the compound (II) and thiourea in equimolecular weight was heated under reflux for five hours, hexamethyldisiloxane was obtained as a volatile product. The ether-soluble part of the nonvolatile product contained thiuroniumchloride (VI) corresponding to the compound (II). The water-soluble part of the nonvolatile product gave methylpolysiloxane when treated with aqueous ammonia. Therefore, it is concluded that the reaction between 3-chloromethylheptamethyltrisiloxane (II) and thiourea gives the corresponding thiuronium chloride (VI) in the first stage and then the fission and recombination of siloxane bonds will take place, as shown below;

5) F. Arndt, *Ber.*, **54**, 2236 (1921).

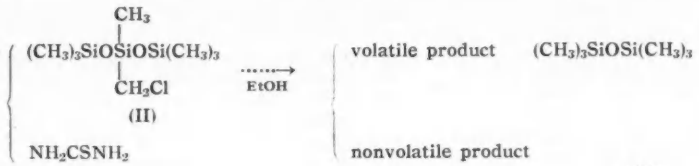

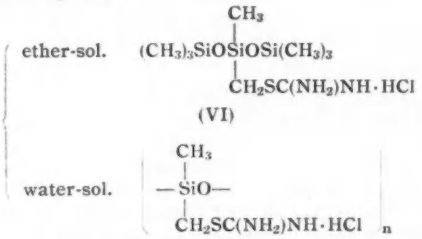

The reaction of 3.5-di(chloromethyl)octamethyltetrasiloxane (III) with thiourea also showed the same type of fission of siloxane bonds and gave polythiuroniumchloride. However in this case no appreciable amount of corresponding thiuroniumchloride was detected.

On the contrary the fission of siloxane bonds did not take place in the case of decamethyltetrasiloxane, which has no chloromethyl group, under the similar condition. Therefore the decrease in electron density on the silicon atom might facilitate the nucleophilic attack of the solvent molecule, as shown in following scheme;

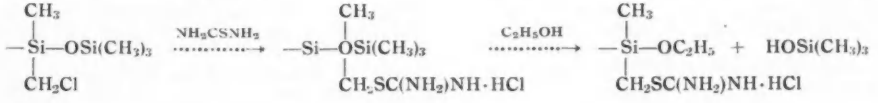

Consequently, the failure in obtaining the partially-reacted molecule in the case of bis(chloromethyl)tetramethyldisiloxane[4] and chloromethylmethylpolysiloxane (I) may be due to the fission of siloxane bonds.

Chloromethylpolysiloxane, which has the three dimensional structure, similarly gave the corresponding water-soluble thiuroniumchloride. Silicic acid was obtained by the treatment of the latter with aqueous ammonia. This is probably an additional evidence for the fission of siloxane bonds.

The Effect of Various Alkalies on the Precipitation Phenomenon of Methylpolysiloxane from the Aqueous Polythiuroniumchloride (V).—The comparison of the reaction time required for the precipitation of methylpolysiloxane in the alkaline decomposition of polythiuronium salt (V) is shown in Table I. The rate of precipitation of methylpolysiloxane became slower in the order of ammonia, sodium carbonate, and sodium bicarbonate, and became faster as their concentration increased. However in the case of sodium hydroxide the higher the alkaline concentration in the region below the equivalent concentration, the faster the rate of

TABLE I

THE EFFECT OF VARIOUS ALKALIES ON THE PRECIPITATION OF METHYLPOLYSILOXANE FROM THE AQUEOUS POLYTHIURONIUM CHLORIDE (V) SOLUTION*

Conc.**	Alkali			
	NaOH	Na_2CO_3	$NaHCO_3$	NH_4OH
6 N	no ppt.	0.2 min.		0.5 min.
1 N	7.0 min.	0.7 ,,	8.5 min.	0.6 ,,
0.1 N	3.2 ,,	10.0 ,,	30.0 ,,	3.3 ,,
0.05 N	10.0 ,,	24.0 ,,		6.5 ,,

* 1 ml. of 10% aq. (V) was quickly mixed with 1 ml. of aq. alkali and the time required till ppt. or turbidity began to appear was measured.

** The equivalent quantity of alkali is about 1 ml. of about 0.5 N.

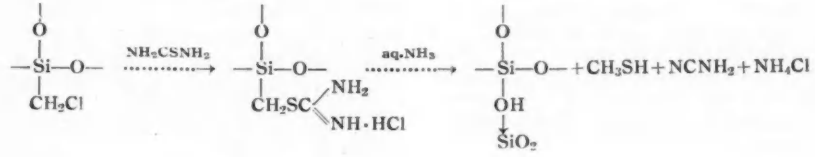

precipitation; on the contrary the higher the concentration in the region above the equivalent concentration, the slower the rate. Finally no precipitate was obtained. This means that sodium methylsilanolate would be produced in high alkaline concentration. In fact, the clear alkaline solution gave precipitation of methylpolysiloxane when neutralized with a dilute aqueous solution of hydrochloric acid.

The Fission of Silicon-Carbon Bonds in Various Silicon-containing Thiuronium Chloride.—The alkaline fission of silicon-carbon bonds in silicon-containing thiuronium chloride seemed to be a type of reaction analogous to the one which was found by Krieble and Elliott[6] in the reaction of chloromethylpolysiloxanes with an aqueous solution of alkali. They observed there the evolution of methylchloride. The effect of various substituents of the silicon atom on the fission of silicon-carbon bonds was compared qualitatively by titrating immediately the amount of methylmercaptan evolved on the decomposition of silicoalkylisothiourea at 100°C, as shown in Fig. 1. The polythiuronium salts of disiloxane and polysiloxane, in which the electron attracting oxygen atom is attached to the silicon atom, was decomposed much faster than the silicoalkylthiuronium salts in which the electron releasing *n*-butyl or *n*-octyl group is attached to the silicon atom. Phenyldimethylsilylmethylthiuronium chloride is situated between these two groups.

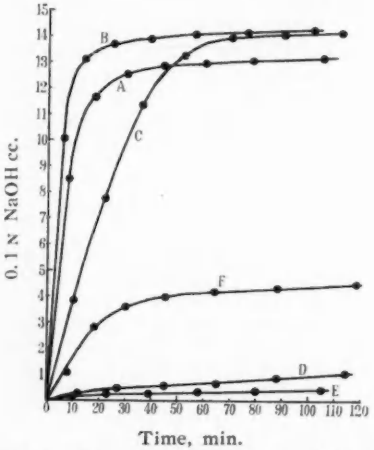

Fig. 1. Rate of alkaline decomposition of silicon-containing thiuronium chlorides.

A, $-\underset{\underset{\underset{

(II). *Anal.* Found: Si, 30.7; Cl, 12.5; Mol. wt. (in benzene), 279; MR_D, 72.06. Calculated for $C_8H_{23}O_2Si_3Cl$: Si, 31.0; Cl, 13.1; Mol. wt., 271; MR_D, 72.40.

(III), *Anal.* Found: Si, 29.6; Cl, 18.4; Mol. wt. (in benzene), 387; MR_D, 95.38. Calculated for $C_{10}H_{28}O_2Si_4Cl$: Si, 29.5; Cl, 18.7; Mol.wt., 379; MR_D, 95.88.

Chloromethylmethylpolysiloxane (I) with Thiourea (1 : 1 mol.).—A mixture of 10.88 g. (0.100 eq.) of (I), 7.62 g. (0.100 mol.) of thiourea, and 25 ml. of absolute alcohol was refluxed on a water bath for seven hours with a reflux condenser equipped with a calcium chloride tube. At the beginning of the refluxing (I) did not dissolve but settled down to the bottom of the flask; however, it gradually came into a homogeneous solution. Removal of the solvent in vacuo gave 22.4 g. of glass-like crude polythiuronium chloride. On dissolving this product in 50 ml. of water a slightly turbid solution was obtained, due to the presence of a minor amount of unreacted (I), and so this aqueous solution was extracted with a small amount of ether and again concentrated to dryness in vacuo to yield 18.27 g. of polythiuronium chloride (V) which contained a small amount of thiourea.

When 3 ml. of 6 N aqueous ammonia was added to a solution of 0.88 g. of (V) in 5 ml. of water a white amorphous precipitate was formed and mercaptan was evolved. The precipitate was centrifuged, washed thoroughly with water, and dried at 100° to give 0.32 g. of crude methylpolysiloxane.

Anal. Found: Si, 39.4; C, 17.8; H, 4.21; Cl, 0.25. Calculated for CH_3OSi: Si, 41.7; C, 17.8; H, 4.48; Cl, 0.0.

In order to identify the methylmercaptan evolved 2.7 ml. of 6 N aqueous sodium hydroxide was added to 0.4 g. of (V) in 10 ml. of water and the mixture was heated on the water bath, and the evolved gas was introduced into a solution of 1.0 g. of mercuric cyanide in 15 ml. of water. The resulted mercaptide (0.4 g.) was recrystallised from alcohol, m.p. 171. The mixed melting point with the known sample did not show any depression. The reaction mixture was filtered to remove the precipitated methylpolysiloxane and the filtrate was evaporated to a few mililiters on a water bath. After cooling 0.4 g. of crude dicyandiamide was obtained in colorless needles and showed the m.p. of 207.5–8° after a recrystallization from water. (207° in literature[5]).

Chloromethylmethylpolysiloxane (I) and Thiourea (2 : 1 mol.).—A mixture of 10.7 g. (0.098 eq.) of (I), 3.8 g. (0.050 mol.) of thiourea, and 25 ml. of absolute alcohol was refluxed for four and a half hours. At the end of the reaction the unreacted (I) remained insoluble. After removing the solvent in vacuo, the residual semisolid was dissolved in 50 ml. of water and the aqueous solutions was extracted with ether. Four and a half grams of the unreacted (I) was recovered as an oil (qualitative test for N and S was negative.) from the ethereal layer and 10.1 g. of crude (V) was obtained as a glass-like solid from the water layer. This product gave an impure methylpolysiloxane on the decomposition with ammonia, the analysis of which was as follows: Qualitative test for N and S was negative; Si, 37.0; Cl, 3.35.

3-Chloromethylheptamethyltrisiloxane (II) with Thiourea.—A mixture of 6.0 g. (0.022 mol.) of (II), 1.68 g. (0.022 mol.) of thiourea, and 10 ml. of absolute alcohol was refluxed for six hours. When the reaction mixture was distilled under reduced pressure, the distilate was caught in a trap cooled in an ice-salt bath and was added into 25 ml. of water to separate 0.8 g. of an insoluble oil, which boiled mostly at 98–101° and had the camphor-like odor, characteristic of hexamethyldisiloxane. The residue which remained was dissolved in 25 ml. of water and extracted with 20 ml. of ether. After drying the ether solution over calcium chloride and evaporating the solvent on a water bath, a crystalline mass of thiuronium chloride (VI) corresponding to (II) was obtained. After repeated washing with petroleum ether it gave colorless needles which amounted to 2.12 g., m.p. 111–2°. Found: Si, 23.8. Calculated for $C_9H_{27}N_2O_2SSi_3Cl$: Si, 24.2.

Its picrate decomposed at 180–1°. Found: Si, 15.5; N, 12.8. Calculated for $C_{15}H_{29}O_9N_5SSi_3$: Si, 15.5; N, 12.9.

One fifth of the water-soluble part of the product was decomposed with 5 ml. of 6 N aqueous ammonia and on standing over night 0.11 g. of methylpolysiloxane was obtained as a precipitate. Found: Si, 41.4; C, 18.3; H, 4.47. Calculated for $CH_3O_{1.5}Si$: Si, 41.4; C, 17.8; H, 4.48.

Another one-fifth gave 0.31 g. of picrate. Found: Si, 6.75; N, 17.58; N/Si atomic ratio = 5.21.

3,5-Di(chlormethyl) octamethyltetrasiloxane (III) and Thiourea.—A mixture of 1.75 g. (0.0046 mol.) of (III), 0.36 g. (0.0048 mol.) of thiourea, and 6 ml. of absolute alcohol was refluxed for five hours. Removing the solvent in vacuo there remained a semisolid and an oil. This was dissolved in 15 ml. of water and extracted with 20 ml. of ether. The ethereal layer gave 0.66 g. of oil. Four-fifths of the water layer, when treated with 6 ml. of 6 N aqueous ammonia, gave 0.133 g. of crude methylpolysiloxane. Found: Si, 40.4; C, 17.9; H, 3.91. Calculated for $CH_3O_{1.5}Si$, 41.7; C, 17.8; H, 4.48.

The residual one-fifth of the water layer gave 0.29 g. of picrate. Found: Si, 7.31; N, 17.74; N/Si atomic ratio = 4.84.

Decamethyltetrasiloxane (VII) and Thiourea.—A mixture of 7.0 g. of (VII), 5.1 g. of thiourea, and 20 ml. of absolute alcohol was refluxed for eight and a half hours. An oil separated on pouring the reaction mixture onto 50 ml. of water. This was washed with a small quantity of water and distilled. Only 5.6 g. of the unreacted starting material was recovered, b.p. 188–193°.

Chlormethylpolysiloxane (IV) and Thiourea.—A mixture of 2.0 g. (0.020 eq.) of (IV), 1.6 g. (0.021 mol.) of thiourea, and 20 ml. of absolute alcohol was refluxed for four hours. The white powder of (IV) gradually became a transparent semisolid and stuck to the bottom of the flask.

After cooling, the upper alcoholic layer was decanted and the residual semisolid was washed several times with alcohol by decantation and dried in vacuo, yielding 2.8 g. of a glassy solid. Found: Si, 17.2; N, 12.8; N/Si atomic ratio=1.5.

Five-tenths of a gram of this product was treated with 10 ml. of water. The insoluble part (about 0.06 g.) was filtered off and the filtrate gave 0.1 g. of an impure amorphous silica on decomposition with 5 ml. of 6 N aqueous ammonia. Found: Si, 44.7; Cl, 0.22. Calculated for SiO_2: Si, 46.6; Cl, 0.0.

The Fission of Silicon-Carbon Bonds in Various Silicon Containing Thiuronium Salts.—The method of the preparation of chlormethyldimethylalkylsilanes where alkyls are methyl, *n*-butyl, *n*-octyl, and chloromethyldimethylsiloxy group and of their corresponding thiuronium chloride has been described in the previous paper.[4]

The general procedure is as follows: A three necked flask of 30 ml. capacity was equipped through ground joints with a side flask of about 5 ml. capacity, a vertical air condenser 30 cm. long, and a nitrogen gas inlet tube, the tip of which reached to the bottom of the main flask. Four mililiters of 0.377 N aqueous sodium hydroxide was placed in the main flask and was heated on a water bath, and a stream of nitrogen gas with a constant flow (23–4 ml./min.) was introduced into it, and then the solution of the sample in the side flask was quickly poured into the main flask. The samples used were in a slight excess over an equivalent amount of sodium hydroxide (0.001508 eq.) and dissolved in 3–5 ml. of water. The evolved methylmercaptan was removed along with the stream of nitrogen gas and led into a two percent aqueous solution of mercuric chloride through the air condencer. The liberated hydrochloric acid was titrated with 0.1 N aqueous sodium hydroxide using methyl orange as the indicator under vigorous shaking. The results are given in Fig. 1. After the reaction, in the case of A a white precipitate was obtained. In B, the reaction mixture was trans-parent and gave an oil, on addition of aqueous dilute hydrochloric acid. In C, the reaction mixture was transparent. No silicon-containing fragment was found in it nor in the flask of the mercuric solution, except for the precipitate of mercaptide which was not analysed quantitatively but showed distinctly the existence of silicon on ignition with sulfuric acid.

In the cases of D, E, and F there remained oils which were insoluble in dilute aqueous hydrochloric acid.

Summary

Chloromethylmethylpolysiloxane (I), 3-chloromethylheptamethyltrisiloxane (II) 3,5-di(chloromethyl)octamethyltetrasiloxane (III), and chloromethylpolysiloxane (IV) were reacted with thiourea in absolute alcohol to give silicon-containing thiuronium chlorides.

Although in the case of (II) the corresponding thiuronium chloride was isolated, an extensive fission and recombination of siloxane bonds took place in every case.

Silicon-carbon bond in the thiuronium chloride derived from (I) was easily cleft by the treatment with an aqueous alkali to give three-dimensional methylpolysiloxane. In a similar manner the thiuronium chloride derived from (IV) gave silicic acid with aqueous alkali.

The fission of silicon-carbon bonds in the silicon-containing thiuronium salts was facilitated by the electron-attracting substituents on the silicon atom.

The author is much indebted to Shinetsu Chem. Ind. Co. for generous supplies of the materials used, to Profs. S. Murahashi and H. Tani for their many helpful suggestions, and to Mr. Konotsune for his help in some of the experiments.

Department of Chemistry,
Faculty of Science,
Osaka University,
Osaka

Formation and Aging of Precipitates. III. Electron Microscopic Studies on Barium Sulfate Precipitates in Aqueous Alcohol

By Eiji SUITO and Kazuyoshi TAKIYAMA

(Received February 7, 1955)

Introduction

It is interesting to examine the precipitates that are formed not only in water but also in other media. Many investigations have been made about precipitates which are produced in more soluble media than water to study their analytical conditions, and those which are produced in less soluble media to prepare the colloidal solutions. The authors reported about the morphology and aging of barium sulfate precipitates in water previously[1], and also examined the change of the shape and size of the precipitates produced by changing the solubility of barium sulfate. This paper is a report on barium sulfate precipitates produced in aqueous alcohol in the relations of the shape and size, the total concentration, the concentration of alcohol and the solubility of barium sulfate.

Solubility of Barium Sulfate in Aqueous Alcohol

As there have been practically no investigations reported about the solubilities of barium sulfate in aqueous alcohol, the authors have measured them by the electric conductivity method, which will be explained by an example as follows.

The electric conductivity was measured by the method of the Wheatstone bridge. The specific conductivity of distilled water was 2.23×10^{-6} mho and that of the saturated aqueous barium sulfate was 5.1×10^{-6} mho. Then the solubility of barium sulfate in water was calculated as 1.2×10^{-5} M. The specific conductivity of 45% alcohol was 5.3×10^{-6} mho and that of the saturated barium sulfate solution in 45% alcohol was 6.6×10^{-6} mho. Then to 15 ml. of 45% alcohol the saturated aqueous barium sulfate was added drop by drop from a micro-burette and the conductivities of these mixed solutions were measured. After 0.11 ml. of the saturated aqueous barium sulfate was added to the aqueous alcohol, the specific conductivity became 6.6×10^{-6} mho. From these results the solubility of barium sulfate in 45% alcohol was calculated as follows:

$$\frac{1.2\times10^{-5}\times0.11}{15.11}=8\times10^{-8}\ (\mathrm{M})$$

The solubilities of barium sulfate in alcohol of various concentrations were measured by the same method and the results are shown in Table I and Fig. 1. As the concentration of the alcohol in which barium sulfate was saturated was somewhat different from that of the alcohol to which the saturated aqueous barium sulfate was added, the percentage of alcohol shown in Table I contains some errors, but they are negligible.

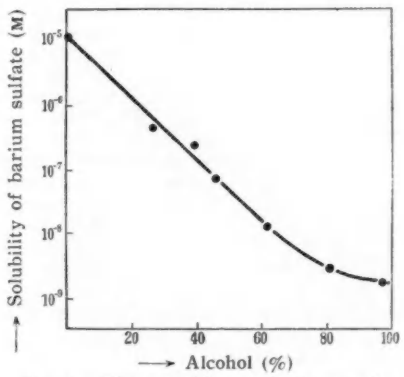

Fig. 1. The solubility of barium sulfate in aqueous alcohol.

TABLE I

SOLUBILITIES OF BARIUM SULFATE IN AQUEOUS ALCOHOL

Concentration of Alcohol %	Solubility of Barium Sulfate M
0	1.2×10^{-5}
30	3×10^{-6}
39	4×10^{-7}
45	8×10^{-8}
62	2×10^{-8}
80	4×10^{-9}
99	2×10^{-9}

Morphology of Barium Sulfate Precipitates in Aqueous Alcohol

The barium sulfate precipitates in aqueous alcohol were prepared as follows. To 10 ml. of alcohol of a certain concentration were added simultaneously 5 ml. of barium hydroxide solution and sulfuric acid which were of the same concentration. The reaction temperature was 18°C. The precipitates produced were observed by an electron microscope.

The conditions of the precipitation and the properties of the precipitated particles are collectively

1) E. Suito and K. Takiyama, This Bulletin, 27, 121, 123 (1954).

shown in Table II. A, B and C groups in Table II are the cases in which the total concentrations of barium sulfate were kept constant and the concentrations of alcohol were changed. In these groups the precipitates produced in water, that is 0% alcohol, are to be compared with the condition of the precipitation reported previously[1]. In D group the concentration of alcohol was kept definite; that is to say, the solubility of barium sulfate was definite, and the total concentration of barium sulfate was changed.

At the total concentration of 0.05 M (A group) the particles precipitated in water were spindle-shaped, as shown in Photo 1, but in aqueous alcohol the shapes of the particles were thin hexagonal plates, and their size became smaller with the increase of the concentration of alcohol as shown in Photos 2, 3 and 4. The hexagonal particles of barium sulfate were found only under these conditions and were not found in the precipitates formed in water nor at the other total concentrations in aqueous alcohol. As the particles of the specimen of No. 4 were very small, namely, the size was below 10 mμ, the shape was not clear.

At the other total concentrations the particles precipitated in the aqueous alcohol were practically diamond-shaped and their size became smaller with the increasing percentage of alcohol in the aqueous alcohol as shown in Table II.

change at the definite solubility was similar to the change of the size of the precipitated particles produced in water medium[1].

At the total concentrations higher than 0.05 M the size of the precipitated particles became extremely small with the addition of alcohol. None of the precipitated particles produced in the aqueous alcohol have changed their shape and size for 2 years on standing in the media.

In these precipitates the similar shaped particles were formed after the same induced period. Namely, the precipitates of diamond shape began to deposit immediately after mixing the reagents and completed their crystallization after 10 to 20 seconds. The precipitates of spindle shape were completly formed directly after mixing the reagents. Such phenomena have been observed both in cases of water and aqueous alcohol media. It seems that the mechanism of the growth of the crystals was similar, when the induced period of the formation of the crystals was identical.

Identification of Crystals by the Electron Micro-Diffraction Method

The electron micro-diffraction method by means of the three stage electron microscope, SM-C3, was applied to analyze the crystal structure of the precipitated particles mentioned above. A few examples of the electron diffraction patterns obtained are shown in Photos 9 (a), (b) and (c).

TABLE II

THE PROPERTIES OF BARIUM SULFATE PRECIPITATES IN AQUEOUS ALCOHOL

Group	No.	Total concentration C_0 (M)	Alcohol concentration (%)	Solubility S (M)	Particle size (mean) (mμ)	Particle shape
A	1	5×10^{-2}	0	1×10^{-5}	470	Spindle
"	2	"	2.5	9×10^{-6}	90	Thin hexagonal plate
"	3	"	10	5×10^{-6}	70	"
"	4	"	50	7×10^{-8}	<10	——
B	5	5×10^{-3}	0	1×10^{-5}	3200	Diamond (rugged)
"	6	"	2.5	9×10^{-6}	3000	"
"	7	"	5	8×10^{-6}	2500	"
"	8	"	7.5	7×10^{-6}	2000	"
"	9	"	10	5×10^{-6}	1100	Diamond (smooth)
"	10	"	15	3×10^{-6}	400	"
"	11	"	50	7×10^{-8}	<10	——
C	12	5×10^{-4}	0	1×10^{-5}	3500	Ellipse
"	13	"	2.5	9×10^{-6}	3100	Diamond (rugged)
"	14	"	10	5×10^{-6}	3000	Diamond (smooth)
"	15	"	25	6×10^{-7}	2000	Spindle (thin rugged)
"	16	"	35	3×10^{-7}	70	Sphere (rugged)
"	17	"	50	7×10^{-8}	<10	——
D	18	5×10^{-2}	10	5×10^{-6}	70	Hexagon
"	19	4×10^{-2}	"	"	710	Diamond (rugged)
"	20	3×10^{-2}	"	"	820	"
"	21	1×10^{-2}	"	"	830	"
"	22	5×10^{-3}	"	"	1600	"
"	23	5×10^{-4}	"	"	3000	Diamond (smooth)

In D group the precipitated particles became larger with the decreasing total concentration of m sulfate as shown in Photos 5~8. This

Photo 9 (a) obtained from the diamond-shaped particles shown in Photo 7 (No. 21) is of coarse Debye-Scherrer rings, because there are not

Electron micrographs of various barium sulfate precipitates

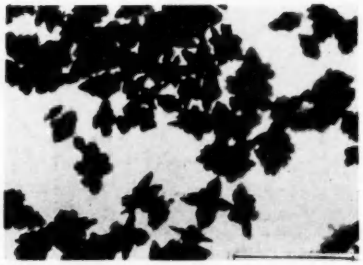

Photo. 1. No. 1. $C_0=5\times10^{-2}$ M, $S=1\times10^{-5}$ M (×20,000)

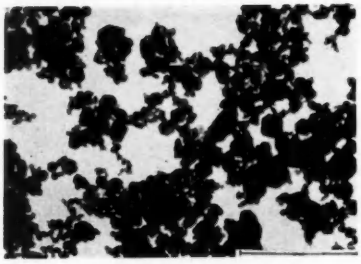

Photo. 2. No. 2. $C_0=5\times10^{-2}$ M, $S=9\times10^{-6}$ M (×20,000)

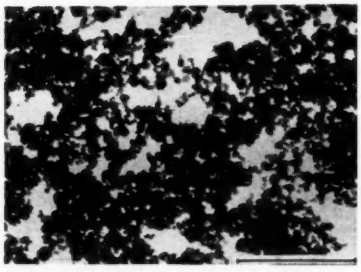

Photo. 3. No. 3. $C_0=5\times10^{-2}$ M, $S=5\times10^{-6}$ M (×20,000)

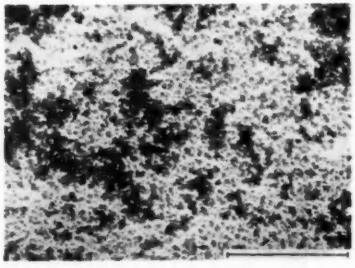

Photo. 4. No. 4. $C_0=5\times10^{-2}$ M, $S=7\times10^{-8}$ M (×20,000)

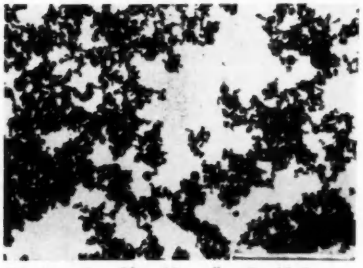

Photo. 5. No. 18. $C_0=5\times10^{-2}$ M, $S=5\times10^{-6}$ M (×20,000)

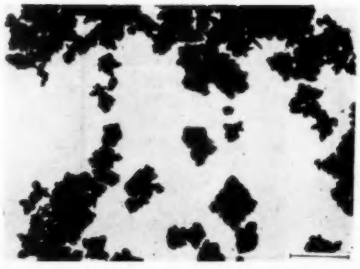

Photo. 6. No. 20. $C_0=3\times10^{-2}$ M, $S=5\times10^{-6}$ M (×10,000)

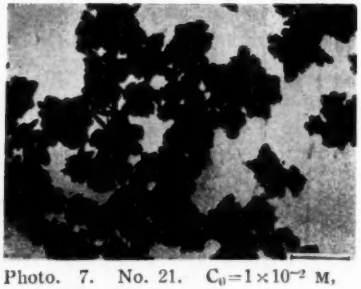

Photo. 7. No. 21. $C_0=1\times10^{-2}$ M, $S=5\times10^{-6}$ M (×10,000)

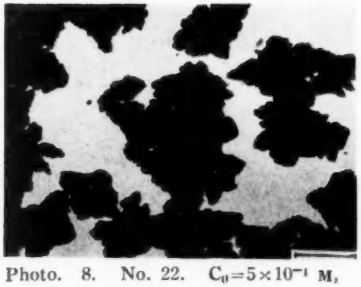

Photo. 8. No. 22. $C_0=5\times10^{-4}$ M, $S=5\times10^{-6}$ M (×10,000)

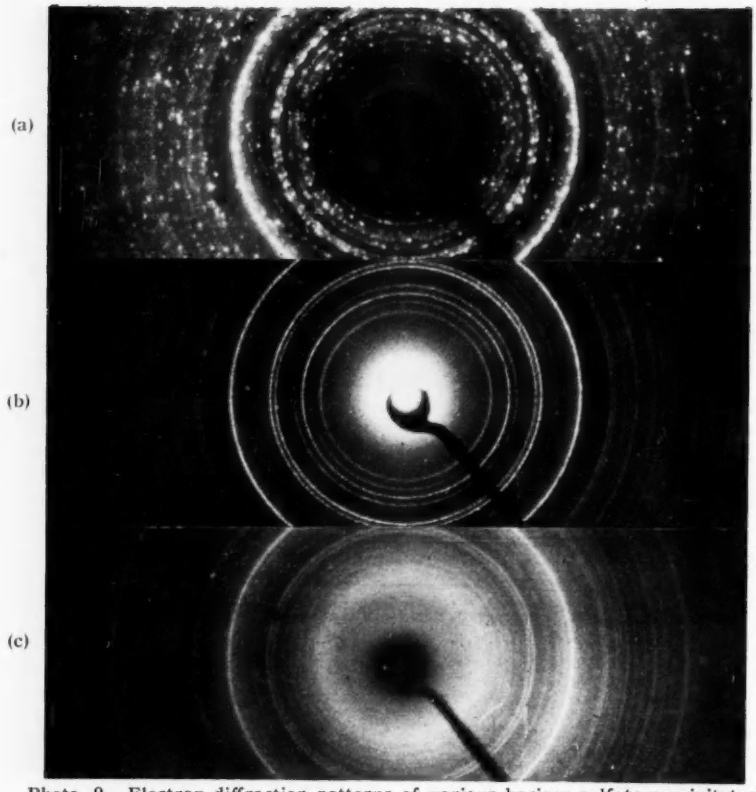

Photo. 9. Electron diffraction patterns of various barium sulfate precipitates.
(a) diamond type (No. 21)
(b) hexagonal type (No. 3)
(c) small particle (No. 4)

many crystalline particles in the selected area (5 μ) of the electron microscope. The patterns obtained from the particles of the hexagonal plates and the small particles shown in Photo 3 (No. 3) and Photo 4 (No. 4) were obtained by the ordinary electron diffraction technique for many crystalline particles, and are very fine as shown in Photos 9 (b) and (c). It is interesting that the pattern obtained from the small particles which are observed as "amorphous" by the electron microscope (<10 mμ) is very sharp, and the particles are obviously crystalline.

The arrangements of the rings of every diffraction pattern are the same as observed with barium sulfate crystals obtained by X-ray diffraction as shown in Fig. 2.

Differences in the intensity of each line in the electron and X-ray diffraction diagrams intimate the orientation of the flat particles on the film of the specimen holder of the electron microscope, though the difference in technique between the electron and X-ray diffractions have to be taken into consideration.

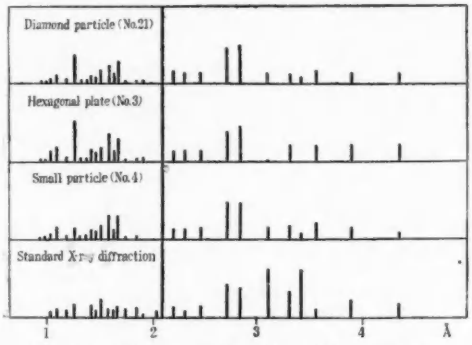

Fig. 2. Electron diffraction diagrams of various barium sulfate precipitates.

Summary

1. The solubilities of barium sulfate in aqueous alcohol were measured.

2. The barium sulfate particles precipitated in aqueous alcohol became smaller with the increasing concentration of alcohol; namely, with the decreasing solubility of barium sulfate.

3. In the case of the aqueous alcohol of the certain percentage (for a definite solubility of barium sulfate) the precipitated particles became larger with the decreasing total concentration of barium sulfate.

4. The barium sulfate precipitates prepared in the aqueous alcohol were practically diamond shaped; and spindle, hexagonal and sphere particles were also found. The shape of the precipitated particles seemed to depend on the induced period of the precipitation.

5. The electron micro-diffraction method was applied to analyze the crystal structure and, of course, the patterns obtained from various types of crystals agreed with those of barium sulfate.

The Institute for Chemical Research, Kyoto University, Takatsuki-Shi, Osaka-Fu